THESIS APPROVAL

GRADUATE SCHOOL, KASETSART UNIVERSITY

Master of Science (Chemistry)

DEGREE

Chemistry — **FIELD**

Chemistry — **DEPARTMENT**

TITLE: Preparation of TiO_2 Supported Activated Carbon for Treatment of Phenol and Acid Orange 7

NAME: Mr. Chalermapan Ngamsopasiriskun

THIS THESIS HAS BEEN ACCEPTED BY

..... **THESIS ADVISOR**

(Associate Professor Apisit Songsasen, Ph.D.)

..... **THESIS CO-ADVISOR**

(Ms. Pornpun Pornsinlapatip, Ph.D.)

..... **THESIS CO-ADVISOR**

(Mr. Surachai Thachepan, Ph.D.)

..... **DEPARTMENT HEAD**

(Assistant Professor Noojaree Prasitpan, Ph.D.)

APPROVED BY THE GRADUATE SCHOOL ON .....

..... **DEAN**

(Associate Professor Gunjana Theeragool, D.Agr.)

Copyright by Kasetsart University All rights reserved

THESIS

PREPARATION OF TiO_2 SUPPORTED ACTIVATED CARBON FOR TREATMENT OF PHENOL AND ACID ORANGE 7

CHALERMPAN NGAMSOPASIRISKUN

A Thesis Submitted in Partial Fulfillment of
the Requirements for the Degree of
Master of Science (Chemistry)
Graduate School, Kasetsart University
2010

Copyright by Kasetsart University All rights reserved

Chalermpan Ngamsopasiriskun 2010: Preparation of TiO_2 Supported Activated Carbon for Treatment of Phenol and Acid Orange 7. Master of Science (Chemistry), Major Field: Chemistry, Department of Chemistry. Thesis Advisor: Associate Professor Apisit Songsasen, Ph.D. 150 pages.

TiO_2/AC was prepared via the sol-gel method, which studied in term of titania precursors. From the characterization results, it was found that TiO_2/AC using titanium(IV) isopropoxide calcined at 400ºC provided the most appropriate properties for performing as the photocatalyst. TGA, Raman and XRD results indicated that this TiO_2/AC catalyst had high crystallinity. SEM and TEM results demonstrated that its surface morphology was particle of AC covered throughout by TiO_2. Moreover, with increasing calcination temperature, its amorphous-to-anatase phase transformation was retarded by the presence of AC. Adsorption of phenol by TiO_2/AC was fitted with the Langmuir isotherm that indicated the monolayer adsorption system, and showed highest thermodynamic stability. All of these properties enhanced the removal efficiency of TiO_2/AC under UV light.

Regarding the photocatalytic activity, TiO_2/AC using titanium(IV) isopropoxide calcined at 400ºC succeeded in degradating phenol and acid orange 7 with the highest efficiency. However, its photocatalytic activity drastically decreased when it was calcined at higher temperature due to the AC was oxidized totally. Besides, the recycling efficiency of catalyst decreased when it was repeatedly used in photocatalytic runs due to the deactivation of catalyst surface.

_____ _____ __ / __ / __

Student's signature Thesis Advisor's signature

Copyright by Kasetsart University All rights reserved

ACKNOWLEDGEMENTS

I would like to express my profound appreciation to my supervisor, Associate Professor Dr. Apisit Songsasen for his valuable guidance and encouragement throughout the span of my study and research. I also wish to express my sincere gratitude to Dr. Pornpun Pornsinlapatip and Dr. Surachai Thachepan, member of the committee. Additionally, I am so grateful to Mr. Suchat Suwannatus, for his kind collaboration and his invention of the photoreactor used in my research.

In addition, I myself would like to thank the Center of Exellecne for Innovation in Chemistry (PERCH-CIC), Commission on Higher Education, Ministry of Education for financial support, and the Department of Chemistry, Faculty of Science, Kasetsart University for all research facilities.

I am deeply in debt to my parents for their unfailing moral support, encouraging me to overcome the obstacles and giving me financial assistance. I wholeheartedly thank my colleagues and my friends for their affection and devoting their valuable time in helping me during my graduate study.

Chalermpan Ngamsopasiriskun

March, 2010

Copyright by Kasetsart University All rights reserved

TABLE OF CONTENTS

		Page
TABLE OF CONTENTS		i
LIST OF TABLES		iii
LIST OF FIGURES		vii
LIST OF ABBREVIATIONS		xv
INTRODUCTION		1
OBJECTIVES		12
LITERATURE REVIEW		13
MATERIALS AND METHODS		23
Materials		23
Methods		24
RESULTS AND DISCUSSION		33
CONCLUSION AND RECOMMENDATIONS		104
Conclusion		104
Recommendations		106
LITRATURE CITED		107
APPENDICES		113
Appendix A	Calculation of crystallite sizes, phase identification using the Sherrer's equation	114
Appendix B	Raw data of all adsorption isotherms	117
Appendix C	Raw data of all photodegradation reactions	123
Appendix D	Calculation of rate constants	142

Copyright by Kasetsart University All rights reserved

TABLE OF CONTENTS (Continued)

Page

Appendix E	Calculation of surface area for phenol adsorption	144
Appendix F	ChV and LC_{50} of intermediates from degradation of phenol and AO7	146
CURRICULUM VITAE		150

Copyright by Kasetsart University All rights reserved

LIST OF TABLES

Table		Page
1	Crystal properties of the three main polymorphs of TiO_2.	3
2	The molecular structure and general properties of phenol and acid orange 7.	11
3	The titania precursors with their volumes, density and equivalent mole of titania.	24
4	Effect of titania precursors and calcination temperatures on the crystallite sizes and phase content of TiO_2/AC and P25 TiO_2.	42
5	The data from Langmuir isotherm of phenol using various catalysts.	53
6	Percentage of phenol removal for the photodegradation of phenol from 200 ml of 100 ppm phenol by various amount of TiO_2/AC (prepared by titanium(IV) isopropoxide as precursor).	55
7	Percentage of phenol removal and rate constant for the photodegradation of phenol from 200 ml of 100 ppm phenol by 0.4g of AC, 0.4g of prepared-TiO_2, 0.4g of P25 TiO_2 and 0.4g of TiO_2/AC (prepared by using titanium(IV) isopropoxide as precursor).	61
8	Percentage of phenol removal and rate constant for the photodegradation of phenol from 200 ml of 100 ppm phenol by 0.4g of prepared-TiO_2.	68
9	Percentage of phenol removal and rate constant for the photodegradation of phenol from 200 ml of 100 ppm phenol by 0.4g of TiO_2/AC (prepared by titanium(IV) isopropoxide as a precursor).	74
10	Percentage of phenol removal and rate constant for the photodegradation of phenol from 200 ml of 100 ppm phenol by 0.4g of TiO_2/AC (prepared by using titanium(IV) n-butoxide as a precursor).	80
11	Rate constant and %removal of phenol from 100 ppm phenol by 0.4g of TiO_2/AC calcined 400ºC using titanium(IV) isopropoxide and titanium(IV) n-butoxide compared to P25 TiO_2.	82

Copyright by Kasetsart University All rights reserved

LIST OF TABLE (Continued)

Table		Page
12	Percentage of AO7 removal for the photodegradation of AO7 from 200 ml of 100 ppm AO7 by 0.2 g of TiO_2/AC (prepared by using titanium(IV) isopropoxide as a precursor) at various pH of solution.	90
13	Percentage of AO7 removal for the photodegradation of AO7 from 200 ml of 100 ppm AO7 by 0.2 g of TiO_2/AC (prepared by using titanium(IV) n-butoxide as a precursor) at various pH of solution.	96
14	Removal of phenol by TiO_2/AC using titanium(IV) isopropoxide as precursor and calcined at 400ºC with three times recycle.	103
15	Removal of AO7 by TiO_2/AC using titanium(IV) isopropoxide as precursor and calcined at 400ºC with three times recycle.	103

Appendix Table

B1	Raw data of the adsorption isotherm of phenol by AC.	119
B2	Raw data of the adsorption isotherm of phenol by AC-400.	120
B3	Raw data of the adsorption isotherm of phenol by TiO_2/AC using titanium(IV) isopropoxide as a precursor.	121
B4	Raw data of the adsorption isotherm of phenol by TiO_2/AC using titanium(IV) n-butoxide as a precursor.	122
C1	Raw data of the photodegradation reaction of phenol by prepared-TiO_2 without calcination.	124
C2	Raw data of the photodegradation reaction of phenol by prepared-TiO_2 calcined at 300ºC.	125
C3	Raw data of the photodegradation reaction of phenol by prepared-TiO_2 calcined at 400ºC.	126
C4	Raw data of the photodegradation reaction of phenol by prepared-TiO_2 calcined at 500ºC.	127

Copyright by Kasetsart University All rights reserved

LIST OF TABLE (Continued)

Appendix Table		Page
C5	Raw data of the photodegradation reaction of phenol by TiO_2/AC prepared from titanium(IV) isopropoxide without calcination.	128
C6	Raw data of the photodegradation reaction of phenol by TiO_2/AC prepared from titanium(IV) isopropoxide calcined at 300ºC.	129
C7	Raw data of the photodegradation reaction of phenol by TiO_2/AC prepared from titanium(IV) isopropoxide calcined at 400ºC.	130
C8	Raw data of the photodegradation reaction of phenol by TiO_2/AC prepared from titanium(IV) isopropoxide calcined at 500ºC.	131
C9	Raw data of the photodegradation reaction of phenol by TiO_2/AC prepared from titanium(IV) n-butoxide without calcination.	132
C10	Raw data of the photodegradation reaction of phenol by TiO_2/AC prepared from titanium(IV) n-butoxide calcined at 300ºC.	133
C11	Raw data of the photodegradation reaction of phenol by TiO_2/AC prepared from titanium(IV) n-butoxide calcined at 400ºC	134
C12	Raw data of the photodegradation reaction of phenol by TiO_2/AC prepared from titanium(IV) n-butoxide calcined at 500ºC	135
C13	Raw data of the photodegradation reaction of AO7 by TiO_2/AC prepared from titanium(IV) isopropoxide calcined at 400ºC at pH 4.0.	136
C14	Raw data of the photodegradation reaction of AO7 by TiO_2/AC prepared from titanium(IV) isopropoxide calcined at 400ºC at pH 7.0.	137
C15	Raw data of the photodegradation reaction of AO7 by TiO_2/AC prepared from titanium(IV) isopropoxide calcined at 400ºC at pH 10.0.	138
C16	Raw data of the photodegradation reaction of AO7 by TiO_2/AC prepared from titanium(IV) n-butoxide calcined at 400ºC at pH 4.0.	139

Copyright by Kasetsart University All rights reserved

LIST OF TABLE (Continued)

Appendix Table		Page
C17	Raw data of the photodegradation reaction of AO7 by TiO_2/AC prepared from titanium(IV) n-butoxide calcined at 400ºC at pH 7.0.	140
C18	Raw data of the photodegradation reaction of AO7 by TiO_2/AC prepared from titanium(IV) n-butoxide calcined at 400ºC at pH 10.0.	141
F1	The ChV and LC_{50} value of each intermediate from degradation of phenol	148
F2	The ChV and LC_{50} value of each intermediate from degradation of AO7	149

Copyright by Kasetsart University All rights reserved

LIST OF FIGURES

Figure		Page
1	Crystal structures of TiO_2 anatase, rutile and brookite.	2
2	Principal processes occurring on the TiO_2 particles	5
3	Secondary reactions with activated oxygen species in the photoelectronchemical mechanism.	6
4	Proposed mechanism of degradation with TiO_2/AC catalysts prepared by MOCVD and sol-gel method.	18
5	FT-IR spectra of (a) AC-TiO_2-P25, (b) AC-TiO_2-P25 after PFBA adsorption and (c) AC-TiO_2-P25 after complete defluoridation.	20
6	Synergistic effect of AC-TiO_2-P25 on photodefluoridation of PFBA	20
7	The image of photoreactor contained UV-lamps and magnetic stirrers.	27
8	The TGA curve of as-prepared TiO_2/AC using titanium(IV) isopropoxide as a titania precursor.	33
9	The TGA curve of as-prepared TiO_2/AC using titanium(IV) n-butoxide as a titania precursor.	34
10	Expected product from the hydrolysis reaction of (a) titanium(IV) isopropoxide and (b) titanium(IV) n-butoxide.	35
11	The XRD patterns of the as-prepared TiO_2/AC using titanium(IV) isopropoxide as a titania precursor with various calcination temperatures.	36
12	The XRD patterns of as-prepared TiO_2/AC using titanium(IV) n-butoxide as a titania precursor with various calcination temperatures.	37
13	The XRD patterns of as-prepared TiO_2/AC using titanium(IV) isopropoxide as a titania precursor at various calcination temperatures.	38
14	The XRD patterns of as-prepared TiO_2/AC using titanium(IV) n-butoxide as a titania precursor at various calcination temperatures.	39
15	The XRD patterns of prepared-TiO_2 using titanium(IV) isopropoxide as a titania precursor at various calcination temperatures.	40

Copyright by Kasetsart University All rights reserved

LIST OF FIGURES (Continued)

Figure		Page
16	Raman spectra of TiO_2/AC using titanium(IV) isopropoxide as a titania precursor with different calcination temperatures.	43
17	Raman spectra of TiO_2/AC using titanium(IV) n-butoxide as a titania precursor with different calcination temperatures.	43
18	Raman spectra of prepared-TiO_2 using titanium(IV) isopropoxide as a titania precursor with different calcination temperatures.	44
19	SEM image and mapping images of TiO_2/AC using titanium(IV) isopropoxide as a titania precursor calcined at 400ºC.	45
20	SEM image and mapping images of TiO_2/AC using titanium(IV) isopropoxide as a titania precursor calcined at 400ºC.	46
21	TEM image of TiO_2/AC using titanium(IV) isopropoxide as a titania precursor calcined at 400ºC	47
22	TEM image of TiO_2/AC using titanium(IV) n-butoxide as a titania precursor calcined at 400ºC	48
23	The Langmuir isotherm of phenol onto activated carbon (AC).	49
24	The Langmuir isotherm of phenol onto activated carbon calcined at 400ºC (AC-400).	50
25	The Langmuir isotherm of phenol onto TiO_2/AC using titanium(IV) isopropoxide as a precursor.	50
26	The Langmuir isotherm of phenol onto TiO_2/AC using titanium(IV) n-butoxide as a precursor.	51
27	Calibration curve of standard phenol.	54
28	The removal of phenol from 200 ml of 100 ppm phenol solution by 0.1 g, 0.2 g, 0.3 g and 0.4 g of TiO_2/AC using titanium(IV) isopropoxide as precursor.	55
29	The removal of phenol from 200 ml of 100 ppm phenol solution by 0.4 g of prepared-TiO_2.	57

Copyright by Kasetsart University All rights reserved

LIST OF FIGURES (Continued)

Figure		Page
30	The removal of phenol from 200 ml of 100 ppm phenol solution by 0.4 g of P25 TiO_2.	57
31	The removal of phenol from 200 ml of 100 ppm phenol solution by 0.4 g of AC.	58
32	The removal of phenol from 200 ml of 100 ppm phenol solution by 0.4 g of TiO_2/AC.	58
33	The removal of phenol from 200 ml of 100 ppm phenol solution by 0.4 g of AC-400, prepared-TiO_2, P25 TiO_2 and TiO_2/AC calcined at 400ºC.	59
34	The relation between $\ln C_o/C$ and time (h) of photodegradation reaction of phenol from 200 ml of 100 ppm phenol solution by 0.4g prepared-TiO_2.	60
35	The relation between $\ln C_o/C$ and time (h) of photodegradation reaction of phenol from 200 ml of 100 ppm phenol solution by 0.4g P25 TiO_2.	60
36	The relation between $\ln C_o/C$ and time (h) of photodegradation reaction of phenol from 200 ml of 100 ppm phenol solution by 0.4g TiO_2/AC.	61
37	The removal of phenol from 200 ml of 100 ppm phenol using 0.4 g of prepared-TiO_2 without calcination.	62
38	The removal of phenol from 200 ml of 100 ppm phenol by 0.4 g of prepared-TiO_2 calcined at 300ºC.	63
39	The removal of phenol from 200 ml of 100 ppm phenol by 0.4 g of prepared-TiO_2 calcined at 400ºC.	63
40	The removal of phenol from 200 ml of 100 ppm phenol by 0.4 g of prepared-TiO_2 calcined at 500ºC.	64
41	The removal of phenol from 200 ml of 100 ppm phenol by 0.4 g of prepared-TiO_2 without calcination and calcined at 300-500ºC.	64

Copyright by Kasetsart University All rights reserved

LIST OF FIGURES (Continued)

Figure		Page
42	The XRD patterns of prepared-TiO_2 using titanium(IV) isopropoxide as titania precursor at various calcination temperatures.	65
43	The relation between lnC_o/C and time (h) of photodegradation reaction of phenol from 200 ml of 100 ppm phenol solution by 0.4g of prepared-TiO_2 without calcination.	66
44	The relation between lnC_o/C and time (h) of photodegradation reaction of phenol from 200 ml of 100 ppm phenol solution by 0.4g of prepared-TiO_2 calcined at 300ºC.	66
45	The relation between lnC_o/C and time (h) of photodegradation reaction of phenol from 200 ml of 100 ppm phenol solution by 0.4g of prepared-TiO_2 calcined at 400ºC.	67
46	The relation between lnC_o/C and time (h) of photodegradation reaction of phenol from 200 ml of 100 ppm phenol solution by 0.4g of prepared-TiO_2 calcined at 500ºC.	67
47	The removal of phenol from 200 ml of 100 ppm phenol by 0.4 g of TiO_2/AC using titanium(IV) isopropoxide without calcination.	69
48	The removal of phenol from 200 ml of 100 ppm phenol by 0.4 g of TiO_2/AC using titanium(IV) isopropoxide calcined at 300ºC.	69
49	The removal of phenol from 200 ml of 100 ppm phenol by 0.4 g of TiO_2/AC using titanium(IV) isopropoxide calcined at 400ºC.	70
50	The removal of phenol from 200 ml of 100 ppm phenol by 0.4 g of TiO_2/AC using titanium(IV) isopropoxide calcined at 500ºC.	70
51	The removal of phenol from 200 ml of 100 ppm phenol by 0.4 g of TiO_2/AC using titanium(IV) isopropoxide without calcination and with calcined at various temperatures.	71
52	The relation between lnC_o/C and time (h) of photodegradation reaction of phenol from 200 ml of 100 ppm phenol solution by TiO_2/AC using titanium(IV) isopropoxide without calcination.	72

Copyright by Kasetsart University All rights reserved

LIST OF FIGURES (Continued)

Figure		Page
53	The relation between lnC_o/C and time (h) of photodegradation reaction of phenol from 200 ml of 100 ppm phenol solution by TiO_2/AC using titanium(IV) isopropoxide calcined at 300ºC.	72
54	The relation between lnC_o/C and time (h) of photodegradation reaction of phenol from 200 ml of 100 ppm phenol solution by TiO_2/AC using titanium(IV) isopropoxide calcined at 400ºC.	73
55	The relation between lnC_o/C and time (h) of photodegradation reaction of phenol from 200 ml of 100 ppm phenol solution by TiO_2/AC using titanium(IV) isopropoxide calcined at 500ºC.	73
56	The removal of phenol from 200 ml of 100 ppm phenol by 0.4 g of TiO_2/AC using titanium(IV) n-butoxide without calcination.	75
57	The removal of phenol from 200 ml of 100 ppm phenol by 0.4 g of TiO_2/AC using titanium(IV) n-butoxide calcined at 300ºC.	75
58	The removal of phenol from 200 ml of 100 ppm phenol by 0.4 g of TiO_2/AC using titanium(IV) n-butoxide calcined at 400ºC.	76
59	The removal of phenol from 200 ml of 100 ppm phenol by 0.4 g of TiO_2/AC using titanium(IV) n-butoxide calcined at 500ºC.	76
60	The removal of phenol from 200 ml of 100 ppm phenol by 0.4 g of TiO_2/AC using titanium(IV) n-butoxide without calcination and with calcined at various temperatures.	77
61	The relation between lnC_o/C and time (h) of photodegradation reaction of phenol from 200 ml of 100 ppm phenol solution by TiO_2/AC using titanium(IV) n-butoxide without calcination.	78
62	The relation between lnC_o/C and time (h) of photodegradation reaction of phenol from 200 ml of 100 ppm phenol solution by TiO_2/AC using titanium(IV) n-butoxide calcined at 300ºC.	78

Copyright by Kasetsart University All rights reserved

LIST OF FIGURES (Continued)

Figure		Page
63	The relation between lnC_o/C and time (h) of photodegradation reaction of phenol from 200 ml of 100 ppm phenol solution by TiO_2/AC using titanium(IV) n-butoxide calcined at 400ºC.	79
64	The relation between lnC_o/C and time (h) of photodegradation reaction of phenol from 200 ml of 100 ppm phenol solution by TiO_2/AC using titanium(IV) n-butoxide calcined at 500ºC.	79
65	The removal of phenol from 200 ml of 100 ppm phenol by 0.4 g of TiO_2/AC calcined 400ºC using titanium(IV) isopropoxide and titanium(IV) n-butoxide compared to P25 TiO_2.	81
66	Calibration curve of standard AO7 at concentration from 5 to 25 ppm adjusted to pH 4.0 .	83
67	Calibration curve of standard AO7 at concentration from 5 to 25 ppm adjusted to pH 7.0 .	84
68	Calibration curve of standard AO7 at concentration from 5 to 25 ppm adjusted to pH 10.0 .	84
69	The removal of AO7 from 200 ml of 100 ppm AO7 solution by 0.2 g of TiO_2/AC at pH 4.0.	85
70	The removal of AO7 from 200 ml of 100 ppm AO7 solution by 0.2 g of TiO_2/AC at pH 7.0.	86
71	The removal of AO7 from 200 ml of 100 ppm AO7 solution by 0.2 g of TiO_2/AC at pH 10.0.	86
72	The removal of AO7 from 200 ml of 100 ppm AO7 solution by 0.2 g of TiO_2/AC calcined at 400ºC at different pH.	87
73	The relation between lnC_o/C and time (h) of photodegradation reaction of AO7 from 200 ml of 100 ppm AO7 solution at pH 4.0 by 0.2g TiO_2/AC.	88

Copyright by Kasetsart University All rights reserved

LIST OF FIGURES (Continued)

Figure		Page
74	The relation between lnC_o/C and time (h) of photodegradation reaction of AO7 from 200 ml of 100 ppm AO7 solution at pH 7.0 by 0.2g TiO_2/AC.	88
75	The relation between lnC_o/C and time (h) of photodegradation reaction of AO7 from 200 ml of 100 ppm AO7 solution at pH 10.0 by 0.2g TiO_2/AC.	89
76	The removal of AO7 from 200 ml of 100 ppm AO7 solution by 0.2 g of TiO_2/AC at pH 4.0.	91
77	The removal of AO7 from 200 ml of 100 ppm AO7 solution by 0.2 g of TiO_2/AC at pH 7.0.	92
78	The removal of AO7 from 200 ml of 100 ppm AO7 solution by 0.2 g of TiO_2/AC at pH 10.0.	92
79	The removal of AO7 from 200 ml of 100 ppm AO7 solution by 0.2 g of TiO_2/AC calcined at 400ºC at different pH.	93
80	The relation between lnC_o/C and time (h) of photodegradation reaction of AO7 from 200 ml of 100 ppm AO7 solution at pH 4.0 by 0.2g TiO_2/AC.	94
81	The relation between lnC_o/C and time (h) of photodegradation reaction of AO7 from 200 ml of 100 ppm AO7 solution at pH 7.0 by 0.2g TiO_2/AC.	94
82	The relation between lnC_o/C and time (h) of photodegradation reaction of AO7 from 200 ml of 100 ppm AO7 solution at pH 10.0 by 0.2g TiO_2/AC.	95
83	Effect of acidic and basic solution to surface of titania.	97
84	Mechanism of titania to generate hydroxyl radical ($^{\bullet}OH$) from hydroxide ion in basis solution	98

Copyright by Kasetsart University All rights reserved

LIST OF FIGURES (Continued)

Figure		Page
85	Possibly proposed mechanism of photodegradation of phenol by oxidation reaction of radical species.	99
86	Possibly proposed mechanism of photodegradation of AO7 by oxidation reaction of radical species.	101

Appendix Figure

A1	The fitting peak of P25 TiO_2 with Lorentzian function.	116

Copyright by Kasetsart University All rights reserved

LIST OF ABBREVIATIONS

M.P.	=	Melting point
B.P.	=	Boiling point
TGA	=	Thermal Gravimetric Analysis
XRD	=	X-ray Diffraction
JCPDS	=	Joint Committee on Powder Diffraction Standard
BET	=	Brunauer-Emmett-Teller
SEM	=	Scanning Electron Microscopy
TEM	=	Transmission Electron Microscopy
FTIR	=	Fourier-Transform Infrared spectroscopy
AO7	=	Acid Orange 7
ChV	=	Chronic toxicity Value
LC_{50}	=	Median Lethal Concentration

Copyright by Kasetsart University All rights reserved

PREPARATION OF TiO_2 SUPPORTED ACTIVATED CARBON FOR TREATMENT OF PHENOL AND ACID ORANGE 7

INTRODUCTION

1. Titanium dioxide (TiO_2)

Titanium dioxide or titania (TiO_2) is naturally discovered in the mineral sources such as ilmenite, rutile, anatase and brookite. Ilmenite ($FeTiO_2$) or titanic iron ore is a grey mineral containing magnetic black iron. It was firstly discovered at Ural Ilmen Mountain (Russia) in 1827 by Kupffer who named it. The majority of the ilmenite mine is used as a raw material for pigment production. The product is titanium dioxide, which is ground into a fine powder and is a highly white substance used as a base in high-quality paint, paper and plastics applications. Rutile is a mineral composed primarily of TiO_2 and found in 1803 by Werner in Spain. It is commonly reddish brown but sometimes yellowish, bluish or violet and naturally contains up to 10% of iron and other impurities as well. The main uses for rutile are the manufacture of refractory ceramic, as a pigment, or for the production of titanium metal. Anatase, earlier called octahedrite, was named by Haüy in 1801. It is always found as small, isolated and sharply developed crystals and a more commonly occurring modification of titanium dioxide. Brookite is a dark brown to greenish black mineral mainly consisting of TiO_2. Brookite occurs rarely compared to the anatase and rutile forms of titanium dioxide. However, it was firstly found by A. Levy in 1825 at Snowen (England)(Carp *et al.*, 2004).

1.1 Crystal structures of titanium dioxide

Titanium dioxide has three crystal structures, anatase (tetragonal), rutile (tetragonal) and brookite (orthorhombic) found in nature (Figure 1). Although their structures are similarly based on octahedrals (TiO_6), they still differ from one another by the distortion of each octahedral and by the assembly patterns of the octahedral chains. Anatase is built up from octahedrals which are mainly connected by their

Copyright by Kasetsart University All rights reserved

verticals. Octahedral structures in rutile are mostly connected by the edges. Both vertical and edge connections are found in the octahedral structure of the brookite form. Although both anatase and rutile are the same tetragonal system, anatase crystal has longer vertical axis than rutile. Meanwhile, brookite crystallizes in the orthorhombic system.

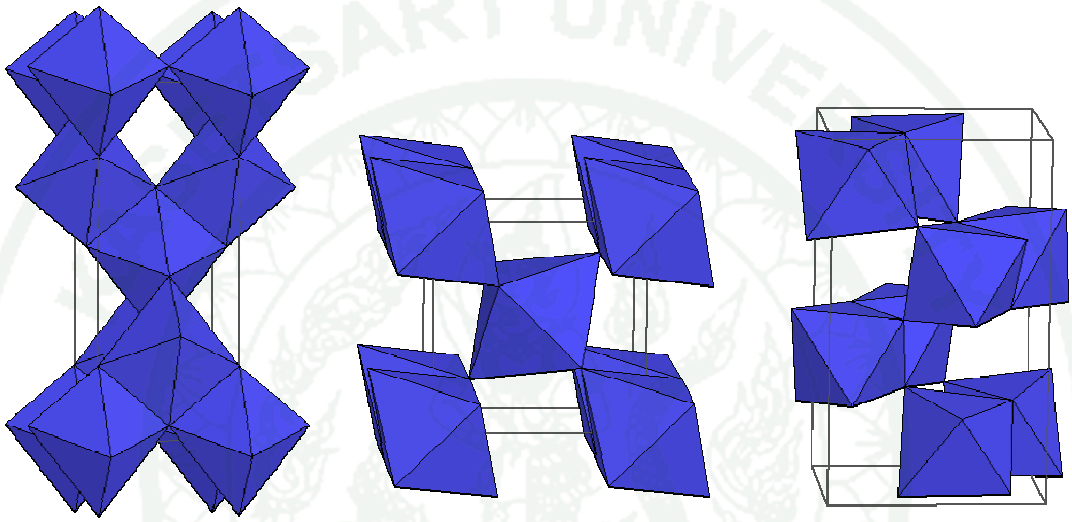

Figure 1 Crystal structures of TiO_2 (a) anatase, (b) rutile and (c) brookite.

Source: Carp *et al.* (2004)

Rutile phase is the most stable phase of titanium dioxide while anatase and brookite are metastable phases. The metastable structures are almost as stable as rutile at normal pressure and temperature because of small difference in the Gibbs free energy (4-20 kJ/mol) between the three phases (Carp *et al.*, 2004). Regarding the band gap energy, 3.26 eV (~380 nm) is the band gap energy of anatase and in rutile 3.05 eV (~406 nm) is its energy (Carp *et al.*, 2004). Other crystal properties of all the three forms of TiO_2 are shown in Table 1.

Copyright by Kasetsart University All rights reserved

Table 1 Crystal properties of the three main polymorphs of TiO_2.

Crystal structure	Crystal	Density (kg/m^3)	Band gap (eV)	Lattice constants (nm)		
				a	b	c
Anatase	Tetragonal	3830	3.26	0.3733	0.3733	0.9370
Rutile	Tetragonal	4240	3.05	0.4584	0.4584	0.2953
Brookite	Orthorhombic	4170	-	0.5436	0.9166	0.5134

Source: Carp *et al.* (2004)

Copyright by Kasetsart University All rights reserved

1.2 Applications of titanium dioxide

At present, titanium dioxide (TiO_2) has been widely used in worldwide applications such as photovoltaic cells, photocatalysis, environmental purification, photoinduced superhydrophilicity as well as an ingredient in a pigment. Because of its chemical stability, non toxicity, low cost and other advantageous properties. With respect to photocatalysis, TiO_2 is close to being an ideal photocatalyst due to its properties as mentioned above. Generally, both anatase and rutile are used as photocatalysts and some research stated that anatase had higher photoactivity than rutile (Yates *et al.*, 1995). There are also other studies which claimed that mixture phases between anatase and rutile provided higher efficiency than the pure phase (Muggli *et al.*, 2001). In these different results, they should rely on the intervening effect of several factors such as specific surface areas, crystallite sizes, pore size distribution as well as preparation methods. In photocatalytic reactions, TiO_2 can degrade not only organic compounds such as hydrocarbons, chlorinated compounds and nitrogen- or sulfur-containing compounds but also inorganic compounds such as nitrogen oxide species (NO_x). Overall, photocatalytic reactions can be generally summarized as shown in Figure 2. Initially, $e^-_{c.b.}$ and $h^+_{v.b.}$ are generated by using photon energy (hν) which has equal or higher energy than band gap energy of TiO_2. Some electrons from valance band ($e^-_{c.b.}$) are excited into the conduction band while holes ($h^+_{v.b.}$) still stay in the valence band and then both of them will move to the TiO_2 surface with a view to reducing or oxidizing. In contrary, $e^-_{c.b.}$ and $h^+_{v.b.}$ are able to recombine again, this can occur at the bulk and at the surface. The recombination process is usually considered as the deactivation process in photocatalytic reaction.

In most studies about photocatalysts, oxygen (O_2) plays a vital role in the primary electron acceptor. In this step, $e^-_{c.b.}$ will transfer to oxygen and further generate H_2O_2 and $^\bullet OH$. Meanwhile, $h^+_{v.b.}$ reacts with adsorbed water molecules on the surface or surface titanol group (>TiOH) and finally hydroxyl radicals are also formed. H_2O_2 contributes to the degradation pathway by acting as an electron acceptor or as a direct source of $^\bullet OH$ due to homolytic scission. All of these reactions are summarized and displayed in Figure 3.

Copyright by Kasetsart University All rights reserved

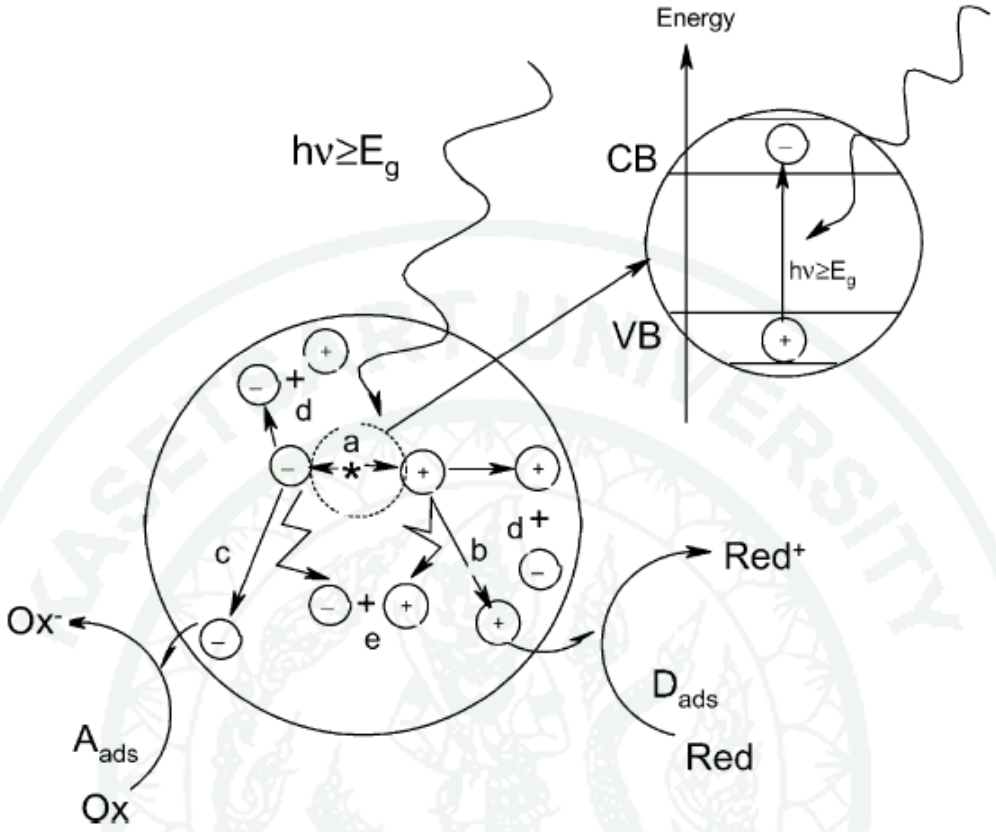

Figure 2 Principal processes occurring on the TiO_2 particles; (a) $e^-_{c.b.} + h^+_{v.b.}$ generation, (b) oxidation of donors (D), (c) reduction of acceptors (A), (d) and (e) $e^-_{c.b.} / h^+_{v.b.}$ recombination at surface and in bulk, respectively.

Source: Mills *et al.* (1997)

Copyright by Kasetsart University All rights reserved

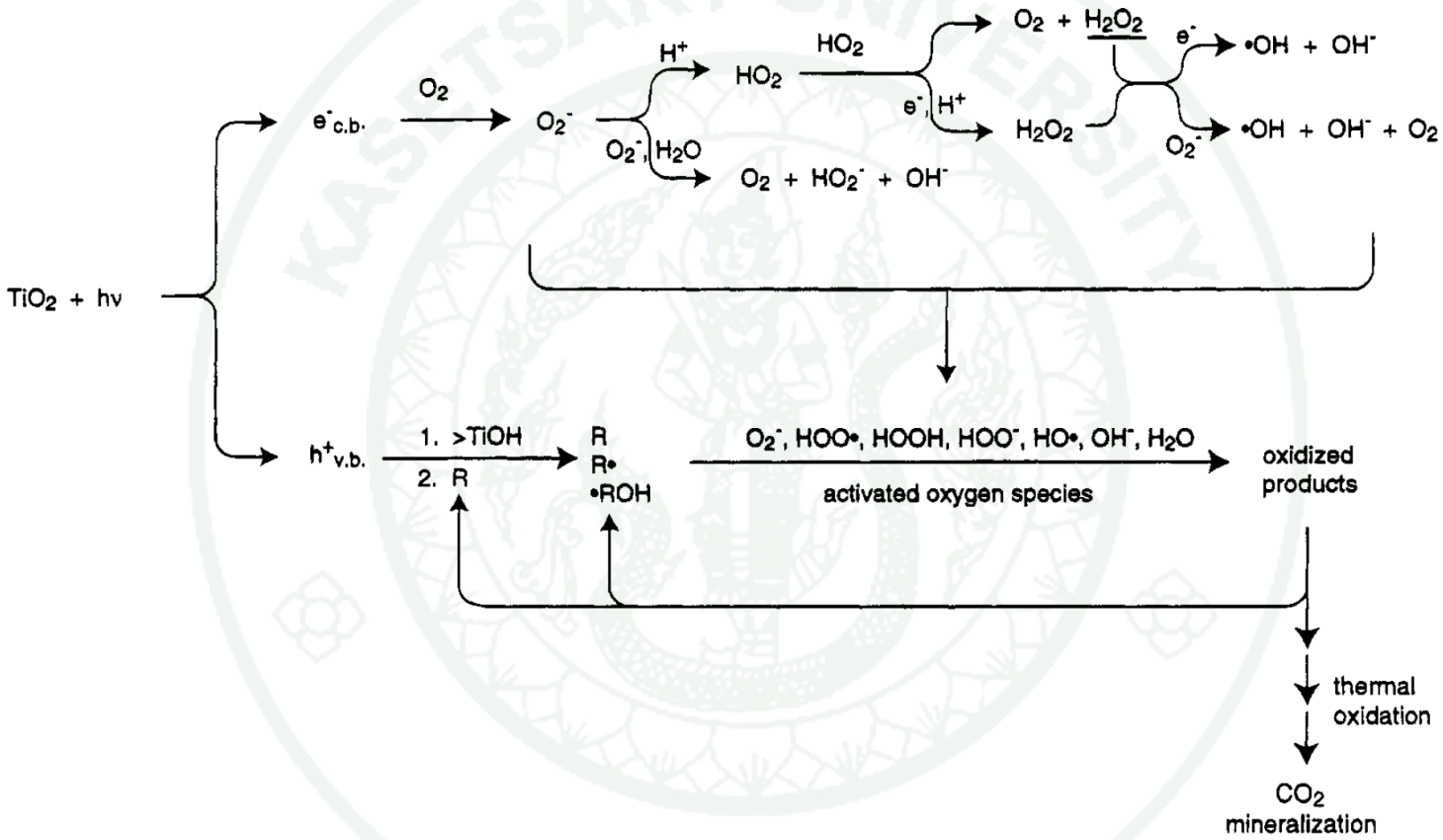

Figure 3 Secondary reactions with activated oxygen species in the photoelectronchemical mechanism.

Source: Hoffman *et al.* (1995)

Copyright by Kasetsart University All rights reserved

1.3 Improving of photocatalytic reaction of titanium dioxide

Recently, the immobilization of TiO_2 onto supporting material has been investigated for photocatalytic activity. A general procedure consists of the fixation of previously prepared titania powder using various techniques such as: electrophoretic deposition, spray coating and immobilization in polymer matrix. Another route is coating of the supporter by in situ catalyst generation, as a result of a combined physical and chemical transformation like chemical vaporization and sol-gel synthesis. Frequently, the fixation of TiO_2 on solid supporter reduces its photocatalytic efficiency. This decline in activity has been related to reduction of active surface, mass-transfer limitation and presence of some cationic impurity (such as Si^{4+}, Na^{+}, Cr^{3+}, Fe^{3+}), which increase the $e^{-}_{c.b.}$ / $h^{+}_{v.b.}$ recombination rate.

Many researchers have studied the hybrid photocatalysts that combine between TiO_2 and adsorbent for investigating the synergistic effect (Carp *et al.*, 2004). Even though the adsorbents such as silica, alumina, zeolite and activated carbon are used in previous study, the activated carbon is a strong adsorbent, has high surface area and high effective adsorption. The main purposes focused on supported TiO_2 are developed in order to:

-immobilize the TiO_2 photocatalyst
-increase the illuminated specific area of the photocatalyst
-increase the adsorption capacity and surface area of the photocatalyst
-influence the selectivity of the photocatalytic reaction

1.4 Preparation method

There are diverse methods to effectively synthesize powder, thin-film and membrane TiO_2 or modified TiO_2, namely co-precipitation, solvothermal, sol-gel, microemulsion, electrochemical, chemical/physical vapor deposition, ion-implantation and ball milling methods. Focusing on the sol-gel method, most of recent

Copyright by Kasetsart University All rights reserved

works usually use this method. It has many advantages over other methods in terms of purity, homogeneity and flexibility in adding activated carbon, ratio control, ease of processing and control over the composition. Generally, there are two known types of titania precursors, non-alkoxide and alkoxide, utilized in the sol-gel method. The former makes use of inorganic salts (such as chlorides, acetylacetonate, etc.), which requires the removal of the inorganic anions after preparation. In other words, the alkoxide route uses metal alkoxides as a starting material. This route has highly been used for preparing metal oxide because metal alkoxide precursors are commercially available in high purity and are easily handled at ambient temperature. Concerning preparation, the sol-gel method is composed of four key steps as follows;

a. Gel formation

This step focuses on gel formation, which is a diphasic material with a solid encapsulating solvent. Before gel formation occurs, a starting material will be hydrolyzed and partially condensed in order to form sol, which is liquid suspension in solid particles. After that, further condensation in three-dimension network is conducive to gel formation. In case of metal alkoxide precursors, all involving reactions are shown below.

Hydrolysis reaction: $\text{Ti-OR} + \text{H}_2\text{O} \longrightarrow \text{Ti-OH} + \text{R-OH}$

Condensation reaction: $\text{Ti-OH} + \text{XO-M} \longrightarrow \text{Ti-O-Ti} + \text{X-OH}$

where X is either H or R (an alkyl group).

b. Aging

To further complete the reaction, gel is left to continue constructing its more networks causing stronger cross-linkage. Moreover, some solvent molecules are expelled by the extensive condensation of gel. This step mainly depends on aging time, temperature as well as pH.

Copyright by Kasetsart University All rights reserved

c. Drying

In order to remove organic solvent or hydrolyzed molecules, metal oxide needs to be heated at the sufficient temperature to dispose them. Additionally, this step is involved in the capillary pressure that has an effect on the pore size of metal oxide. Therefore, many factors, such as heating rate, pressure rate and time, are taken into serious consideration with a view to controlling the pore structure of metal oxide.

d. Calcination

This final step emphasizes on crystallization of metal oxide. Calcination is used in order to remove the dormant organic part and to crystallize phase of metal oxide. However, it will inevitably cause a decrease in surface area, loss of surface hydroxyl groups and even phase transformation.

2. Phenol

Phenol is categorized as one of the aromatic compounds, in which a hydroxyl group is attached directly to a benzene ring as illustrated in Table 2. Pure phenol is a white crystalline solid, smelling of disinfectant. The crystals are often rather wet and discolored. Phenol is slightly acidic and has a limited solubility in water. Its molecule is difficult to lose the H^+ ion from the hydroxyl group, resulting in the highly water-soluble phenoxide anion $C_6H_5O^-$. Additionally, concerning natural contamination, high concentration of phenol and its derivatives are found in nature. They contaminate in wastewater derived from different chemical industries such as resin manufacturing, petrochemical, oil-refineries, paper making as well as iron smelting. However, phenol is highly corrosive and moderately toxic. It causes many effects on humans by burning the skin and other tissues that it comes into contact with. This gives severe skin burning and if inhaled serious internal corrosion. Thus, current research aims to study how to dispose this toxic compound widespread in nature.

Copyright by Kasetsart University All rights reserved

3. Acid orange 7

Acid orange 7 (AO7), the synthetic dyes, is one of the most common azo dye stuffs. Generally, azo dyes are used to color many different products such as textile, paper, cosmetics, tanned lather and drugs. It represents more than 50% of the all dyes used in textile industries (Esther *et al.*, 2004). Those are characterized by the presence of azo groups (–N=N–) in association with aromatic systems and auxochromes (–OH, $–SO_3$, etc.). Due to their large degree of aromaticity, most azo dyes are known to be largely non biodegradable in aerobic conditions and can be changed to more hazardous intermediates in anaerobic conditions (Hammami *et al.*, 2008). An acid orange 7 (Table 2) is representative of mono-azo dye. It is soluble and stable in water and has been reported is to be concentration is carcinogenic to human even low concentration.

Copyright by Kasetsart University All rights reserved

Table 2. The molecular structure and general properties of phenol and acid orange 7.

Structure	Properties			
	Molecular formula	Molecular weight (g/mol)	M.P. (ºC)	B.P. (ºC)
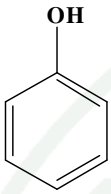	C_6H_5OH	94.11	40.5	181.7
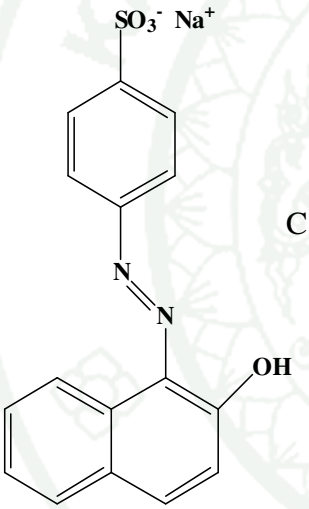	$C_{16}H_{11}SO_4N_2Na$	350.32	164	-

Source: Guo *et al.*(2010)

Copyright by Kasetsart University All rights reserved

OBJECTIVES

This work aims to study the preparation with sol-gel, characterization with various techniques and photocatalytic applications of TiO_2 supported activated carbon (TiO_2/AC). There are three main objectives that this work focuses on;

1. To study the effect of titania precursors on the as-prepared TiO_2/AC in terms of its phase transformation, crystallinity, surface morphology as well as the adsorption activity.

2. To study the effect of calcination temperature between 300 and 500ºC on the phase transformation, crystallinity as well as surface morphology compared to prepared-TiO_2 and P25 TiO_2.

3. To study the removal of phenol and AO7 using the TiO_2/AC due to on both adsorption and photodegradation under UV light. In addition, adsorption isotherm, the %removal and rate constants of TiO_2/AC are compared to prepared-TiO_2 and P25 TiO_2.

4. To study the recyclability of the TiO_2/AC for removal of phenol and AO7.

Copyright by Kasetsart University All rights reserved

LITERATURE REVIEW

This section will give a review of works by some previous researchers on the preparation of titanium dioxide supported activated carbon (TiO_2/AC) by various methods to degrade pollutants. The recent studies on photocatalytic activity of TiO_2/AC on degradation of various pollutants are reviewed as follows.

Arana *et al.* (2003) studied the photoreactivity of titanium dioxide supported activated carbon (TiO_2/AC) on the degradation of phenol by Fourier-transform infrared spectroscopy (FTIR), total organic carbon measurement (TOC) and UV-Vis spectroscopy. The experiment was performed by suspended TiO_2 (Degussa-P25, Merck) and AC (ref. 102186, Merck) in solution of phenol, 4-aminophenol and salicylic acid. The photoactivity of TiO_2/AC to decomposition of phenol, 4-aminophenol and salicylic acid were observed by FTIR technique. They observed strong interaction of phenol, 4-aminophenol and salicylic acid with surface of AC containing catalyst which improved the TiO_2 catalytic efficiency. The optimal degradation condition was 0.5 g of TiO_2/AC and 100 mg/l (250 ml) of phenol (4-aminophenol or salicylic acid) solution irradiated by UV-lamp for 4 h.

Colon *et al.* (2003) studied photocatalytic activity of TiO_2 supported activated carbon. The catalyst was prepared by sol-gel process and through sulfate pretreatment (TiO_2/ACS). The catalyst was characterized by X-ray powder diffractometry (XRD), scanning electron microscopy (SEM), Brunauer-Emmett-Teller surface area measurement (BET), X-ray photoelectron spectroscopy (XPS) and thermal gravimetric and differential thermal analysis (TG-DTA). The synergistic effect of AC and sulfate in catalyst could increase surface area and stabilize anatase phase of TiO_2, which improved the photodegradation efficiency of TiO_2/ACS. The optimal degradation condition was 0.45 g of TiO_2/ACS and 50 mg/l (450 ml) of phenol solution for 2 h.

Copyright by Kasetsart University. All rights reserved

Tryba *et al.* (2003) prepared titanium dioxide supported activated carbon (CWZ14, Gryfskand) (TiO_2/AC) through hydrolytic precipitation from tetraisopropyl orthotitanate (97%, Aldrich) and followed by heat treatment at 650-900^oC for 1 h under nitrogen atmosphere. The catalyst was characterized by Brunauer-Emmett-Teller surface area measurement (BET), X-ray powder diffractometry and thermal gravimetric analysis (TGA). The removal of phenol from its aqueous solution under UV-irradiation was measured on TiO_2/AC. Surface area of TiO_2/AC decreased drastically in comparison with AC but the efficiency of phenol removal irradiate by UV-lamps was high. The sample heated at 900^oC, which consisted mainly of rutile phase, showed the highest total removal of phenol. The optimal degradation condition was 0.3 g of TiO_2/AC and 50 mg/l (500 ml) of phenol solution for 6 h.

Fu *et al.* (2004) prepared photocatalyst, titanium dioxide supported activated carbon fiber (Zichuan Carbon Fibers, China) (TiO_2/ACF) by a molecular adsorption–deposition (MAD) method based on titanium tetrachloride followed by calcination in a stream of Ar gas. The catalyst was characterized by Brunauer-Emmett-Teller surface area measurement (BET), X-ray powder diffractometry, thermal gravimetric analysis (TGA), scanning electron microscopy (SEM) and X-ray photoelectron spectroscopy. From SEM observation, TiO_2 was deposited on almost each carbon fiber with a coating thickness of about 100 nm. When calcination temperature raised up to 900◦C, it showed anatase phase of TiO_2. The TiO_2/ACF showed high photocatalytic activity in photodegradation of highly concentrated methylene blue solutions.

Carpio *et al.* (2005) prepared titanium dioxide supported activated carbon (Darco G-60, Aldrich) (TiO_2/AC) in two forms, as powder and pellet by sol-gel process based on titanium isopropoxide (97%, Aldrich) then thermal treatment at 325^oC for 5 h, considering the thermal stability of AC. Both forms of TiO_2/AC were characterized by X-ray fluorescence spectroscopy (XRF), scanning electron microscopy with energy dispersive X-ray microanalysis (SEM-EDX) and Brunauer-Emmett-Teller surface area measurement (BET). Photoactivity of phenol degradation under UV-lamp showed that 2.13×10^{-4} M of phenol can be removed by using this

Copyright by Kasetsart University All rights reserved

method. Powder-TiO_2/AC showed higher photodegradation efficiency than pellet-TiO_2/AC but recovery of powder-TiO_2/AC from solution was more difficult.

Li *et al.* (2005) prepared titanium dioxide supported activated carbon (TiO_2/AC) by hydrolysis precipitation method from tetrabutyl orthotitanate (99.9%, Aldrich) and use it to degrade methyl orange. TiO_2/AC was characterized by Raman spectroscopy, X-ray photoelectron spectroscopy (XPS) and scanning electron microscopy (SEM). It was observed that TiO_2/AC had higher photodegradation efficiency than pure TiO_2 powder, as well as a mixture of TiO_2 powder with activated carbon. The optimum degradation condition was 0.5 g of TiO_2/AC and 12×10^{-3} M (250 ml) of methyl orange at pH 6 with 40 W of UV-lamps for methyl orange photodegradation. The photodegradation efficiency of TiO_2/AC decreased from 97.4% to 14.2% after 20 trials.

Yuan *et al.* (2005) prepared the TiO_2 supported activated carbon fibers (TiO_2/ACF), both solids were linked by epoxy resin, followed by calcination at various temperatures in N_2 atmosphere. The catalyst was characterized by Brunauer-Emmett-Teller surface area measurement (BET), X-ray powder diffractometry, thermal gravimetric analysis (TGA), scanning electron microscopy (SEM) and transmission electron microscopy (TEM). When increased calcination temperature, epoxy resin on surface of TiO_2 was decomposed. The sample calcined at 460◦C exhibited the highest photocatalytic activity. The optimal degradation condition was 0.35 g of TiO_2/AC and 85 mg/l (350 ml) of methylene blue solution.

Codero (2007) studied the influence of inorganic compounds employed in preparation of TiO_2 supported activated carbons (TiO_2/AC). Activation of activated carbon, impregnated with $ZnCl_2$, H_3PO_4 and KOH were performed under N_2 flow at 450ºC by 1 h. The catalyst was characterized by Brunauer-Emmett-Teller surface area measurement (BET), Fourier transform infrared spectroscopy (FTIR) and scanning electron microscopy (SEM). The photodegradation process was performed by adding of 10 mg of AC and 15 mg of TiO_2-P25 under stirring in solution of 100mg/l (25 ml) 4-chlorophenol for 80 min. From FTIR spectra, the TiO_2-AC which was impregnated

Copyright by Kasetsart University All rights reserved

by 5% (w/w) $ZnCl_2$ (TiO_2/AC- $ZnCl_2$-5%) showed strong interaction with 4-chlorophenol. Impregnation of 5% $ZnCl_2$ significantly improved the photodegradation efficiency of TiO_2/AC- $ZnCl_2$-5%.

Li *et al.* (2007) developed titanium dioxide supported activated carbon (TiO_2/AC) that was prepared by sol-gel method from tetrabutyl orthotitanate (99.9%, Aldrich) as a precursor. The AC performed as a barrier which controlled the growth of TiO_2 particles. The catalyst was characterized by X-ray powder diffractometry (XRD), scanning electron microscopy (SEM), Brunauer-Emmett-Teller surface area measurement (BET), X-ray photoelectron spectroscopy (XPS) and thermal gravimetric analysis. The optimal condition was 20 mg/l (200 ml) of methylene blue (MB) and 0.5 g of TiO_2/AC for 3 h. The efficiency of MB degradation of TiO_2/AC and TiO_2 powder were 98% and 61%, respectively.

Matos *et al.* (2007) studied the influence of catalyst TiO_2/AC which was prepared from titanium dioxide (Degussa-P25, Merck) and activated carbon (ref. 102186, Merck) on the removal of phenol in aqueous solution on consecutive run. The catalyst was prepared by direct mixing of AC (0.01 g) and TiO_2 (0.05 g), and then added 1×10^{-3} M of phenol solution (20 ml) under stirring for 15 h. The catalyst was characterized by Fourier transform infrared spectroscopy (FTIR) and X-ray powder diffractometry (XRD). The photodegradation efficiency was determined by the numbers of photocatalytic runs. The TiO_2/AC showed higher efficiency on the consecutive runs than TiO_2 or AC alone.

Subramani (2007) prepared titanium dioxide supported activated carbon (TiO_2/AC) by impregnating anatase-TiO_2 (M/s, Aldrich) onto the activated carbon (M/s, Loba Chemie, India) surface through hydrothermal route. The content of AC was 1.0 g and varied the content of TiO_2 from 0.1 to 0.5 g. The catalyst was characterized by Brunauer-Emmett-Teller surface area measurement (BET), X-ray powder diffractometry and scanning electron microscopy (SEM). XRD patterns indicated that anatase phase of TiO_2 was deposited on AC. The dispersion of TiO_2

Copyright by Kasetsart University All rights reserved

particles on the carbon surface was confirmed by SEM. The appropriate content of TiO_2 was 0.2 g, which exhibited the highest surface area.

Wang *et al.* (2007) prepared titanium dioxide on activated carbon (Darco G-60, Aldrich) (TiO_2/AC) by acid catalyzed sol-gel method, using titanium isopropoxide (97%, Aldrich) as a precursor. The catalyst was calcined at various temperatures. The catalyst was characterized by Brunauer-Emmett-Teller surface area measurement (BET), thermal gravimetric analysis (TGA), X-ray powder diffractometry (XRD), scanning electron microscopy (SEM) and UV-Visible spectrophotometry. Calcination temperature and content of AC affected to photodegradation efficiency. The optimal calcination temperature was 450^{o}C and content of AC was 20% by weight of TiO_2/AC. Photocatalytic efficiency on the degradation of Chromotrope 2R (C2R) was observed by UV-Vis spectrophotometry. The optimal condition was 50 mg/l (800 ml) of C2R solution and 0.8 g of TiO_2/AC irradiated by UV-lamp for 2 h.

Li *et al.* (2008) prepared TiO_2 supported carbon (TiO_2/C) by sol–gel process. The key factors affecting the methylene blue (MB) oxidation efficiency were investigated, including the initial concentration of MB, the pH value and the catalysts concentration. Total organic carbon (TOC) analysis indicated complete mineralisation of MB. The results showed that pure TiO_2 and TiO_2 mixed carbon required 580 min and 460 min for complete the photodegradation of MB, while the TiO_2/C required for 320 min. This indicated that the TiO_2/C showed the highest photodegradation efficiency. The optimal condition was a MB concentration of 20 mg/l at pH 6 with catalyst concentration of 2.5 g/l for the fastest rate of MB degradation.

Yanhui (2008) prepared anatase titania nanoparticles at low temperature (75ºC) by hydrolysis of titaniumn-butoxide in acidic condition. The prepared TiO_2 nanoparticles were loaded on activated carbon (TiO_2/AC) in a rotatory evaporator under vacuum, and then the composite photocatalyst was employed for the removal of phenol from water. The optimal condition was 400 ml of 100 mg/l phenol solution and 0.6 g of photocatalyst contained 0.4 g of titania and 0.2 g of AC under UV irradiation. The AC with strong adsorbent activity provided sites for the adsorption of

Copyright by Kasetsart University All rights reserved

phenol, and the adsorbed phenol migrated continuously onto the surface of TiO_2 particles, which were located mainly at the exterior surface of the activated carbon. Some phenol remained adsorbed on the catalyst when no traces of phenol were detected in the water. This adsorbed phenol could be degraded by illuminated titania while maintaining UV irradiation. The photocatalyst was used for six cycles with degraded rate of phenol still higher than 80%.

Zhang *et al.* (2008) prepared TiO_2 supported activated carbon photocatalysts by sol–gel and metal organic chemical vapor deposition (MOCVD) in order to investigate effect of preparation methods on the structure and catalytic performance of TiO_2/AC catalysts. The TiO_2 by MOCVD was deposited on the surface of AC through the heterogeneous reaction, forming a TiO_2/AC hybrid film as evidenced by SEM and N_2 adsorption tests. Photocatalytic activity was performed by degradation of 100 mg/l methyl orange (MO) with flow rate of 1.2 m^3/h and 2.0 g of catalyst for 2 hours. The hybrid TiO_2/AC film could capture the intermediates produced during the degradation of the target pollutant resulting in efficient mineralization. The TiO_2/AC catalysts by MOCVD that is showed in Figure 4 exhibited a Ti-O-C bond in layer of TiO_2+AC, which showed more stability of TiO_2 on AC than sol-gel method.

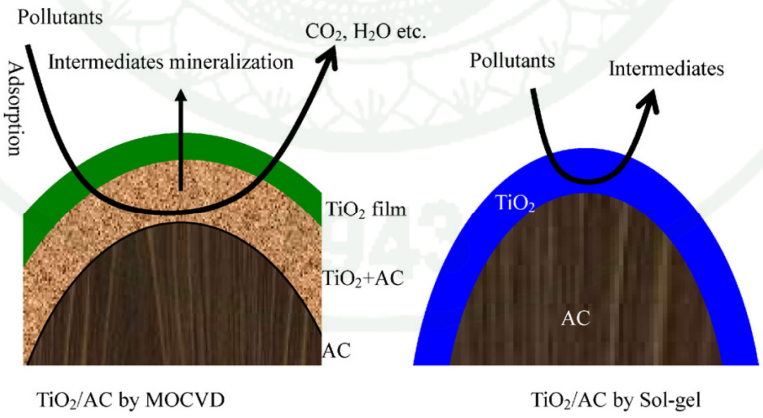

Figure 4 Proposed mechanism of degradation with TiO_2/AC catalysts prepared by MOCVD and sol-gel method.

Source: Zhang *et al.* (2008)

Copyright by Kasetsart University All rights reserved

Mao *et al.* (2009) studied the photocatalytic activity and the promoting effect of titania incorporated with carbon (TiO_2/C) for removing the pollutant in wastewater. The TiO_2/C composite photocatalysts with various ratios of TiO_2 to carbon were prepared by the sol–gel method. The degradation of methyl orange (MO), as the model reaction, was carried out in the aqueous slurry solution using these photocatalysts at 20ºC. Experimental results revealed that the ratio of TiO_2 to carbon largely affected the performance of composite catalyst. The optimal weight ratio of 1:1 for the highest photocatalytic capability was found. The photocatalytic performances of TiO_2/C catalysts were also found better than those of TiO_2 incorporated with activated carbon. The optimal condition was 500 ml of 40 mg/l MO with 0.05 g of catalyst and degradation time was 2 hours. The better promoting effect might be attributed to the larger pores of carbon that allow a faster diffusion of the adsorbed MO from carbon toward TiO_2 and the high electrical conductivity of carbon which can reduce the recombination of electrons and holes generated in TiO_2.

Ravichandran *et al.* (2010) prepared and characterized the activated carbon loaded TiO_2-P25 by various techniques. Percentage of AC that loaded TiO_2-P25 was varied in the range of 4-12%. The photocatalytic efficiency of activated carbon loaded TiO_2-P25 (10AC-TiO_2-P25) (0.1 g) was evaluated by photodefluoridation of 100 mg/l (100ml) pentafluorobenzoic acid (PFBA) under UV irradiation at neutral pH. The 10%AC-TiO_2-P25 showed the highest efficiency for photodegradation. The FTIR spectra of AC-TiO_2-P25 photocatalyst before and after the adsorption of PFBA and after complete defluoridation on irradiation are shown in Figure 5a-c. Adsorption bands of C-F stretching (1650, 1613, 1527, 1490, 1402 and 1290 cm^{-1}) appear on the absorption spectra of the catalyst after PFBA adsorption, it indicates that the PFBA adsorbed on surface of catalyst (Figure 5b). After irradiation of AC-TiO_2-P25 with the adsorbed PFBA, peaks in this range disappear giving a spectrum (Figure 5c) similar to the spectrum of the catalyst alone (Figure 5a). This confirms that the adsorbed PFBA molecules on AC are being transferred to the TiO_2-P25, where they are degraded under irradiation as shown in Figure 6. The efficiency of AC-TiO_2-P25 is due to synergy effect of activated carbon.

Copyright by Kasetsart University All rights reserved

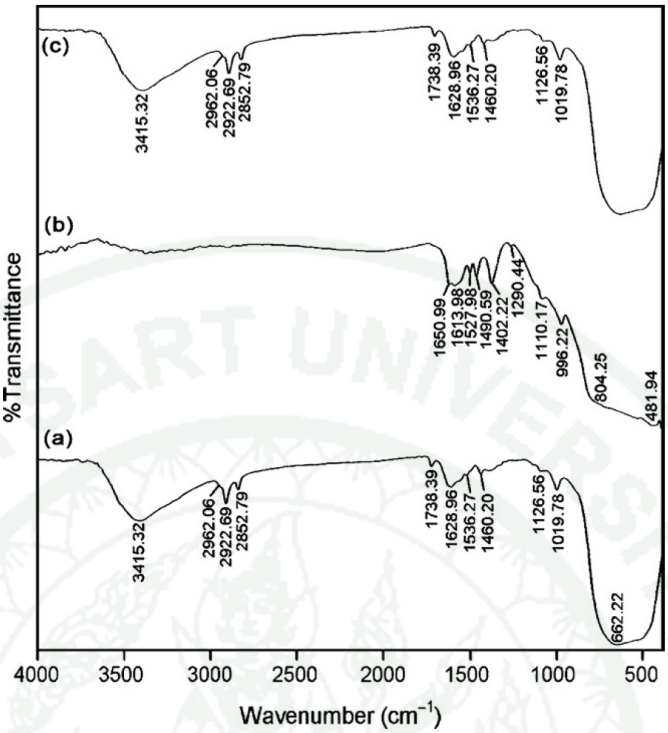

Figure 5. FT-IR spectra of (a) AC-TiO_2-P25, (b) AC-TiO_2-P25 after PFBA adsorption and (c) AC-TiO_2-P25 after complete defluoridation of PFBA.

Source: Ravichandran *et al.* (2010)

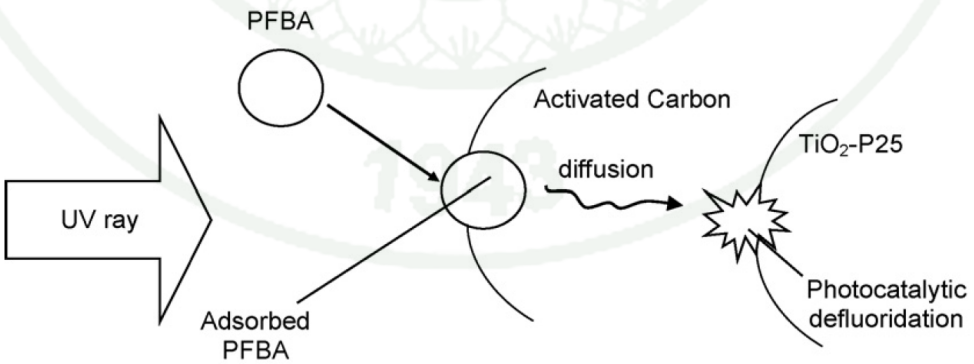

Figure 6. Synergistic effect of AC-TiO_2-P25 on photodefluoridation of PFBA

Source: Ravichandran *et al.* (2010)

Copyright by Kasetsart University All rights reserved

Wang *et al.* (2009) developed the TiO_2 photocatalysts deposited on activated carbon (TiO_2/AC) by dip-hydrothermal method at 180 ºC using peroxotitanate as a precursor and then calcinated at 300–800ºC. The catalysts were characterized by X-ray diffraction (XRD), scanning electron microscopy (SEM), Raman spectroscopy and the nitrogen absorption. Their photocatalytic activity was evaluated by degradation of 250 ml of 50 mg/l methyl orange (MO) with 0.5 g of catalysts for 1 hour. The results showed that TiO_2 particles of anatase type were deposited on the activated carbon surface. The TiO_2/AC calcinated at 600 ºC exhibited the best photocatalytic performance. For the comparison, the same photocatalysis experiment was carried out for two mixtures of commercial TiO_2 (Degussa P25) with AC and synthetic TiO_2 with AC. It was found that the composite catalyst TiO_2/AC was better than the two mixtures. Besides, different from fine powdered TiO_2, the granular TiO_2/AC photocatalysts could be easily separated from the bulk solution and reused, its photocatalytic ability was hardly decreased after a five-cycle for MO degradation.

Wang *et al.* (2009) studied the effect of porosities of as a supported for preparation of TiO_2 immobilized on granular activated carbons (TiO_2/AC). The catalyst was prepared by a dip-hydrothermal method using peroxotitanate as precursor, calcined at 600ºC. The TiO_2/AC composites were characterized by X-ray diffraction, scanning electron microscopy (XRD), X-ray photoelectron spectroscopy (XPS) and the nitrogen absorption. Their photocatalytic activity was evaluated by degradation of 250 ml of 50 mg/l methyl orange (MO) with 0.5 g of catalysts for 1 hour methyl orange (MO). The results showed that TiO_2 nanoparticles of anatase type were deposited on the activated carbon surface. The porosity of activated carbon had significant influence on the adsorption, the amount of TiO_2 deposited on the external surface of AC and the activity of composite photocatalysts. The composite TiO_2/AC made from proper mesoporosity AC exhibited higher catalytic activity than the mixture of powdered TiO_2 with AC.

Zhu and Zou (2009) studied two types of commercially activated carbons (AC), pellets and granules, affected on TiO_2 nanoparticles coated AC (TiO_2/AC) which were prepared using a sol–gel method. Color and trace organics remaining in

Copyright by Kasetsart University All rights reserved

the actual treated effluent were adsorbed by TiO_2/AC. The adsorbed organic compounds were then decomposed using a photocatalytic process and the AC were regenerated for reuse. The efficiency of the process was assessed by photodegradation of 40 mg/l methylene blue (MB) with flow rate 1 l/h and 50 g of catalyst. The TiO_2/AC-granules achieved better efficiency in MB removal than TiO_2/AC-pellets, with around 90% within 1 h of treatment.

Copyright by Kasetsart University All rights reserved

MATERIALS AND METHODS

Materials

1. Titanium(IV) tetra-n-butoxide ($C_{16}H_{36}O_4Ti$, Lab Grade, Merck, Hohenbrunn, Germany)
2. Titanium(IV) tetraisopropoxide ($C_{12}H_{28}O_4Ti$, Lab Grade, ACROS, New Jersey, USA)
3. Activated carbon (C, AR Grade, Fluka Chemika, Steinheim, Switzerland)
4. Isopropanol (C_3H_7OH, AR Grade, Sentmenat, Spain)
5. Degussa P25 Titinium(IV) dioxide nanopowder (99.9% , Aldrich, Riedstr., Germany)
6. Phenol (C_6H_5OH, AR Grade, Carlo Erba, Van de Reuil, France)
7. Acid orange 7 ($C_{16}H_{12}N_2O_4S$, AR Grade, Aldrich, Riedstr., Germany)

Copyright by Kasetsart University All rights reserved

Methods

1. Catalyst preparation

The photocatalyst, titanium dioxide supported activated carbon (TiO_2/AC), was prepared by sol-gel process. Initially, 10.0 ml of titanium(IV) isopropoxide as a precursor was added into the suspended solution of 2.0 g of activated carbon and 40.0 ml of isopropyl alcohol under stirring condition at 30ºC. The black condensed-mixture was slightly appeared by undergoing the hydrolysis and condensation reactions within 30 minutes after the addition of precursor. This stirring condition was held at 30ºC for one hour. Consequently, the black slurry was obtained and then dried at 120ºC in the oven for one hour in order to evaporate the remaining isopropyl alcohol and by-product residues generated from hydrolysis reaction. Finally, the TiO_2/AC was calcined in the furnace at various temperatures (300ºC-500ºC) for one hour to obtain the crystalline phase of TiO_2 and remove of volatile fractions. Additionally, the effect of titania precursor was also studied by using 11.22 ml of titanium(IV) n-butoxide in place of titanium(IV) isopropoxide through sol-gel process.

Table 3 The titania precursors with their volumes, density and equivalent mole of titania.

Titania precursors	Chemical formula	Density (g/ml)	Volume (ml)	Amount of titanium (mole)
Titanium(IV) isopropoxide	$C_{12}H_{28}O_4Ti$	0.937	10.00	3.30×10^{-2}
Titanium(IV) n-butoxide	$C_{16}H_{36}O_4Ti$	1.000	11.22	3.30×10^{-2}

Copyright by Kasetsart University All rights reserved

2. Catalyst characterization

1.1 Thermal Gravimetric Analysis (TGA)

The range of calcination temperature of the prepared TiO_2/AC catalyst was obtained from TGA (TGA 7 Perkin Elmer analyzer). 4.0-5.0 mg of Al_2O_3 as protecting material was loaded onto platinum pan, and then 10.0 mg of sample was added. The temperature program was carried out by setting up temperature from 50ºC to 600ºC with an increasing rate of 10ºC/minute under nitrogen gas condition.

1.2 X-ray powder Diffraction (XRD)

2.2.1. Determination of the crystalline phase

The crystalline phase was obtained by a Philips Pw 1083 X-ray diffractometer (XRD) operated at 40 kV and 35 mA and a Philips X´ Pert X-ray diffractometer operated at 40 kV and 30 mA, both of which used Cu Kα radiation source at λ of 1.54 Å. XRD data were collected from 2θ of 20-60 degree. The ground sample was coated on the inverse side of clear adhesive tape, and then it was pressed to obtain the smooth surface of the sample. The crystalline phases of all samples were identified by comparison with the Joint Committee on Powder Diffraction Standards (JCPDS) files.

2.2.2. Determination of the crystallite size

The crystallite size was calculated by Scherrer's equation as follows; (Patterson *et al.,* 1939)

$$d = \frac{k\lambda}{\beta Cos\theta_B}$$

Copyright by Kasetsart University All rights reserved

where d is the crystallite size (nm)

k is the constant whose value is approximately 0.9

λ is the wavelength of the X-ray radiation source (0.154 nm for Cu Kα)

β is the full width at half maximum intensity (FWHM) (radians)

θ_B is the Bragg angle at the position of the maximum peak.

1.3 Scanning Electron Microscopy (SEM)

The morphology of the prepared TiO_2/AC catalysts was determined by SEM and recorded by a JEOL JSE-5600Lv scanning electron microscope fitted with tungsten filament. Each of the powdered samples was spread on carbon tape mounted on an SEM stub and coated with Pt/Pd particles prior to SEM operation.

1.4 Transmission Electron Microscopy (TEM)

The morphology and particle size of all the prepared TiO_2/AC catalysts were investigated by TEM recorded by a JEOL 1200 EX electron microscope fitted with a standard tungsten filament and operated at 100 keV. Images were recorded digitally using a Mega View II digital camera with Soft Imaging System GmbH analysis 3.0 image analysis software and/or on KODAK Electron Image Film SO-163. Samples diluted in ethanol solution were deposited onto Formvar-coated, carbon-reinforced, 3-mm-diameter copper electron microscope grids and left to air-dry prior to analysis.

1.5 Raman Spectroscopy

The Raman shifts of TiO_2/AC and prepared-TiO_2 were observed on a Renishaw Raman Imaging Microscope operated with green laser. Silicon plate was used as a calibrating material, which showed the evident Raman shift at 520 nm^{-1}. Each of the crushed samples was deposited on a glass plate and a little acetone solution was dropped in order to make the sample tightly attach to the surface of the plate.

Copyright by Kasetsart University All rights reserved

3. Photoreactor

The photoreactor as shown in Figure 7 was used for study the photodegradation reaction of phenol and acid orange 7 by TiO_2/AC catalyst. UV-lamp, Hg vapor fluorescent lamp, was employed as light source. The reactor contained two sets of magnetic stirrer, ventilator and eight UV-lamps (120W). Furthermore, this reactor could control the inside temperature at 30ºC during the reaction for 4 hours.

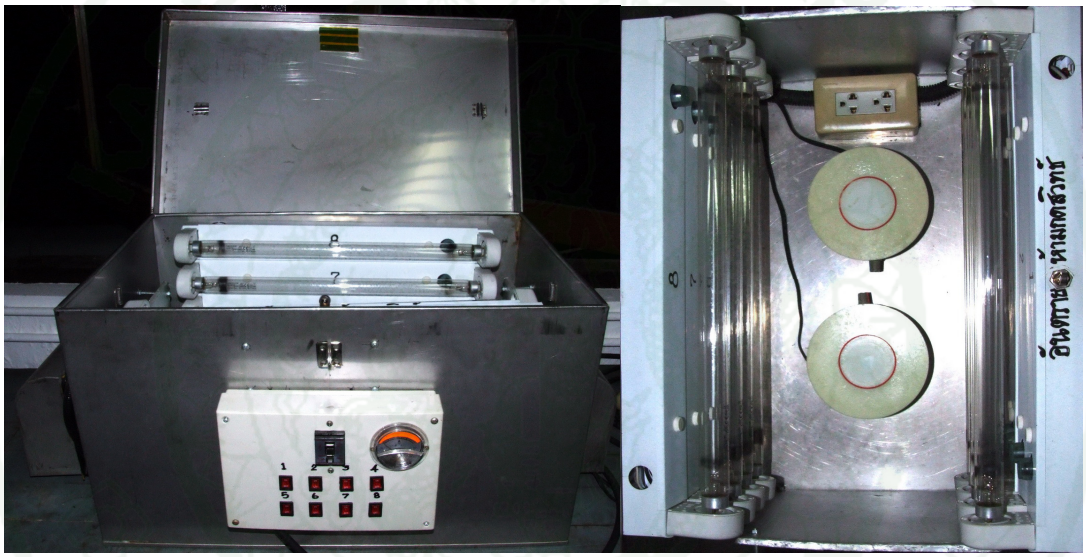

Figure 7 The image of photoreactor contained UV-lamps and magnetic stirrers.

Copyright by Kasetsart University All rights reserved

4. Preparation of solution for photodegradation reaction

4.1. Preparation of phenol solution

100 ml of 1000 ppm stock phenol solution was prepared by weighing 0.1000 g of standard phenol, and then it was dissolved in distilled water with a certain volume in a 100 ml volumetric flask.

500 ml of 100 ppm of phenol solution was prepared by diluting 50 ml of the stock phenol solution with distilled water. The phenol solution was then sonicated in order to obtain a homogeneous solution

4.2. Preparation of acid orange 7 solution

100 ml of 1000 ppm stock AO7 solution was prepared by weighing 0.1000 g of standard AO7, and then it was dissolved in distilled water with a certain volume in a 100 ml volumetric flask.

500 ml of 100 ppm of AO7 solution was prepared by diluting 50 ml of stock AO7 solution with distilled water. The AO7 solution was then sonicated in order to obtain a homogeneous solution.

5. Photocatalytic experiments

5.1. Photocatalytic degradation of phenol

Firstly, 0.4 g (2.0 g/l) of the TiO_2/AC photocatalyst was added into 200 ml of 100 ppm phenol solution. The degradation reaction was operated under dark condition for one hour and then operated under UV-irradiation with 15 W of eight UV lamps. The system was first left in the dark in order to attain the adsorption equilibrium before the degradation. In this condition, the solution was continually

Copyright by Kasetsart University All rights reserved

stirred at a constant temperature (30ºC) in the photoreactor during the period of degradation.

To monitor the reaction, the sample was collected by a syringe in order to measure the amount of initial (before the addition of TiO_2/AC photocatalyst) and remaining concentration of phenol in each period of time. For avoidance of the catalyst contamination in the collected sample, stirrer was switched off 15 minutes before collecting the sample. All of the collected samples were left overnight in the dark condition and then centrifuged for 5 minutes to reduce the dispersion of the fine-powdered catalyst. After that, the centrifugate was transferred into a vial. Finally, all samples were diluted with distilled water to a certain volume and their concentrations were measured by a JASCO 7800 UV-Vis spectrophotometer at wavelength 270 nm.

5.2. Photocatalytic degradation of AO7

Initially, 0.2 g (1.0 g/l) of the TiO_2/AC photocatalyst was added into 200 ml of 100 ppm AO 7 solution at pH 4.0, 7.0 and 10.0, respectively. The degradation reaction was operated under dark condition for one hour and then operated under UV-light with 15 W of eight UV lamps. The system was first left in the dark in order to attain the adsorption equilibrium before the degradation. In this condition, the solution was continually stirred under the constant temperature (30ºC) in the photoreactor during the period of degradation.

To monitor the reaction, the sample was collected by a syringe in order to measure the amount of initial (before the addition of TiO_2/AC photocatalyst) and remaining concentration of AO7 in each period of time. For avoidance of the catalyst contamination in the collected sample, stirrer was switched off 15 minutes before collecting the sample. All of the collected samples were left overnight in the dark condition and then centrifuged for 5 minutes to reduce the dispersion of the fine-powdered catalyst. After that, the centrifugate was transferred into a vial. Finally, all samples were diluted with distilled water to a certain volume and their concentrations were measured by a JASCO 7800 UV-Vis spectrophotometer at wavelength 485 nm.

Copyright by Kasetsart University. All rights reserved

6. Concentration measurement of phenol and AO7

6.1. Preparation of solution for linear calibration curves

6.1.1. The calibration curve of phenol solution

Various concentrations of phenol (5, 10, 15, 20 and 25 ppm) were prepared by diluting from 100 ppm of phenol solution (as prepared in section 4.1). The series of phenol concentrations were measured by a JASCO7800 UV-Vis spectrophotometer at wavelength 270 nm.

6.1.2. The calibration curve of AO7

Various concentrations of AO7 (5 to 25 ppm) were prepared by diluting from 100 ppm of AO7 solution (as prepared in section 4.2). The series of AO7 concentrations were measured by a JASCO7800 UV-Vis spectrophotometer at wavelength 485 nm.

6.2. Determination of phenol concentration

The decreasing concentration of phenol was followed by measuring absorbance of collected samples by a JASCO-7600 UV-Vis spectrophotometer. The measurement was operated at wavelength 270 nm and distilled water was used as a blank and reference solution.

6.3. Determination of AO7 concentration

The decreasing concentration of AO7 was followed by measuring absorbance of collected samples by a JASCO-7600 UV-Vis spectrophotometer. The measurement was operated at wavelength 485 nm and distilled water was used as a blank and reference solution.

Copyright by Kasetsart University All rights reserved

7. Adsorption isotherm of phenol

7.1. Concentration of equilibrium state

A 0.05 g of catalyst was loaded in each eleven of 50-ml elrenmeyer flasks, and then 25 ml of various concentrations (50, 100,150, 200, 250, 300, 350, 400, 450 and 500 ppm) of phenol and reference (distilled water) were added into each elrenmeyer flask. Afterwards, the flasks were agitated in a shaker under the constant shaking rate (200 rpm) for 6 hours. Then the catalyst was filtered out, the remain phenol was determined by a JASCO7600 UV-Vis spectrophotometer at wavelength 270 nm.

7.2. Contact time

The 0.05 g of catalyst was loaded in each of twelve 50 ml elrenmeyer flasks, after that 25 ml of 400 ppm phenol solution (the appropriate concentration from 7.1) was poured in each of six flasks and reference (distilled water) was poured into the rest flasks. Continually, all flasks were agitated in a shaker under the constant shaking rate (200 rpm), and then one phenol and one reference flask were withdrawn from the shaker every one hour until that finished. Then the catalyst was filtered out, the remain phenol was determined by a JASCO-7600 UV-Vis spectrophotometer at wavelength 270 nm.

7.3. Adsorption isotherm

The 0.05 g of catalyst was loaded in each of six 50 ml elrenmeyer flasks, and then 25 ml of various concentrations (300, 350, 400, 450, 500 ppm) of phenol and reference (distilled water) were poured in each elrenmeyer flask. Consecutively, all flasks were agitated in a shaker under the constant shaking rate (200 rpm) for 4 hours (the contact time from 7.2). Then the catalyst was filtered out, the remain phenol was determined by a JASCO-7600 UV-Vis spectrophotometer at wavelength 270 nm.

Copyright by Kasetsart University All rights reserved

8. Recycling of the catalyst

After photodegradation experiments, the catalyst was covered with phenol (or AO7) molecules due to the adsorption ability of catalyst. The catalyst was filtrated and separated from solution, therefore, it could be regenerated for further photocatalytic runs. The regeneration was done by double treating the used catalyst in 20 ml of distilled water with sonicating for 10 minutes. Lastly, suspension solution was filtrated and dried in oven at temperature of 120ºC.

Copyright by Kasetsart University All rights reserved

RESULTS AND DISCUSSION

1. Catalyst characterization

1.1 Effect of calcination temperature

Suitable calcination temperature was determined because it could affect the properties of the prepared catalysts. This is because the calcination temperature should be less than the maximum oxidizing temperature of activated carbon and high enough for amorphous TiO_2 to change to anatase structure. TGA and XRD techniques were used to characterize the as-prepared catalyst for appropriate calcination temperature.

1.1.1. Thermal gravimetric analysis (TGA)

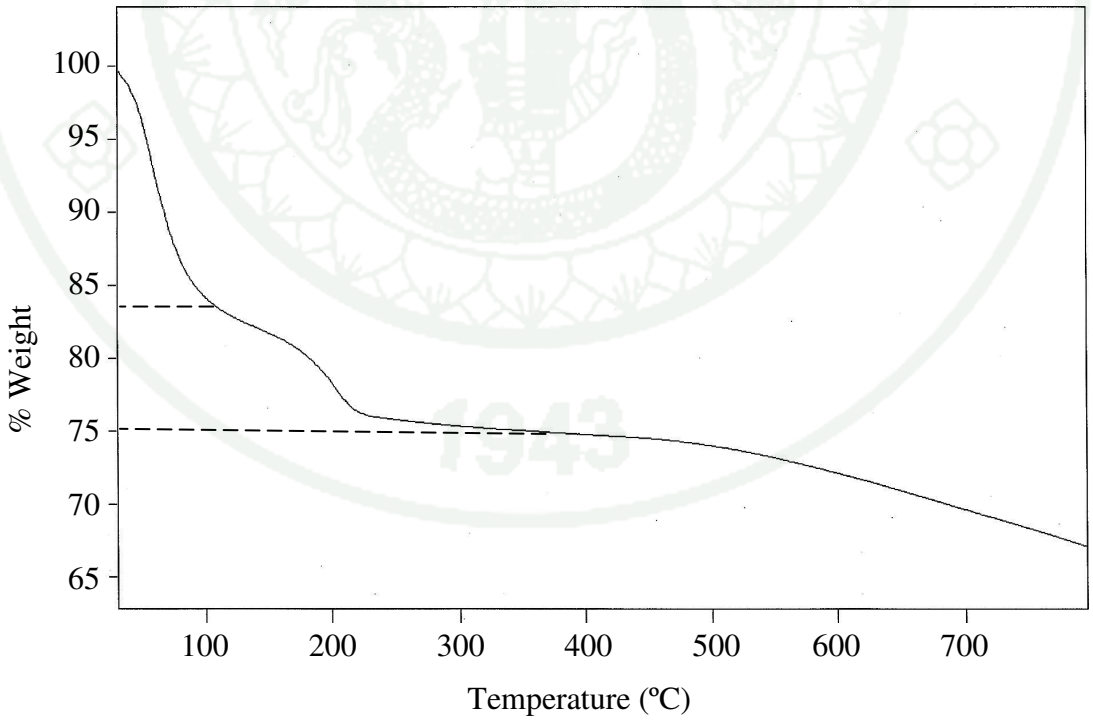

Figure 8 The TGA curve of as-prepared TiO_2/AC using titanium(IV) isopropoxide as a titania precursor.

Copyright by Kasetsart University All rights reserved

The TGA curve (Figure 8) of the as-prepared TiO_2/AC using titanium(IV) isopropoxide as a precursor after drting at 120ºC, presents three main steps of weight loss. Initially, at 125ºC shows 17% weight loss by evaporation of the absorbed water and organic molecules. The next step, weight loss of 8% at 400ºC exhibits evaporation of tightly-absorbed solvent or the by-product of hydrolysis reaction. The last step, at 400ºC shows the first oxidation reaction of the activated carbon.

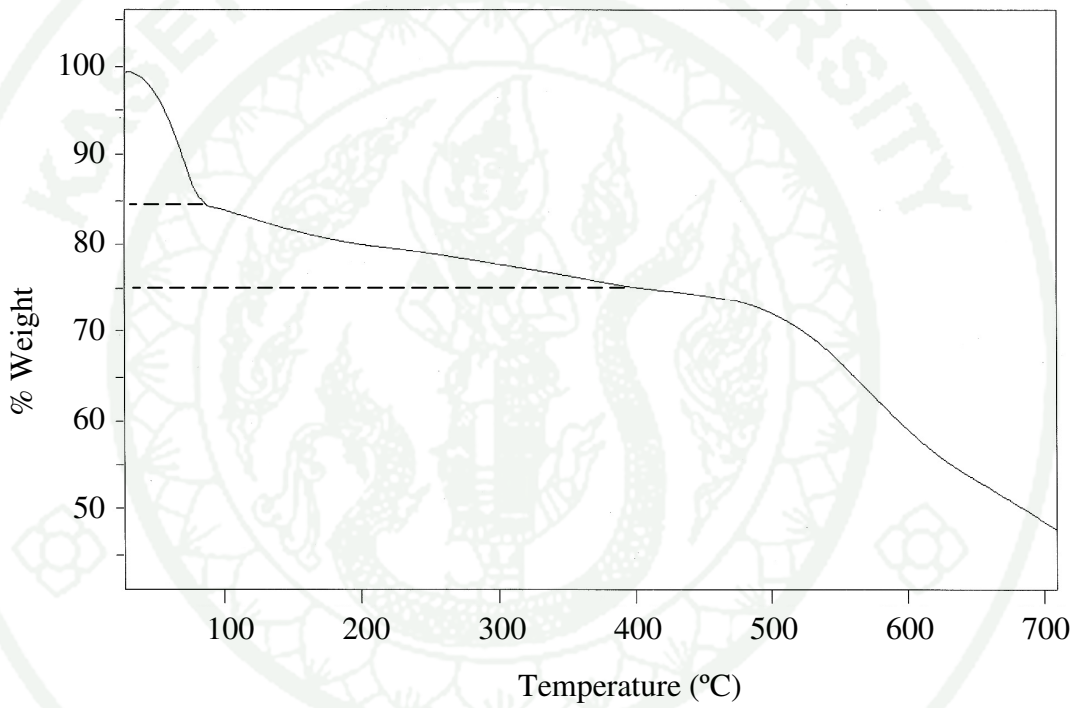

Figure 9 The TGA curve of as-prepared TiO_2/AC using titanium(IV) n-butoxide as a titania precursor.

The TGA curve (Figure 9) of the as-prepared TiO_2/AC using titanium(IV) n-butoxide as a precursor after drying at 120ºC also presents three main steps of weight loss. Firstly, at 100ºC shows 15% weight loss by evaporation of the absorbed water molecules. The next step, weight loss of 12% at 400ºC exhibits evaporation of tightly-absorbed solvent or the by-product of hydrolysis reaction. Finally, at 400ºC indicates the first oxidation reaction of activated carbon.

Copyright by Kasetsart University All rights reserved

The last step of both TGA curves of the as-prepared TiO_2/AC catalysts, was due to the oxidation reaction of the activated carbon, because the carbon of TiO_2/AC (black color) became ash (gray color) after characterization by a TGA. On the other hand, the first and second decomposition steps of the two titania precursors as shown in Figure 10a and 10b are different due to the boiling point of the by-product of the hydrolysis, isopropanol and n-butanol, which were the by-products when titanium(IV) isopropoxide and titanium(IV) n-butoxide were used as precursor, respectively.

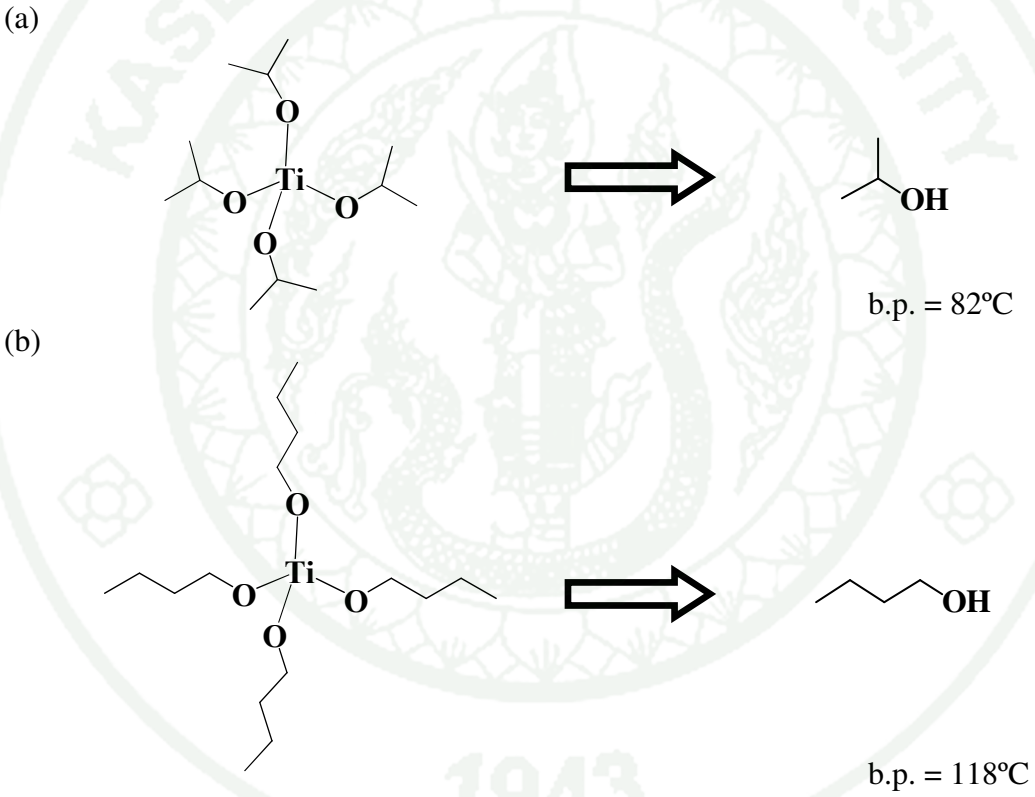

Figure 10 Expected product from the hydrolysis reaction of (a) titanium(IV) isopropoxide and (b) titanium(IV) n-butoxide.

In the preparation step, the precursor was hydrolyzed in sol-gel process, and then it produced isopropanol (Figure 10a) and n-butanol (Figure 10b) when titanium(IV) isopropoxide and titanium(IV) n-butoxide were used, respectively. In case of titanium(IV) isopropoxide precursor (Figure 10a), the boiling point of

Copyright by Kasetsart University All rights reserved

isopropanol is 82ºC indicating that it is easy to be removed at 120ºC under the drying step. However, small amounts of isopropanol are still remained and adsorbed on the surface of the catalyst, which can be removed at higher temperature (125ºC-400ºC), showing 8% weight loss. In case of titanium(IV) butoxide precursor (Figure 10b), the boiling point of n-butanol is 118ºC indicating that it more difficult to be removed than isopropanol at 120ºC under drying step. This may be reason for higher percentage of weight loss (10%) between 100ºC to 400ºC in the TGA curve when titanium(IV) n-butoxide was used as a precursor.

1.1.2. X-ray powder diffraction (XRD)

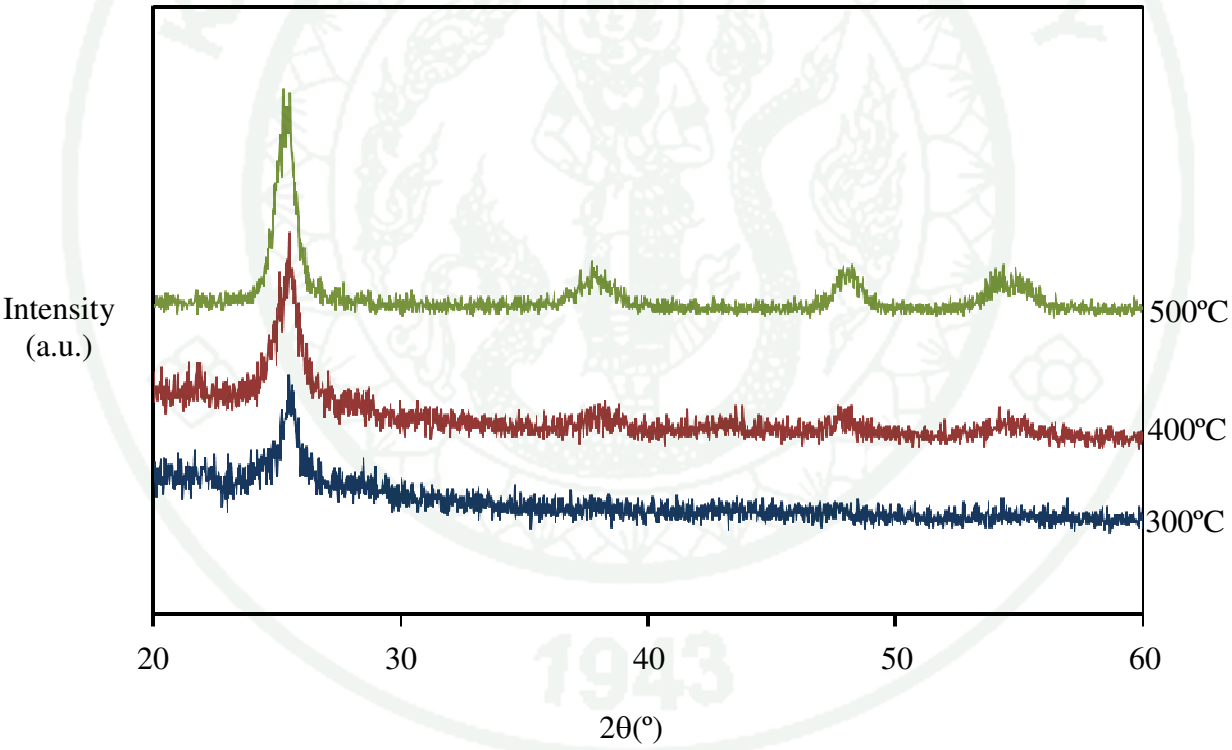

Figure 11 The XRD patterns of the as-prepared TiO_2/AC using titanium(IV) isopropoxide as a titania precursor with various calcination temperatures.

Copyright by Kasetsart University All rights reserved

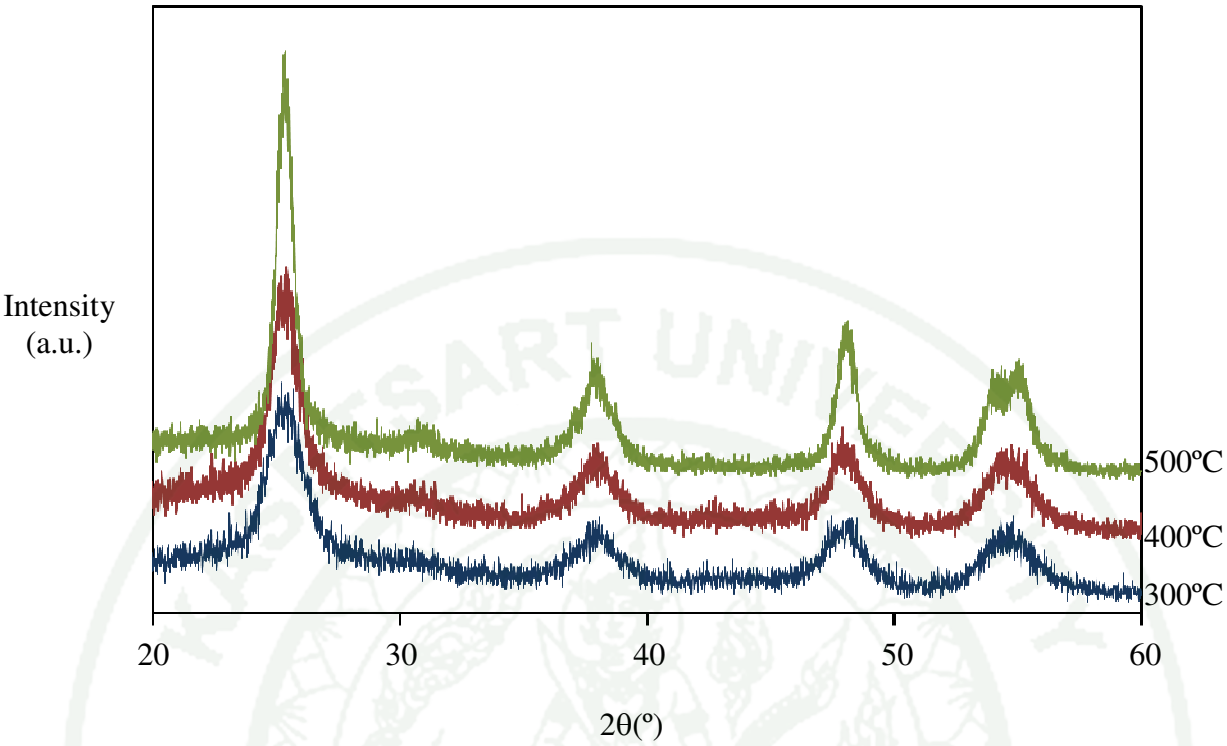

Figure 12 The XRD patterns of as-prepared TiO_2/AC using titanium(IV) n-butoxide as a titania precursor with various calcination temperatures.

The XRD patterns of TiO_2/AC catalysts with various calcination temperatures using titanium(IV) isopropoxide and titanium(IV) n-butoxide as a titania precursor are shown in Figure 11 and Figure 12, respectively. TiO_2/AC catalyst calcined at 300ºC shows broad diffraction pattern, indicating the amorphous phase of TiO_2/AC. For the TiO_2/AC catalyst calcined at 400ºC, anatase structure firstly appears in diffraction pattern, which is indentified at 2θ of 25.4º, 38.1º, 48.2º, 53.9º and 55.1º, corresponding to the standard XRD pattern (JCPDS file No.21-1272). At calcination temperature 500ºC, the characteristic peaks of anatase phase has more sharpness and prominence than that at 400ºC, particularly, at 2θ of 25.4º.

According to the results for TGA analysis and X-ray diffraction of as-prepared TiO_2/AC, the calcination temperature at 400ºC was selected as the appropriate temperature for the preparation of TiO_2/AC catalyst, because the volatile fraction was completely eliminated, the oxidation of the activated carbon was not occurred, and titania exhibited the anatase phase.

Copyright by Kasetsart University All rights reserved

1.2 Phase transformation

1.2.1. X-ray powder diffraction (XRD)

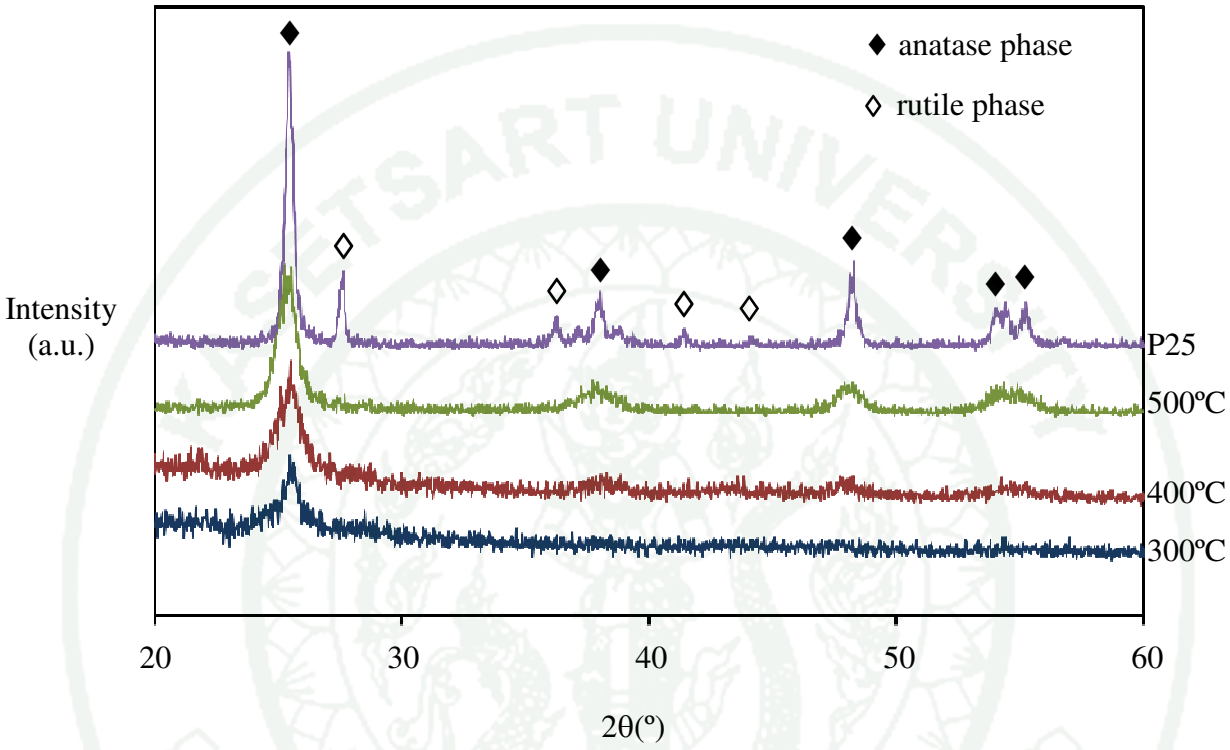

Figure 13 The XRD patterns of as-prepared TiO_2/AC using titanium(IV) isopropoxide as a titania precursor at various calcination temperatures.

The XRD patterns of TiO_2/AC calcined at 300ºC to 500ºC as shown in Figure 13 exhibit amorphous and anatase phase, depending on calcination temperature. At calcination temperature of 300ºC, it shows broad diffraction pattern indicating the amorphous structure of TiO_2/AC. Then, it changes to anatase structure when calcination temperature was raised up to 400ºC. Anatase structure is identified at 2θ of 25.4º, 38.1º, 48.2º, 53.9º and 55.1º, corresponding to the standard XRD pattern (JCPDS file No.21-1272). At 500ºC, the characteristic peaks of anatase phase have more sharpness and prominence than lower calcination temperatures with all characteristic peaks, especially, at 2θ of 25.4º. The crystallite sizes of TiO_2/AC using titanium(IV) isopropoxide as precursor which calculated from Scherrer's equation (Patterson *et al.,* 1939), was found to increase from 6 to 12 nm with increasing

Copyright by Kasetsart University All rights reserved

calcination temperature in the anatase phase. This implied that the higher calcination temperature, the larger particles of TiO_2/AC.

XRD pattern of Degussa P25 TiO_2 as shown in Figure 13 consists of mixed phase in the ratio of 75% anatase to 25% rutile. The XRD peaks at 2θ of 25.4º and 27.6º show the obvious characteristic peak of anatase and of rutile structure (at 2θ of 27.5°, 36.1°, 41.3°, 44.2° and 55.5°, JCPDS files No. 21-1276), respectively. The crystsllite size of Degussa P25 was found to be 29.42 nm, which was different from that reported in Table 4, as it was prepared through a different process and did not have activated carbon as a supporter.

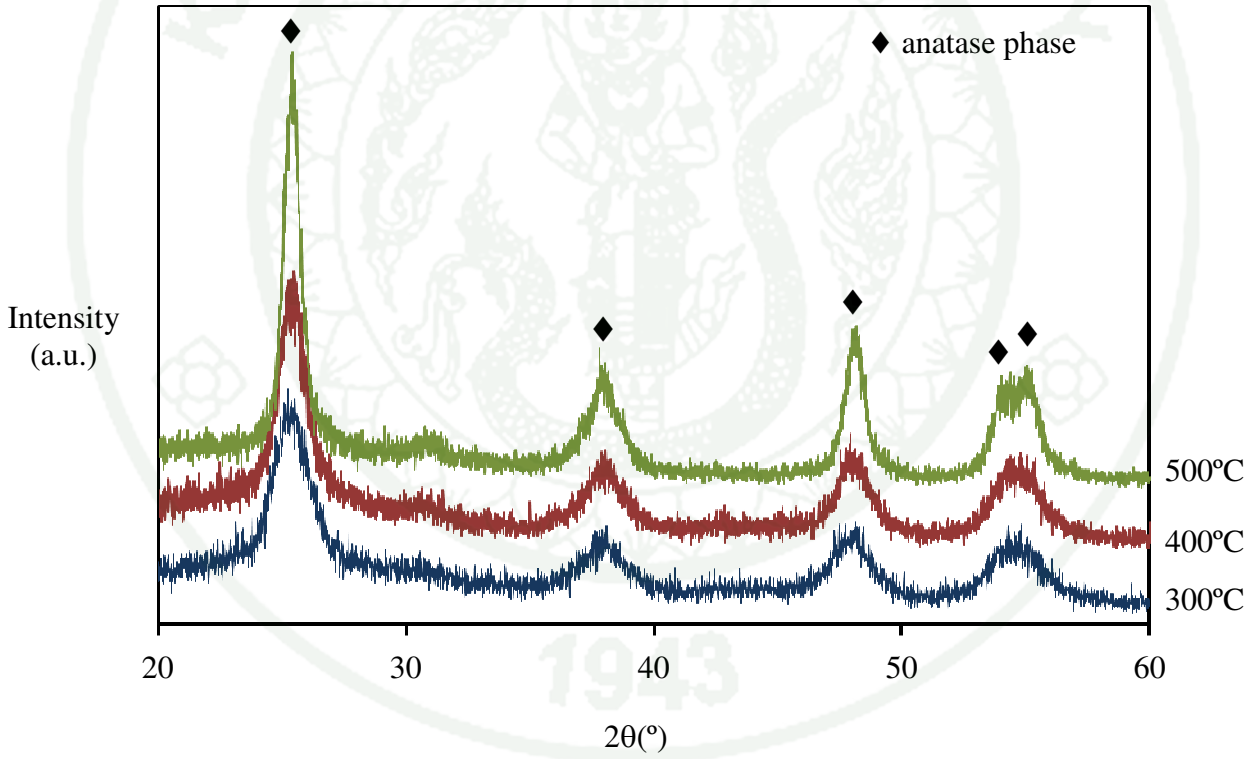

Figure 14 The XRD patterns of as-prepared TiO_2/AC using titanium(IV) n-butoxide as a titania precursor at various calcination temperatures.

The XRD patterns of the anatase structure of TiO_2/AC using a titanium(IV) n-butoxide as a precursor are shown in Figure 14. The anatase structure, that was identified at 2θ of 25.4º, 38.1º, 48.2º, 53.9º and 55.1º, corresponding with the

Copyright by Kasetsart University All rights reserved

standard XRD pattern (JCPDS file No.21-1272), firstly appeared at calcination temperature of 300ºC.

At calcination temperature of 500ºC, a characteristic peak of anatase structure (at 2θ of 25.4º) has more sharpness and prominence than lower temperature. The crystallite sizes of TiO_2/AC using titanium(IV) n-butoxide as a precursor which calculated from Scherrer's equation increase from 6 to 14 nm with increasing calcination temperature in the anatase phase. These indicated that the higher the calcination temperature, the larger the crystallite size of TiO_2/AC.

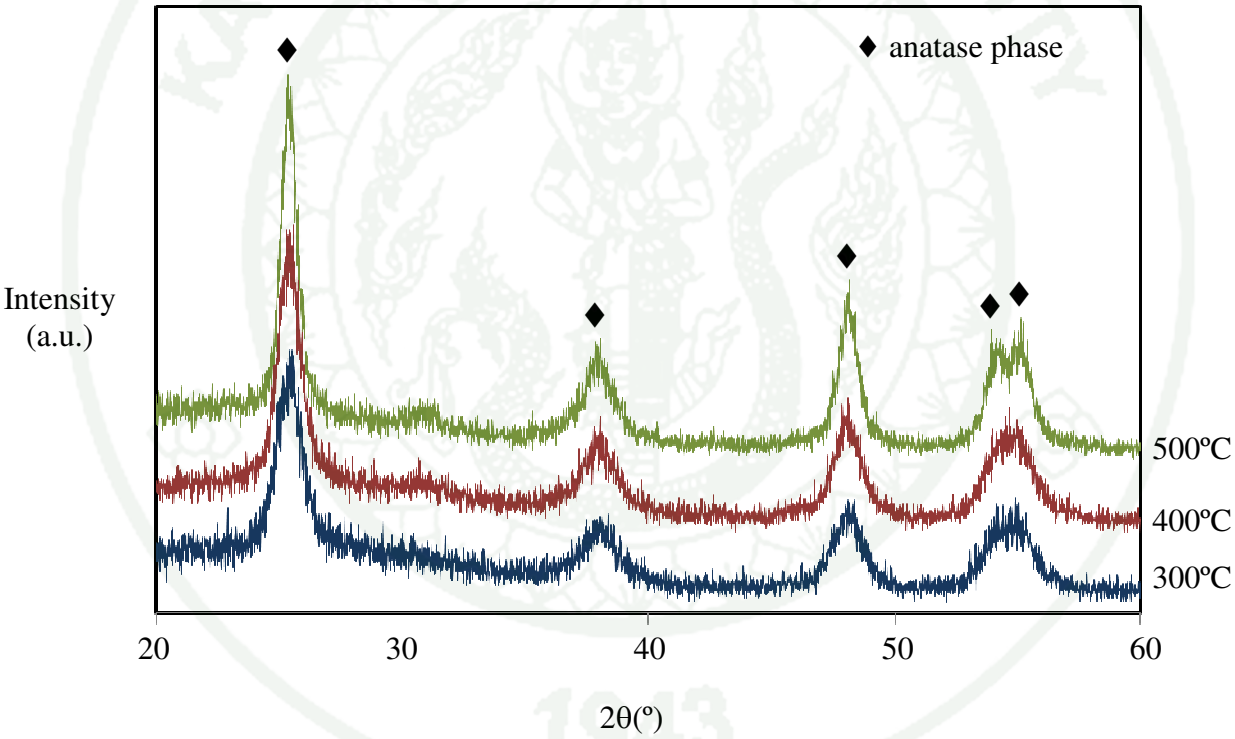

Figure 15 The XRD patterns of prepared-TiO_2 using titanium(IV) isopropoxide as a titania precursor at various calcination temperatures.

Figure 15 shows the XRD patterns of TiO_2 using titanium(IV) isopropoxide as a precursor at various calcination temperatures. All of the XRD patterns exhibited the anatase phase (at 2θ of 25.4º, 38.1º, 48.2º, 53.9º and 55.1º, JCPDS file No.21-1272). From the results in Table 4, the crystallite sizes of the prepared-TiO_2, which calculated from Scherrer's equation (Patterson *et al.,* 1939),

Copyright by Kasetsart University All rights reserved

increased from 9 to 14 nm with increasing calcination temperature in anatase phase. This also indicates that the higher the calcination temperature, the larger the crystallite size of TiO_2.

In comparing the XRD patterns of TiO_2/AC using two different types of titania precursors, which the characteristic similarity and difference of the prepared catalysts can be discussed as follows;

First, both of catalysts (TiO_2/AC using titanium(IV) isopropoxide and TiO_2/AC using titanium n-butoxide) show the anatase phase (at 2θ of 25.4º, 38.1º, 48.2º, 53.9º and 55.1º, corresponding with the standard XRD pattern) after calcination at high temperature. The rutile phase dose not appeare because the calcination temperature used is lower than 550ºC (Zhang *et al.*, 2006).

Second, similar crystallinity are found in TiO_2/AC using titanium(IV) isopropoxide and that using titanium(IV) n-butoxide as precursor at calcination temperature of 500ºC. This indicates that the different titania precursors organic contents (Ti-O-R) in different titania precursors dose not change the formation of Ti-O-Ti.

Third, as shown in Table 4 the crystallite sizes of TiO_2/AC using titanium(IV) n-butoxide was larger than that of TiO_2/AC using titanium(IV) isopropoxide at 400ºC which might be due to the thermal decomposition of the remaining titamium(IV) n-butoxide resulting in rapid agglomeration of TiO_2. However, with increasing temperature, the crystallite sizes of TiO_2/AC and TiO_2 were increased.

From the comparison, it can be concluded that TiO_2/ACwhich prepared from both titanium precursors have similar characteristics. The crystallite size of TiO_2/AC using titanium(IV) isopropoxide as a precursor appered to be smaller than when the titanium(IV) n-butoxide was used.

Copyright by Kasetsart University. All rights reserved

Table 4 Effect of titania precursors and calcination temperatures on the crystallite sizes and phase content of TiO_2/AC and P25 TiO_2.

Sample	Titania precursor	Calcination temperature (ºC)	2θ (degree)	Cosθ	β (degree)	β (radian)	Crystallite size (nm)[a]
TiO_2	Titanium(IV) isopropoxide	300	25.41	0.975	0.83	0.01457	9.74
		400	25.42	0.975	0.74	0.01300	10.92
		500	25.41	0.975	0.57	0.00996	14.25
TiO_2/AC	Titanium(IV) isopropoxide	300	25.46	0.975	1.25	0.02193	6.74
		400	25.43	0.975	0.87	0.01521	9.34
		500	25.34	0.975	0.64	0.01124	12.62
	Titanium(IV) n-butoxide	300	25.37	0.975	1.24	0.02169	6.54
		400	25.38	0.975	0.91	0.01591	8.92
		500	25.38	0.975	0.56	0.00979	14.50
P25 TiO_2	-	-	25.42	0.975	0.27	0.00476	29.84

[a]The crystallite size was calculated by using Sherrer' s equation (Patterson *et al.,* 1939).

Copyright by Kasetsart University All rights reserved

1.2.2. Raman spectroscopy

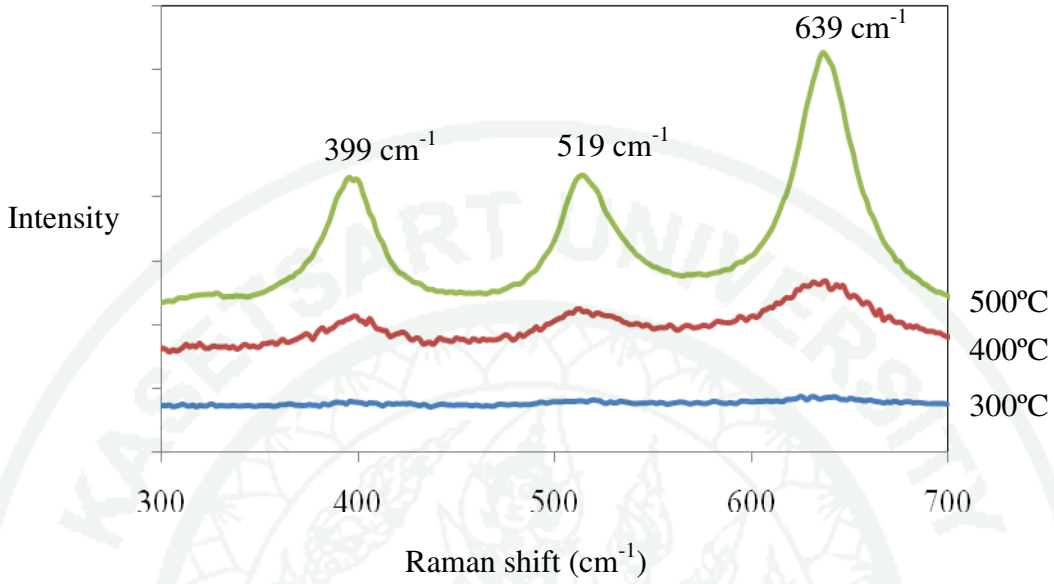

Figure 16 Raman spectra of TiO_2/AC using titanium(IV) isopropoxide as a titania precursor with different calcination temperatures.

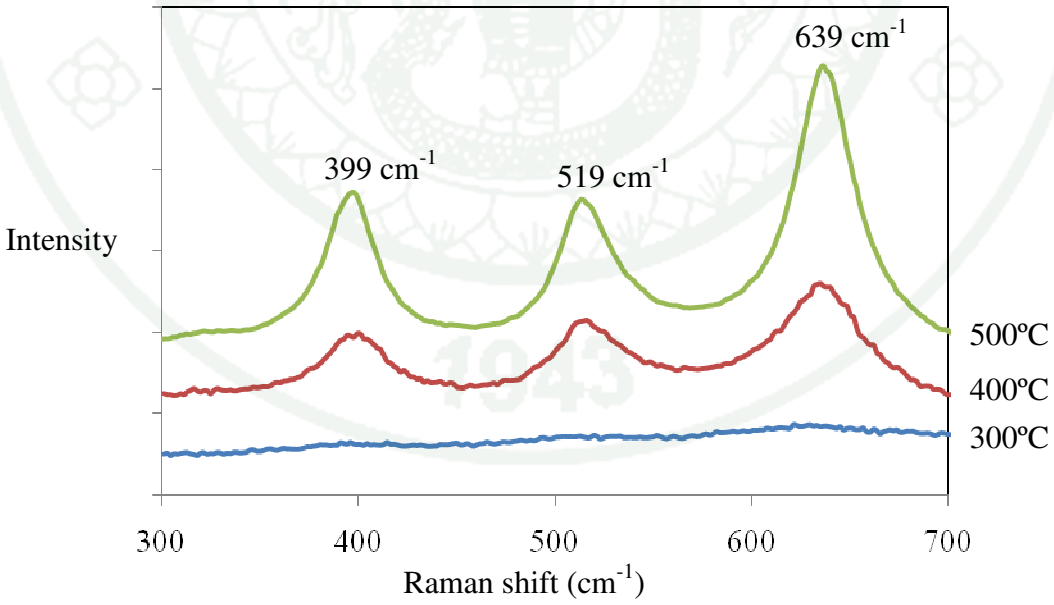

Figure 17 Raman spectra of TiO_2/AC using titanium(IV) n-butoxide as a titania precursor with different calcination temperatures.

Copyright by Kasetsart University All rights reserved

As shown in Figure 16 and 17, TiO_2/AC using titanium(IV) isopropoxide and titanium(IV) n-butoxide as a titania precursor show anatase phase at 400ºC and 500ºC which can be confirmed by the presence of Raman shifts of Ti-O bond at 399 cm^{-1}, 519 cm^{-1} and 639 cm^{-1}, respectively (Gnaser *et al.*, 2007). For lower calcination temperature (300ºC), the TiO_2/AC was still in amorphous phase as indicated by broad Raman shifts. When compared to the XRD data, the Raman results also provided the significant data as to the phase identification and phase transformation between 300ºC and 500ºC.

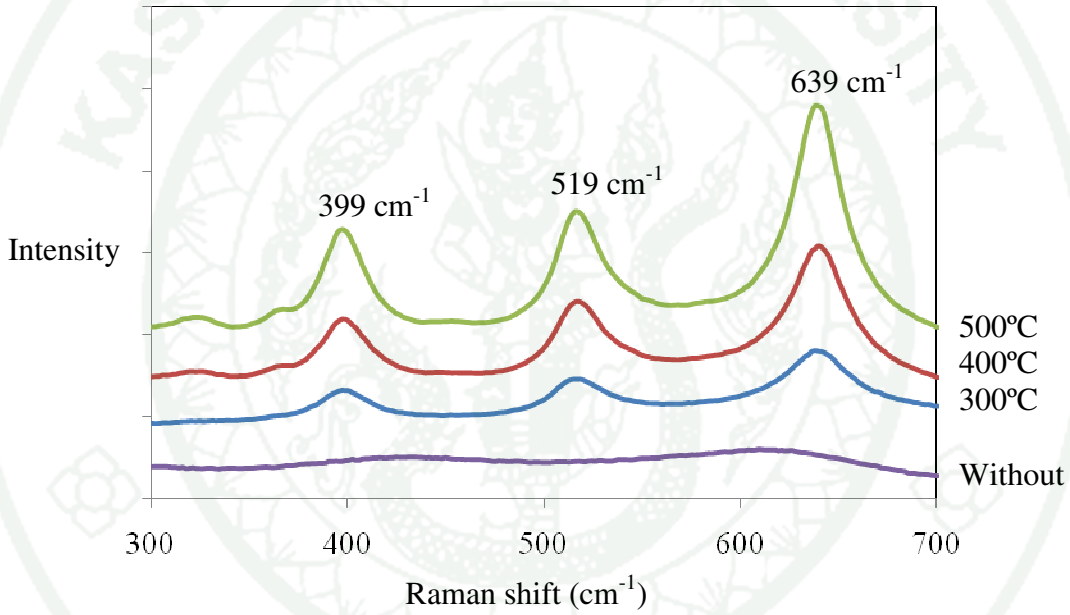

Figure 18 Raman spectra of prepared-TiO_2 using titanium(IV) isopropoxide as a titania precursor with different calcination temperatures.

The Raman spectra of TiO_2 (prepared by titanium(IV) isopropoxide as a titania precursor) as shown in Figure 18 demonstrate the anatase phase at calcination temperature of 300ºC to 500ºC. Anatase phase was identified with a set of Raman shifts at 399 cm^{-1}, 519 cm^{-1} and 639 cm^{-1}, respectively. For the prepared-TiO_2 without calcination, it can be seen that the TiO_2 showed broad spectrum indicating less Ti-O bonds forming and amorphous structure. Hence, in analogy with the XRD data, the Raman results confirm the amorphous-to-anatase phase transformation between 300ºC and 500ºC.

Copyright by Kasetsart University All rights reserved

From the results in Figure 16 to 18, it may be concluded that activated carbon could delayed the phase transition of TiO_2 from amorphous to anatase phase. The anatase phase of the prepared-TiO_2 already appeared at the calcination temperature of 300ºC

2. Morphology

2.1. Scanning electron microscope (SEM)

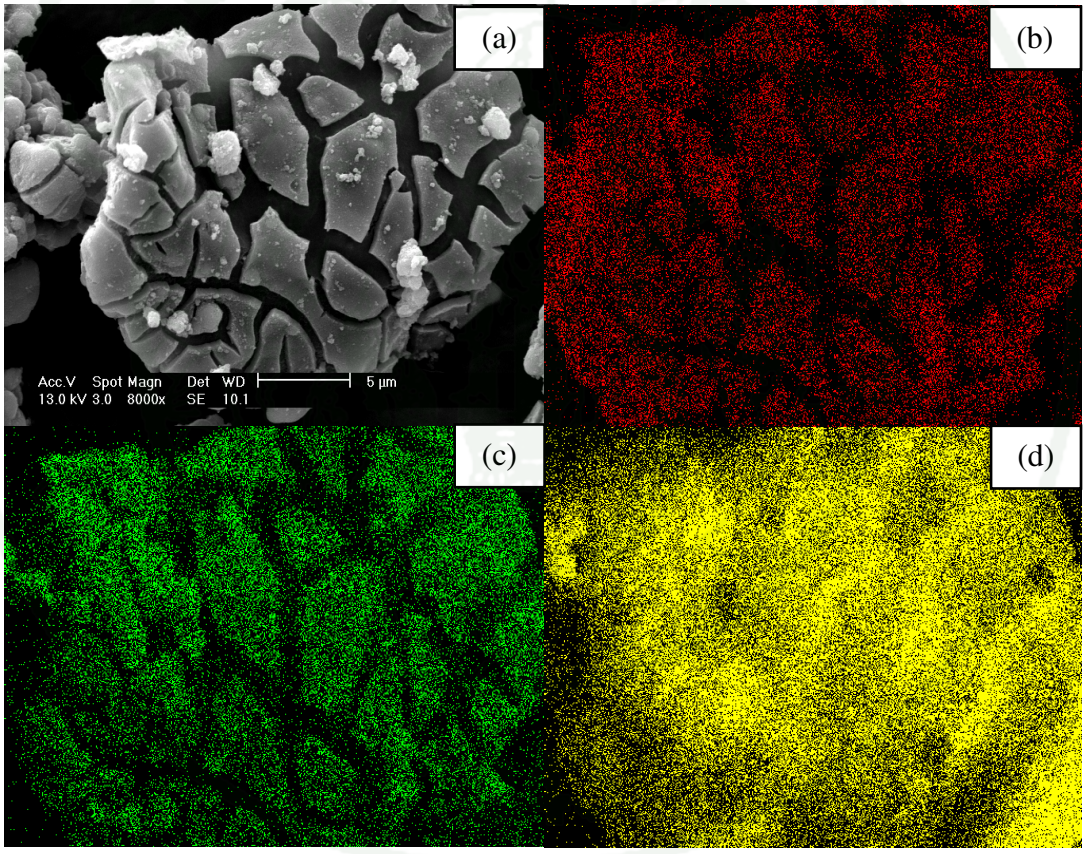

Figure 19 SEM image and mapping images of TiO_2/AC using titanium(IV) isopropoxide as a titania precursor calcined at 400ºC;
(a) SEM image, (b) mapping image of Ti, (c) mapping image of O and (d) mapping image of C

Copyright by Kasetsart University All rights reserved

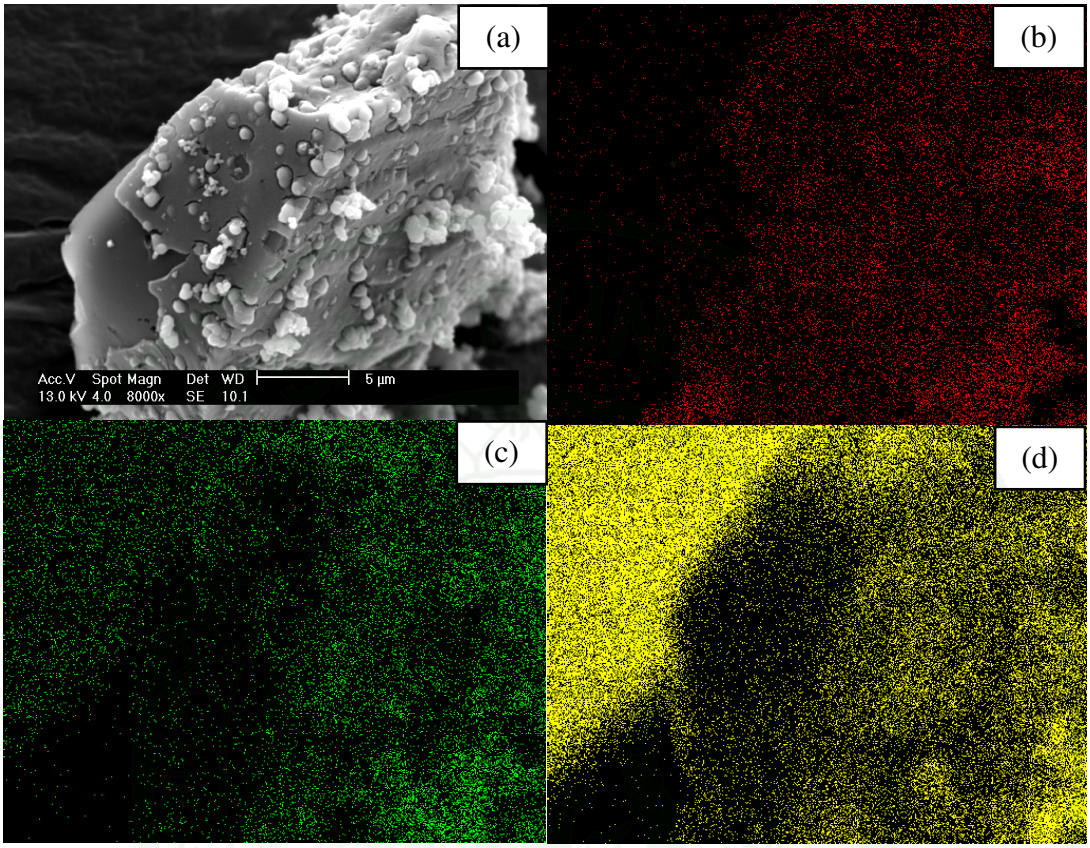

Figure 20 SEM image and mapping images of TiO_2/AC using titanium(IV) isopropoxide as a titania precursor calcined at 400ºC;
(a) SEM image, (b) mapping image of Ti, (c) mapping image of O and (d) mapping image of C

Figure 19 and 20 show surface morphology (Figure 19a and 20a) and mapping images (Figure 19b-c and 20b-c) of TiO_2/AC prepared by titanium(IV) isopropoxide and titanium(IV) n-butoxide, respectively. From SEM result of both catalysts, it can be seen that mapping image of Ti and O matched with the bright zone of SEM image and mapping image of C matched with the dark zone of SEM image. This can be indicated that TiO_2 (bright zone) could covered and spread on surface of AC (dark zone).

Copyright by Kasetsart University All rights reserved

Noticeably, the surface morphology of TiO_2/AC prepared by titanium(IV) n-butoxide (Figure 19a) had more TiO_2-film spreading throughout the AC than TiO_2/AC prepared by titanium(IV) isopropoxide (Figure 20a). This may be because the titanium(IV) n-butoxide precursor had bulky ligands that could slow the rate of hydrolysis reaction. Hence, the titanium(IV) n-butoxide was gradually hydrolyzed which caused more continuous TiO_2-film covered on AC surface than titanium(IV) isopropoxide.

2.2. Transmission electron microscope (TEM)

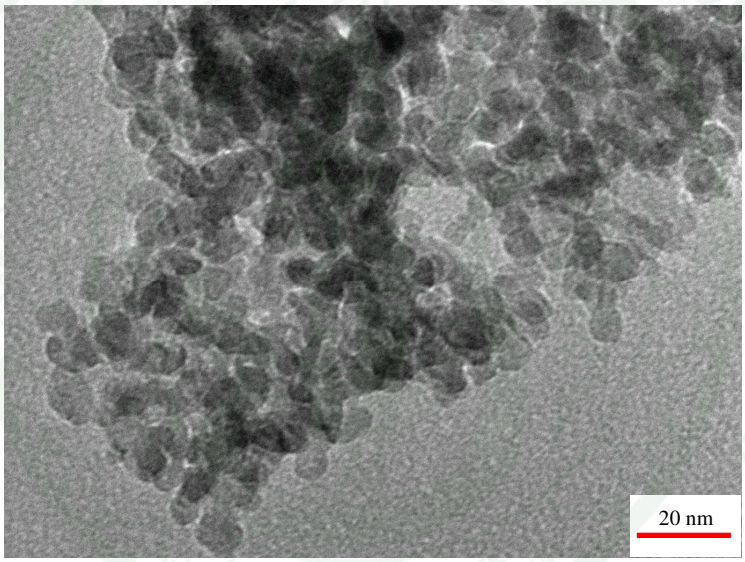

Figure 21 TEM image of TiO_2/AC using titanium(IV) isopropoxide as a titania precursor calcined at 400ºC

Copyright by Kasetsart University All rights reserved

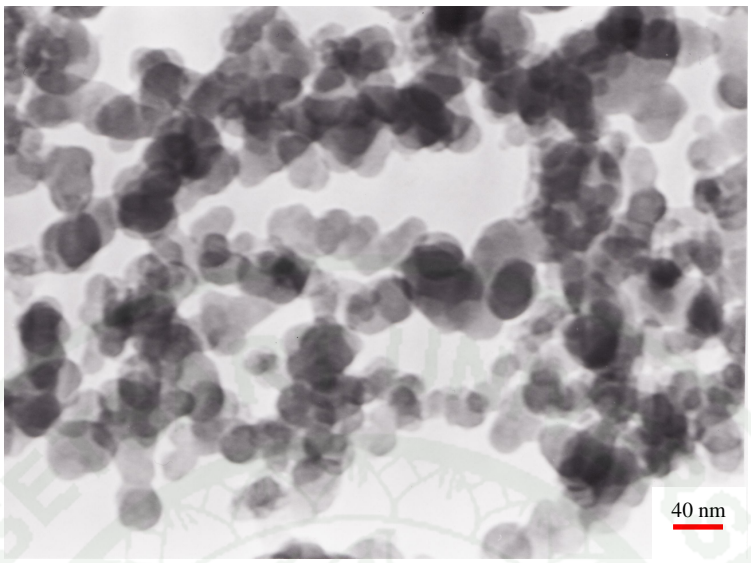

Figure 22 TEM image of TiO_2/AC using titanium(IV) n-butoxide as a titania precursor calcined at 400ºC

The crystallite sizes of TiO_2/AC calcined at 400ºC with different precursors were determined by TEM images as shown in Figure 21 and 22, respectively. The TiO_2/AC using titanium(IV) isopropoxide had crystallite size of 10 nm, approximately. There results were in agreement with the XRD results. For the TiO_2/ AC using titanium(IV) n-butoxide, its crystallite size was approximately 20 nm probably might be due to thermal decomposition of remaining titamium(IV) n-butoxide resulting in rapid agglomeration of TiO_2.

Copyright by Kasetsart University All rights reserved

3. Adsorption Isotherm

The adsorption isotherm indicates how the adsorption molecules distribute between the liquid phase and the solid phase when the adsorption process reaches an equilibrium state. The analysis of the adsorption data by fitting to different isotherm models is an important step to find the suitable model that can be used for design purpose (Hameed *et al.*, 2007). Several models have been published in the literature to describe the experimental data of adsorption isotherms. From the results in the present experiments, the adsorption data were fitted to the Langmuir isotherm model that indicated the monolayer adsorption system, which composed of chemisorptions and physisorption. Therefore, the Langmuir isotherm was used to describe the relationship between the amount of phenol adsorbed and its equilibrium concentration. The Langmuir isotherm of AC, AC-400, TiO_2/AC using titanium(IV) isopropoxide and titanium (IV) n-butoxide as precursors are shown in Figure 23 to 26.

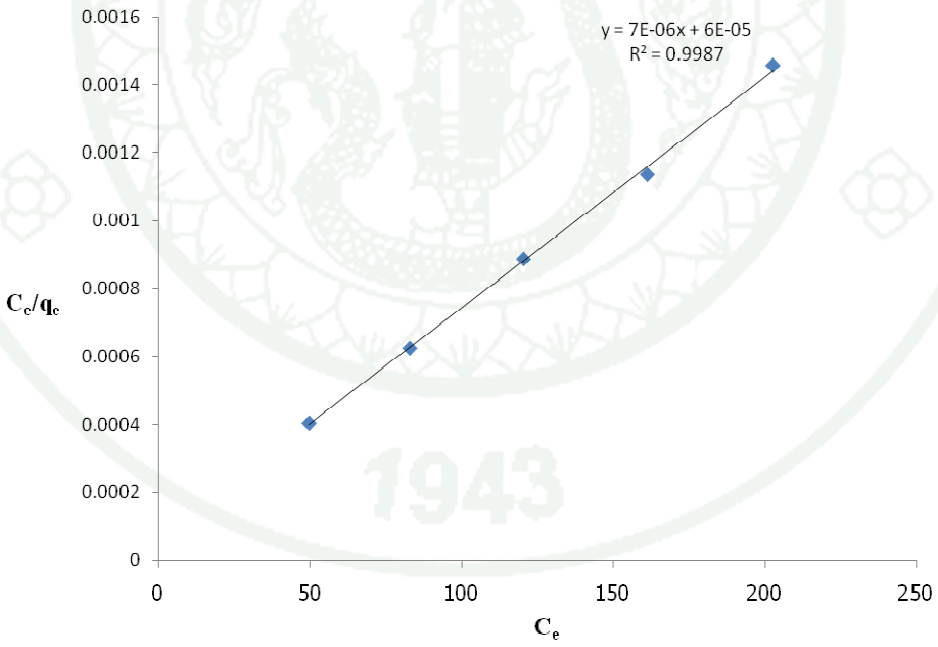

Figure 23 The Langmuir isotherm of phenol onto activated carbon (AC).

Copyright by Kasetsart University All rights reserved

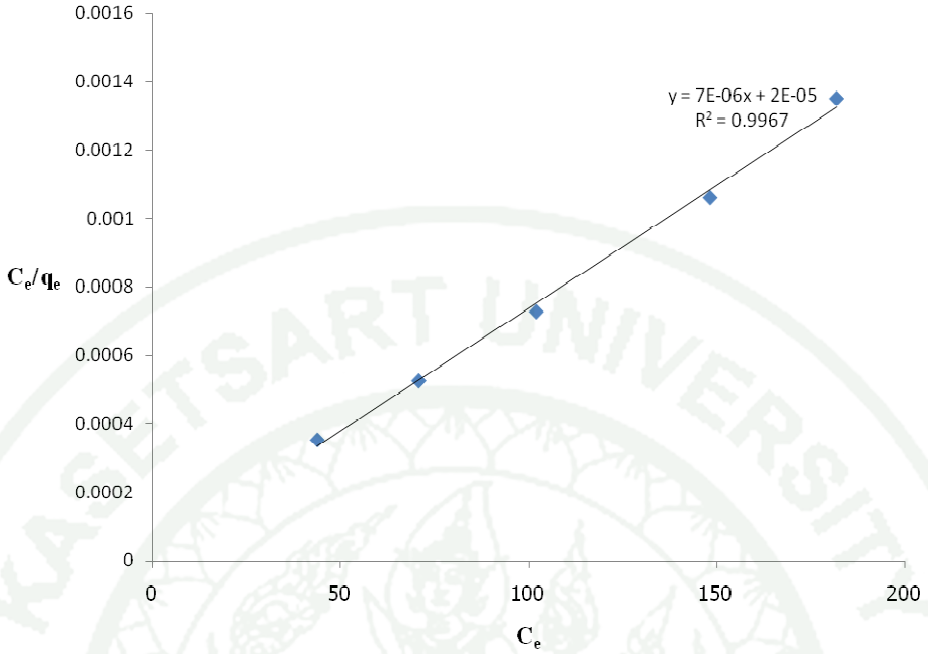

Figure 24 The Langmuir isotherm of phenol onto activated carbon calcined at 400ºC (AC-400).

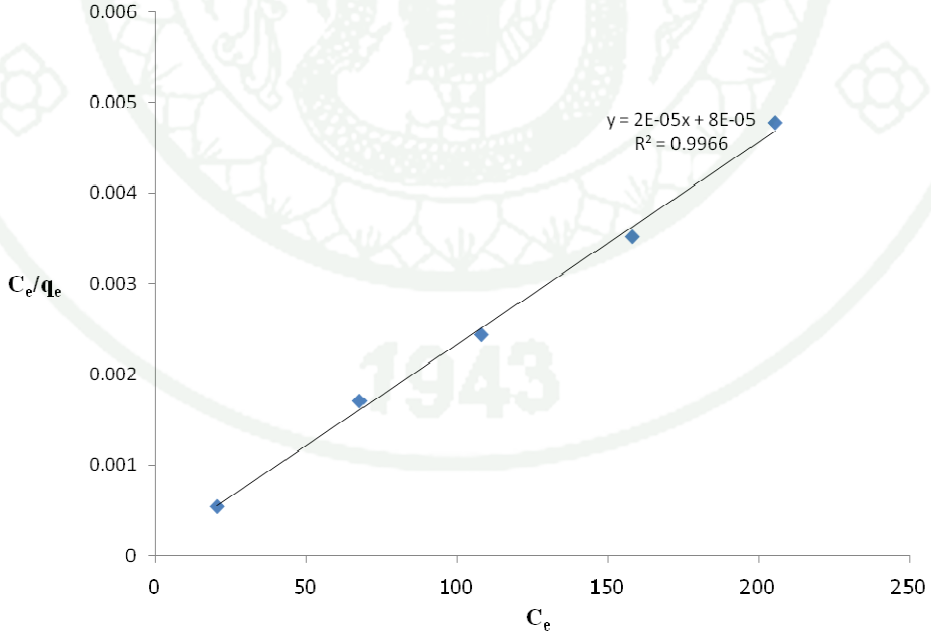

Figure 25 The Langmuir isotherm of phenol onto TiO_2/AC using titanium(IV) isopropoxide as a precursor.

Copyright by Kasetsart University All rights reserved

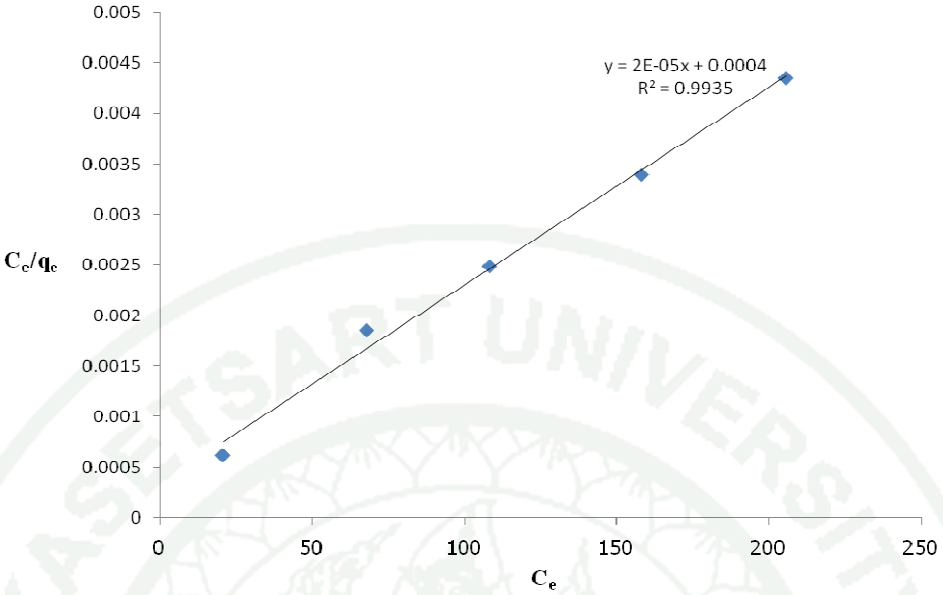

Figure 26 The Langmuir isotherm of phenol onto TiO_2/AC using titanium(IV) n-butoxide as a precursor.

The Langmuir adsorption constant (b), adsorption capacity (Q), contact time and R^2 of each catalysts (TiO_2/AC, AC and AC-400) are reported in Table 5. A Langmuir adsorption constant (b) of catalyst exhibited that thermodynamic stability of catalyst while it adsorbed phenol, and adsorption capacity (Q) of catalyst showed that how much the phenol could be adsorbed by catalyst. For the Langmuir isotherm, the procedure used to fit adsorption isotherm was adapted from Hameed *et al.*, which plotted a graph between C_e/ q_e and C_e. The relative coefficient (R^2) which obtained from plotted was close to 1. The Langmuir adsorption constant (b) and adsorption capacity (Q) from Langmuir equation as followed:

$$\frac{C_e}{q_e} = \frac{1}{bQ} + \frac{C_e}{Q}$$

C_e = liquid-phase concentration of phenol at equilibrium (mg/l)

q_e = equilibrium of solid-phase absorbed concentration (mg/g)

b = adsorption constant of Langmuir adsorption isotherm (l/mg)

Q = the maximum surface coverage (monolayer formation) (mg/g)

Copyright by Kasetsart University All rights reserved

Table 5 shows that Langmuir constant of AC and AC-400 are 34.9×10^{-2} and 11.7×10^{-2} l/mg respectively with similar maximum adsorption capacity (Q) of 1.4×10^{5} mg/g. These implied that the calcination at 400ºC caused decreasing adsorption activity of AC-400 due to the lost of some functional groups at the surface of AC by increasing of calcination temperature, but still had adsorption capacity as before calcination (Dabrowski *et al.*, 2005). The AC-400 was used as a reference comparing with TiO_2/AC photocatalyst.

The TiO_2/AC photocatalysts prepared form titanium(IV) isopropoxide and titanium(IV) n-butoxide as a precursor have similar Q-value at 5.0×10^{4} mg/g, and their Langmuir constant are 25.0×10^{-2} l/m and 5.0×10^{-2} l/mg, respectively. The Langmuir constant indicated that the catalyst had adsorption ability of phenol in terms of thermodynamic stability. These indicated that both of TiO_2/AC using titanium(IV) isopropoxide and titanium(IV) n-butoxide had more thermodynamic stability than Degussa P25 TiO_2. Moreover, the Q-value could be calculated together with size of phenol (Zhang *et al.*, 2006) in order to obtain estimated surface area of catalyst as shown in Appendix E.

Regarding the surface area, The BET surface area of AC, AC-400 and TiO_2/AC (prepared by using titanium(IV) isopropoxide).were 1110, 1056 and 441 m^2/g. It could be indicated that surface area from BET was similar trend with estimated surface area that was calculated from Q-value.

Copyright by Kasetsart University All rights reserved

Table 5 The data from Langmuir isotherm of phenol using various catalysts.

Sample	Precursor	Langmuir constant (b) (l/mg)	Adsorption capacity (Q) (mg/g)	Surface area [b] (m^2)	Contact time (h.)	R^2
AC	-	34.9×10^{-2}	1.4×10^{5}	$2.14x10^{3}$	3	0.9967
AC-400	-	11.7×10^{-2}	1.4×10^{5}	$2.14x10^{3}$	1	0.9987
TiO_2/AC calcined at 400ºC	Titanium(IV) isopropoxide	25.0×10^{-2}	5.0×10^{4}	$7.66x10^{2}$	1	0.9966
	Titanium(IV) n-butoxide	5.0×10^{-2}	5.0×10^{4}	$7.66x10^{2}$	1	0.9935
Degussa P25 [a]	-	3.3×10^{-4}	3.1×10^{3}	47	1	0.9900

[a] J.Matos et al. (1998)

[b] Calculation of surface area of phenol was shown in Appendix E.

Copyright by Kasetsart University All rights reserved

4. Removal of phenol

4.1. Calibration curve of standard phenol

A sereies of solution of phenol was quantified by UV-Vis spectrophotometry. The absorbance of maximum wavelenght at 270 nm was plotted against concentration of phenol from 5 to 25 ppm, as shown in Figure 27.

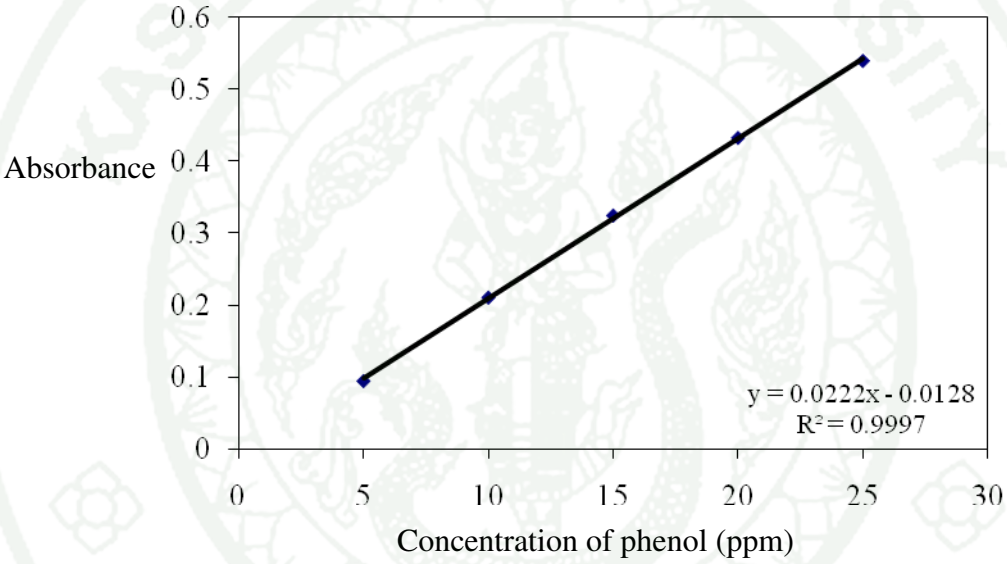

Figure 27 Calibration curve of standard phenol at concentration from 5 to 25 ppm

4.2. Optimal amount of catalyst

The various amounts of TiO_2/AC using titanium(IV) isopropoxide as a precursor were used to remove phenol from 200 ml of 100 ppm phenol solution. As shown in Figure 28, the removal results of catalyst are composed of adsorption activity (first 60 min) and photodegradation activity (after 60 min). From Table 6, it indicates that the higher amount of catalyst, the higher removal efficiency. Therefore, 0.4 g of catalyst was selected to remove phenol and acid orange 7.

Copyright by Kasetsart University All rights reserved

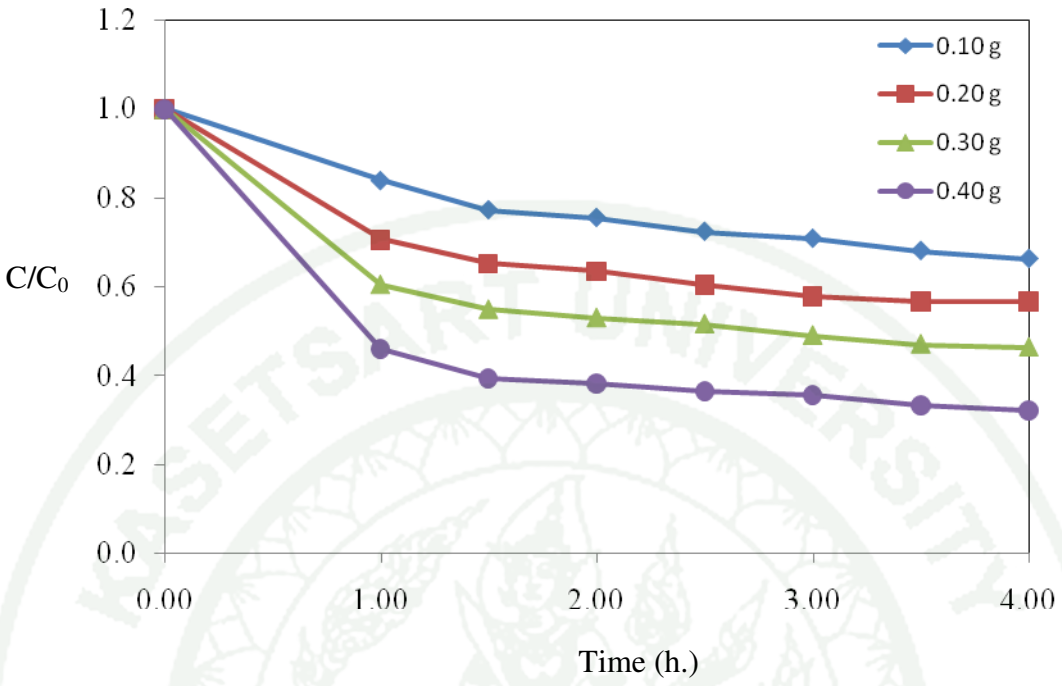

Figure 28 The removal of phenol from 200 ml of 100 ppm phenol solution by 0.1 g, 0.2 g, 0.3 g and 0.4 g of TiO_2/AC using titanium(IV) isopropoxide as precursor.

Table 6 Percentage of phenol removal for the photodegradation of phenol from 200 ml of 100 ppm phenol by various amount of TiO_2/AC (prepared by titanium(IV) isopropoxide as precursor).

Catalysts	Amount of catalyst (g)	% Removal		
		Adsorption	Degradation	Total
TiO_2/AC	0.10	16.17±0.035	14.04±0.063	30.22±0.098
	0.20	29.47±0.025	13.92±0.049	43.39±0.074
	0.30	39.56±0.016	14.12±0.013	53.69±0.029
	0.40	54.14±0.034	13.88±0.047	68.03±0.081

Copyright by Kasetsart University All rights reserved

4.3. Photodegradation of phenol

The concentration of phenol after reached adsorption equilibrium (first hour) and photodegraded in each 30 minutes interval under artificial UV light were quantified by UV-Vis spectrophotometry at the maximum wavelenght of 270 nm. The removal results are shown in Figure 29 to 33, which composed of adsorption activity (first 60 min) and photodegradation activity (after 60 min). Figure 29, 30, 31 and 32 show the removal of phenol using prepared-TiO_2, P25 TiO_2, AC and TiO_2/AC (prepared by using titanium(IV) isopropoxide as a precursor) respectively, under the same condition, 200 ml of 100 ppm phenol solution with 0.4 g of catalyst. The prepared-TiO_2 and TiO_2/AC photocatalyst were calcined at 400ºC. The %removal of phenol using prepared-TiO_2 and P25 TiO_2 were only 5.55% and 13.80%. Nevertheless, the % removal using TiO_2/AC and AC were 67.95% and 57.26% respectively, but AC showed only adsorption activity. The results indicated that the TiO_2/AC photocatalyst was more effective for removal of phenol than AC, prepared-TiO_2 and P25 TiO_2. The reason for the higher %removal of phenol using P25 than prepared-TiO_2 may due to the mixed-phase of P25 TiO_2. As previous studies, the mixing phase between anatase (75%) and rutile (25%) of P25 TiO_2 could improve the photocatalytic activity of TiO_2.(Carp *et al.*, 2004)

Copyright by Kasetsart University All rights reserved

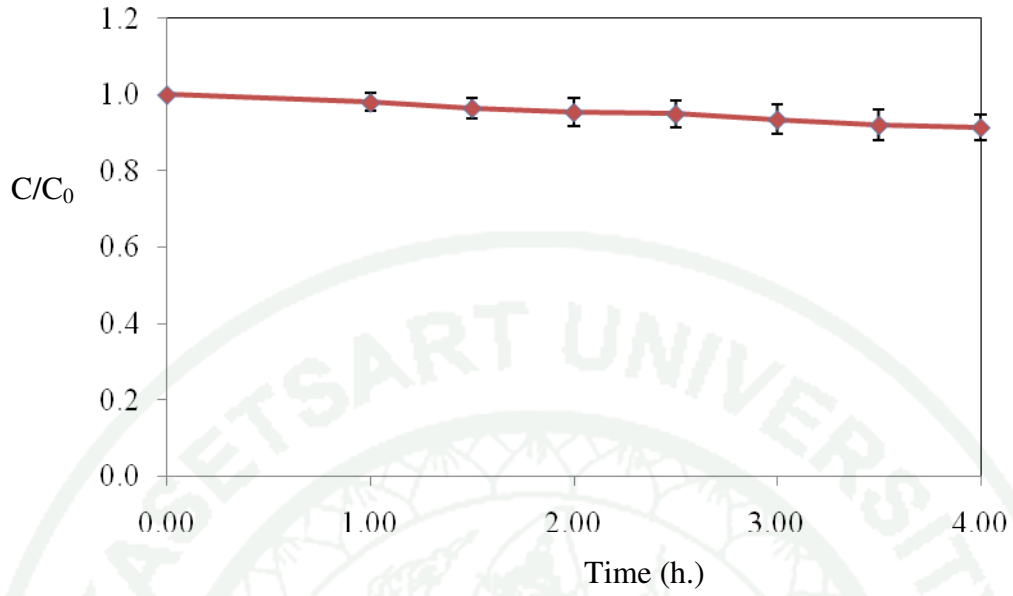

Figure 29 The removal of phenol from 200 ml of 100 ppm phenol solution by 0.4 g of prepared-TiO_2.

C/C_0 is the ratio of remaining concentration of phenol devide by initial concentration.

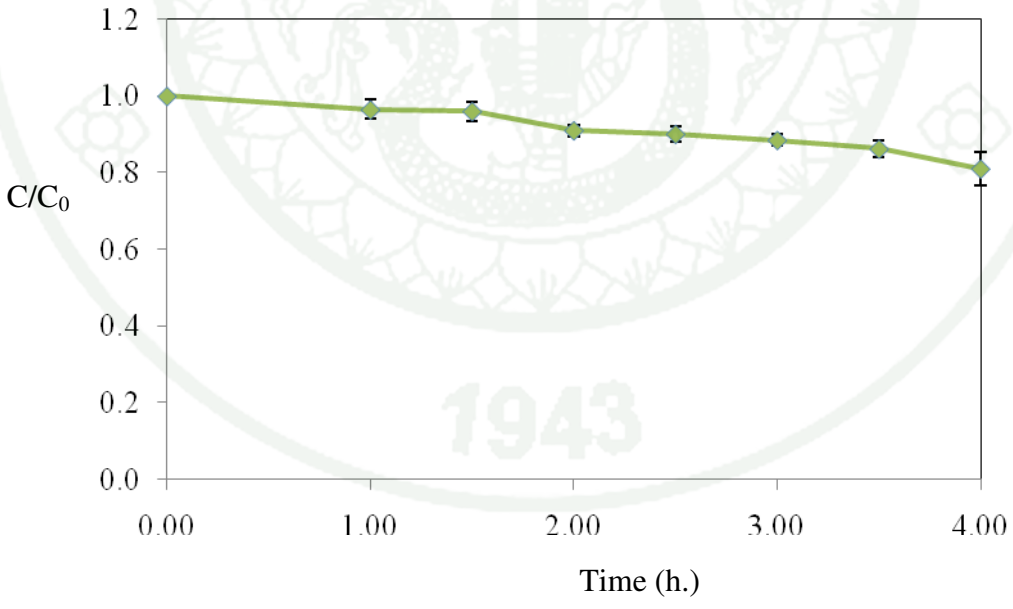

Figure 30 The removal of phenol from 200 ml of 100 ppm phenol solution by 0.4 g of P25 TiO_2.

Copyright by Kasetsart University All rights reserved

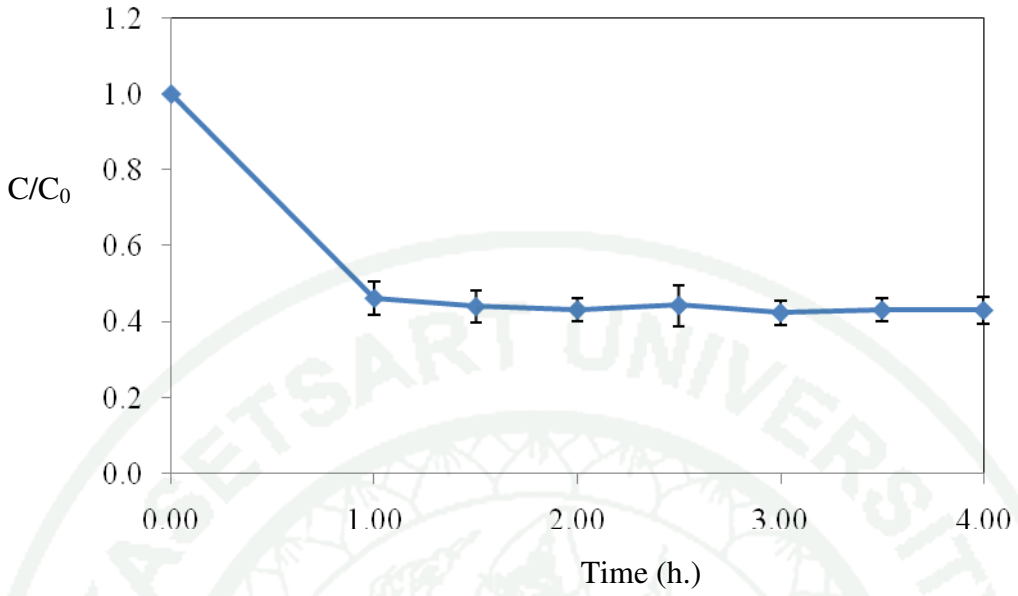

Figure 31 The removal of phenol from 200 ml of 100 ppm phenol solution by 0.4 g of AC.

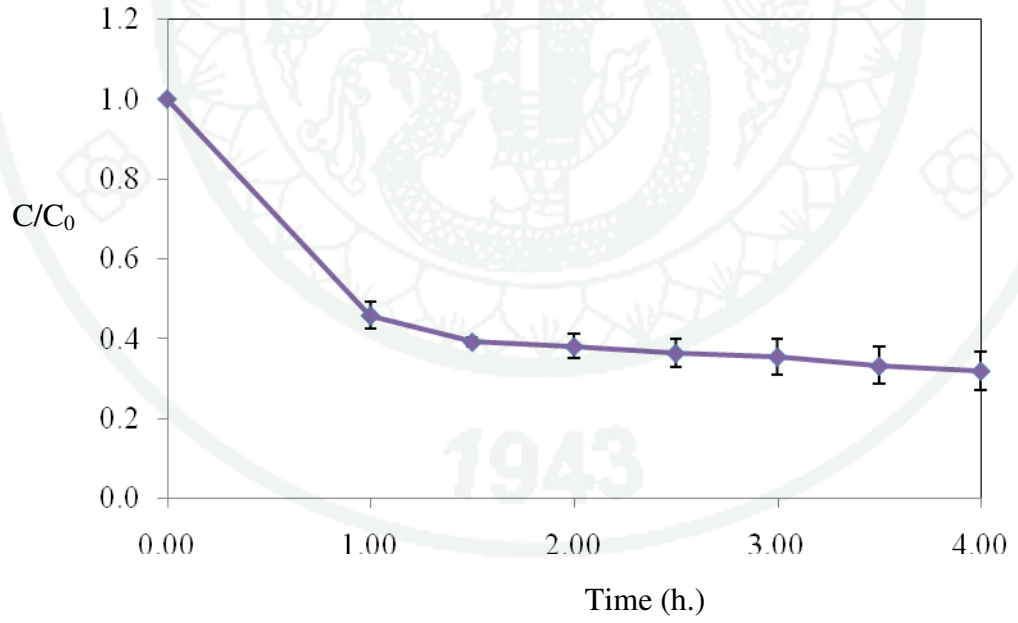

Figure 32 The removal of phenol from 200 ml of 100 ppm phenol solution by 0.4 g of TiO_2/AC.

Copyright by Kasetsart University All rights reserved

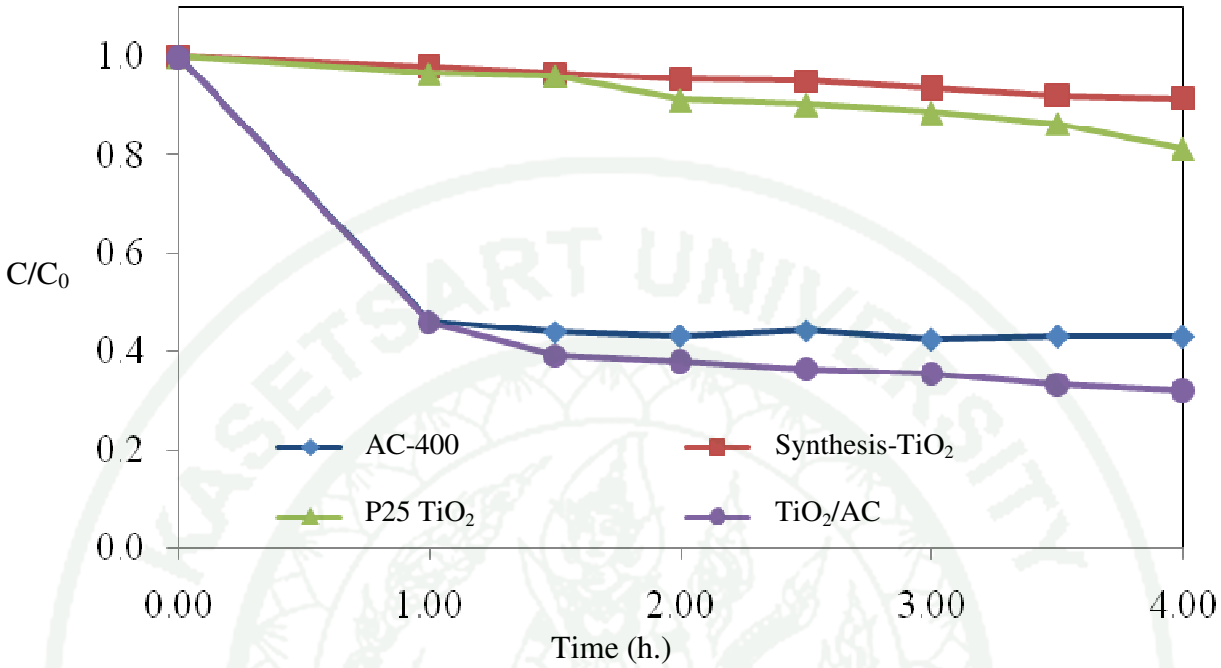

Figure 33 The removal of phenol from 200 ml of 100 ppm phenol solution by 0.4 g of AC-400, prepared-TiO_2, P25 TiO_2 and TiO_2/AC calcined at 400ºC.

In case of TiO_2/AC photocatalyst, %removal of phenol was higher than prepared-TiO_2 and P25 TiO_2. Propose that the rate of degradation was the first order reaction from the plotting between $\ln(C_0/C)$ and time as shown in Figure 34 to 36. The rate constant (k) is related to the slope of the plot which can be calculated by assumption that the degradation of phenol is first order reaction. The rate constant (k) of photocatalytic degradation of phenol with different catalysts are shown in Table 7. The calculation in full is shown in Appendix D. However, the rate of degradation of AC-400 colud not be determined, because it showed only adsorption activity.

Copyright by Kasetsart University All rights reserved

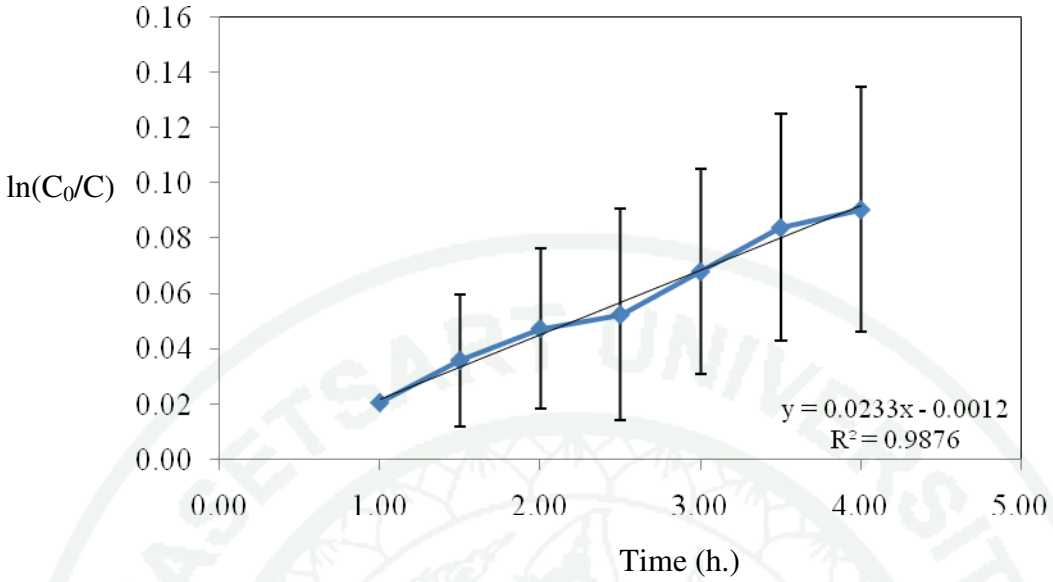

Figure 34 The relation between $\ln C_0/C$ and time (h) of photodegradation reaction of phenol from 200 ml of 100 ppm phenol solution by 0.4g prepared-TiO_2.

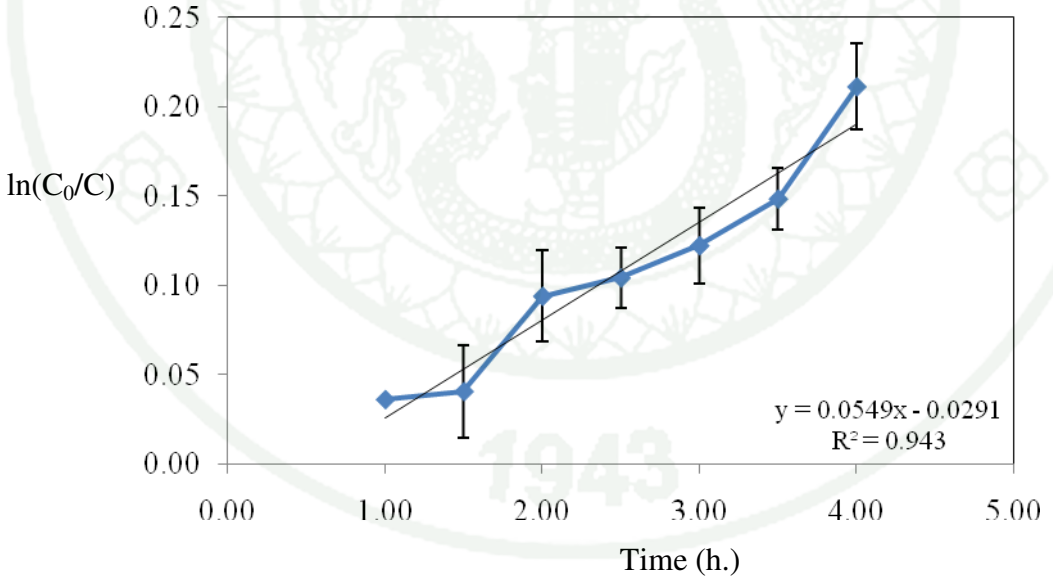

Figure 35 The relation between $\ln C_0/C$ and time (h) of photodegradation reaction of phenol from 200 ml of 100 ppm phenol solution by 0.4g P25 TiO_2.

Copyright by Kasetsart University All rights reserved

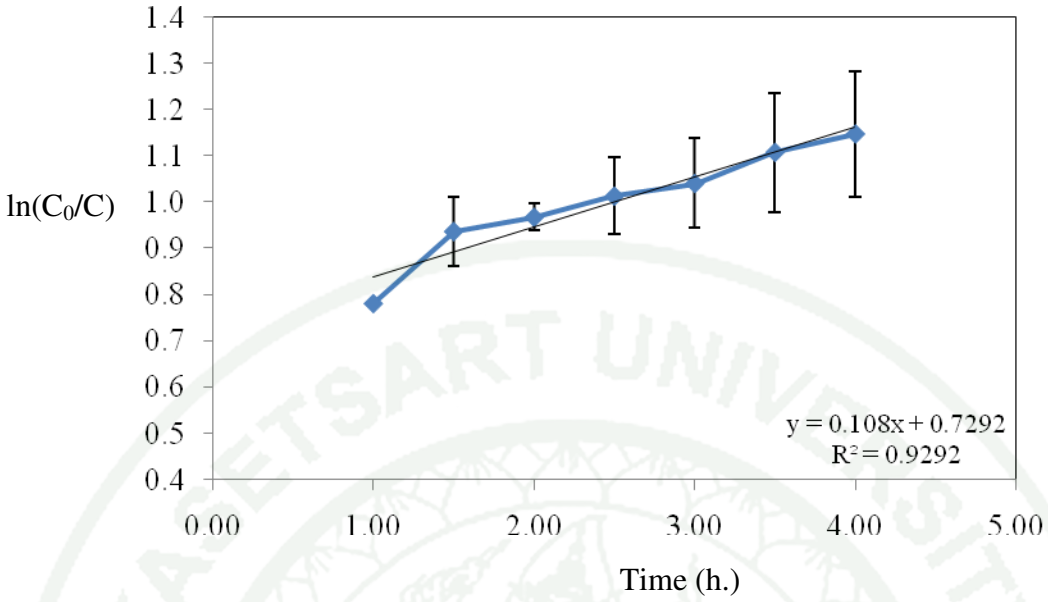

Figure 36 The relation between $\ln C_0/C$ and time (h) of photodegradation reaction of phenol from 200 ml of 100 ppm phenol solution by 0.4g TiO_2/AC.

Table 7 Percentage of phenol removal and rate constant for the photodegradation of phenol from 200 ml of 100 ppm phenol by 0.4g of AC, 0.4g of prepared-TiO_2, 0.4g of P25 TiO_2 and 0.4g of TiO_2/AC (prepared by using titanium(IV) isopropoxide as precursor).

Catalysts	% Removal	R^2	Rate constant[a] (h^{-1})
Prepared-TiO_2	8.60	0.9876	0.0233
P25 TiO_2	18.95	0.9340	0.0520
AC-400	57.01	-*	-*
TiO_2/AC	68.03	0.9292	0.1080

* No photodegradation occur.

[a] Rate constants obtained form slope of graph in Figure 34 to 36.

Copyright by Kasetsart University All rights reserved

The rate constant of the photodegradation using TiO_2/AC was faster than using prepared-TiO_2 and P25 TiO_2 due to the particle of TiO_2 of TiO_2/AC which was smaller than the prepared-TiO_2 and P25 TiO_2. This may be because the titania precursor was hardly hydrolyzed by adsorption of AC in preparation step, therefore TiO_2 particle was gradually occurred by do not had agglomeration effect. It can be concluded that the supporting of AC could improve the photocatalytic activity of TiO_2 under the artificial UV light.

The prepared-TiO_2 catalysts with various calcination temperatures and without calcination were used to degrade phenol under UV-irradiation and the results are shown in Figure 37 to 41.

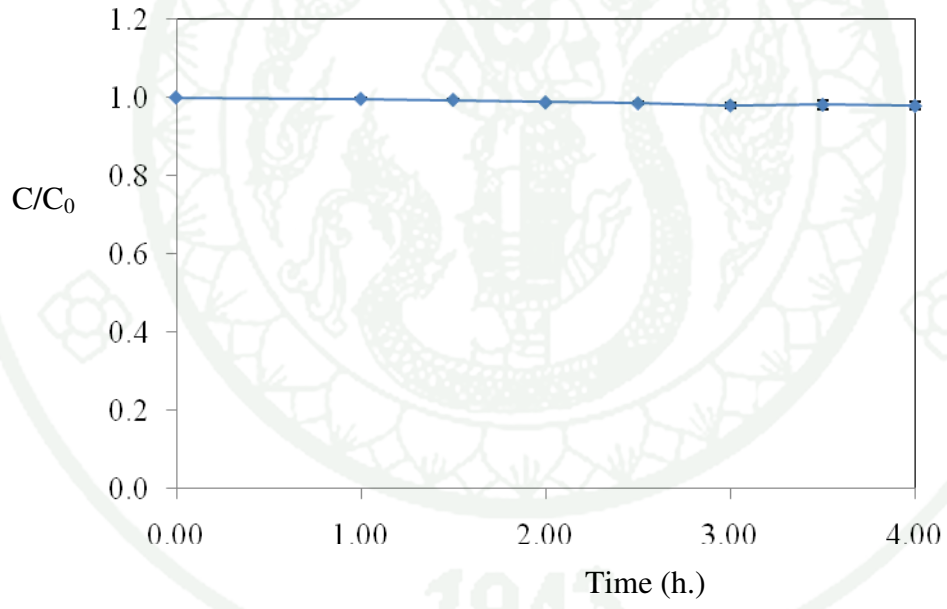

Figure 37 The removal of phenol from 200 ml of 100 ppm phenol using 0.4 g of prepared-TiO_2 without calcination.

Copyright by Kasetsart University All rights reserved

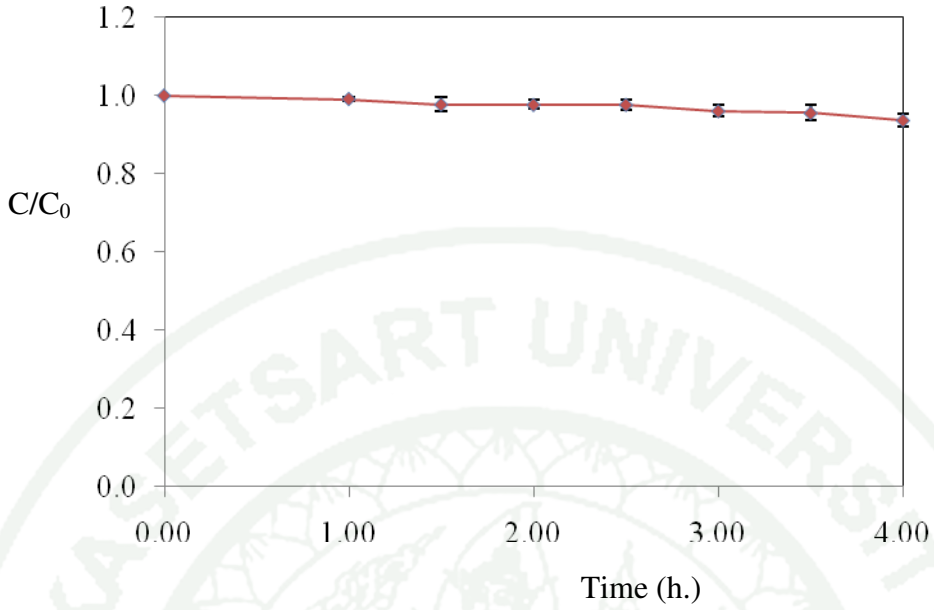

Figure 38 The removal of phenol from 200 ml of 100 ppm phenol by 0.4 g of prepared-TiO_2 calcined at 300ºC.

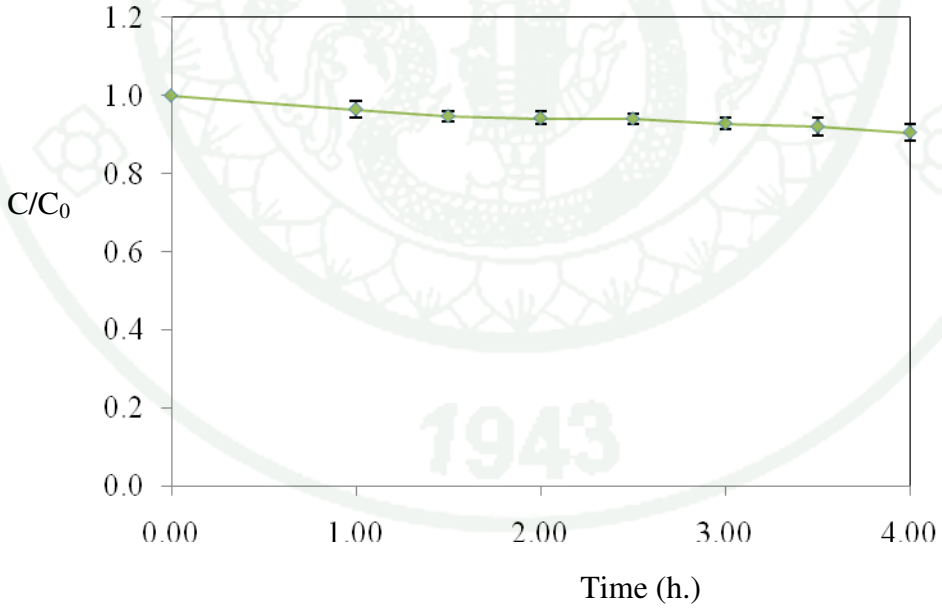

Figure 39 The removal of phenol from 200 ml of 100 ppm phenol by 0.4 g of prepared-TiO_2 calcined at 400ºC.

Copyright by Kasetsart University All rights reserved

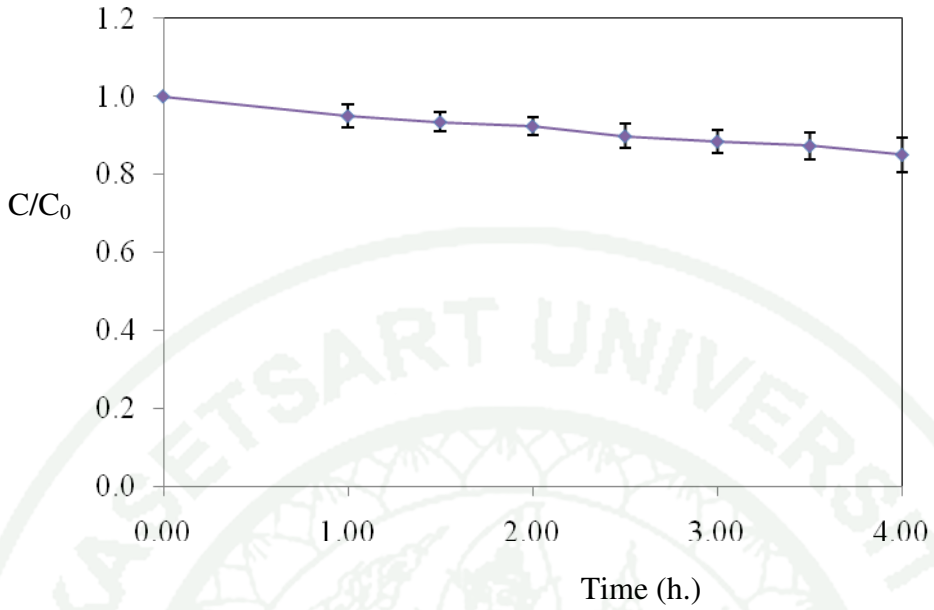

Figure 40 The removal of phenol from 200 ml of 100 ppm phenol by 0.4 g of prepared-TiO_2 calcined at 500ºC.

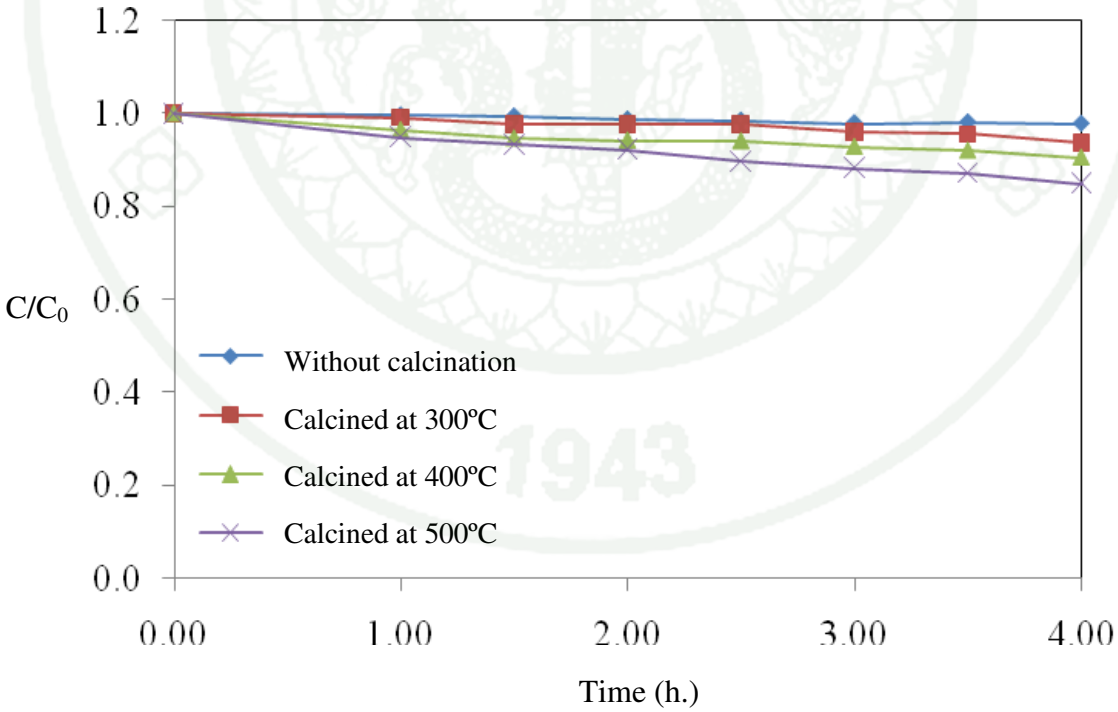

Figure 41 The removal of phenol from 200 ml of 100 ppm phenol by 0.4 g of prepared-TiO_2 without calcination and calcined at 300-500ºC.

Copyright by Kasetsart University All rights reserved

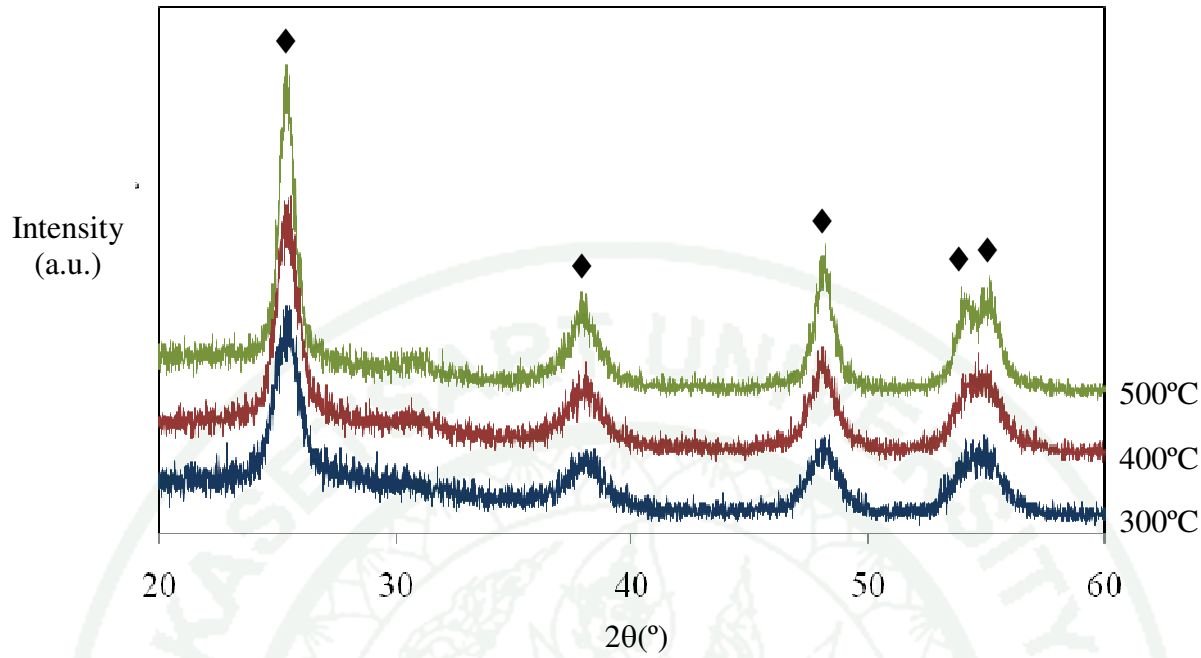

Figure 42 The XRD patterns of prepared-TiO_2 using titanium(IV) isopropoxide as titania precursor at various calcination temperatures.

(♦ for the anatase phase)

The removal of phenol from solution using prepared-TiO_2 without calcination and with calcined at 300ºC, 400ºC and 500ºC are shown in Figure 41 which composed of adsorption activity (first 60 min) and photodegradation activity (after 60 min). The %removal of prepared-TiO_2 without calcination was 3.29%. which lower than the prepared-TiO_2 calcined at 300ºC, 400ºC and 500ºC which were 6.28%, 9.45% and 15.03% respectively.(Table 8).

Figure 42 shows the XRD patterns of prepared-TiO_2 at various calcination temperatures. The XRD patterns of all calcined prepared-TiO_2 exhibit the anatase phase (at 2θ of 25.4º, 38.1º, 48.2º, 53.9º and 55.1º, JCPDS file No.21-1272). As calculated from the Sherrer's equation, the crystallite size of prepared-TiO_2 calcined 300ºC, 400ºC and 500ºC were 9.5, 10.7 and 14.0 nm, respectively. This implied that the higher calcination temperature, the higher cystallinity and the larger crystallite size of TiO_2.

Copyright by Kasetsart University All rights reserved

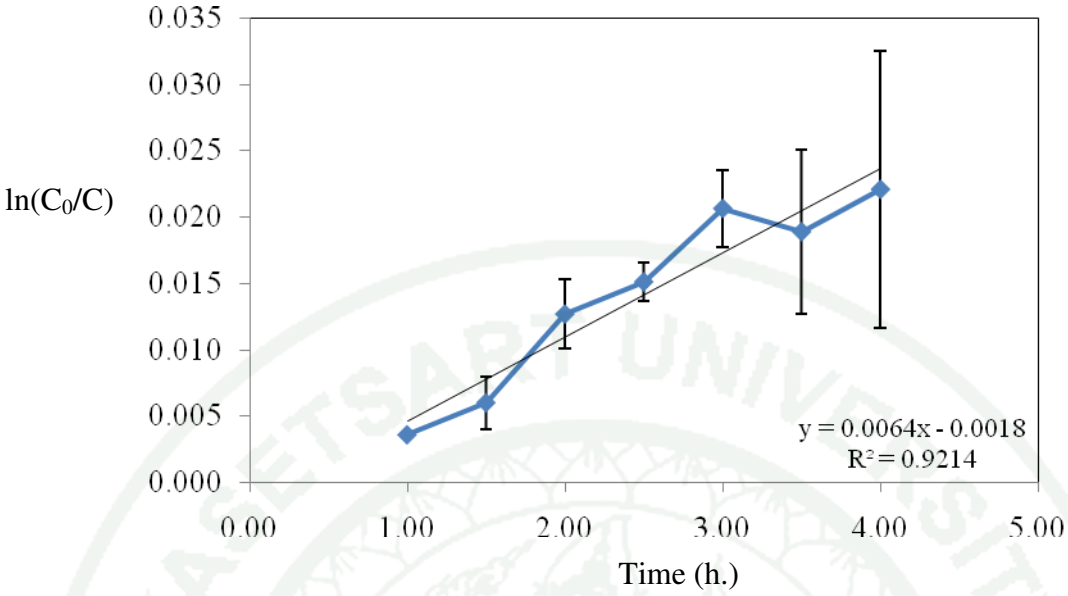

Figure 43 The relation between $\ln C_0/C$ and time (h) of photodegradation reaction of phenol from 200 ml of 100 ppm phenol solution by 0.4g of prepared-TiO_2 without calcination.

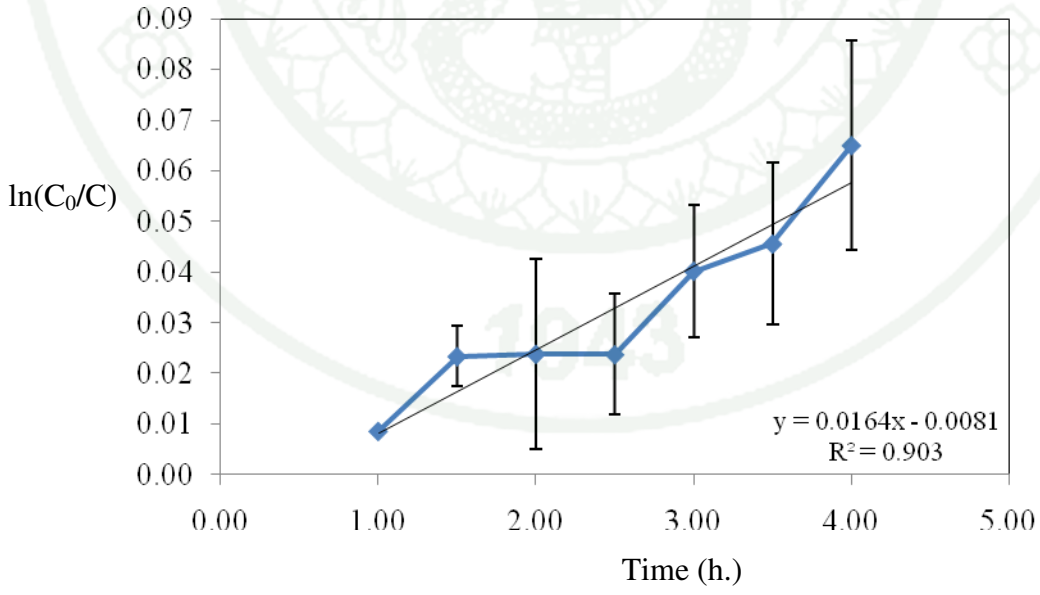

Figure 44 The relation between $\ln C_0/C$ and time (h) of photodegradation reaction of phenol from 200 ml of 100 ppm phenol solution by 0.4g of prepared-TiO_2 calcined at 300ºC.

Copyright by Kasetsart University All rights reserved

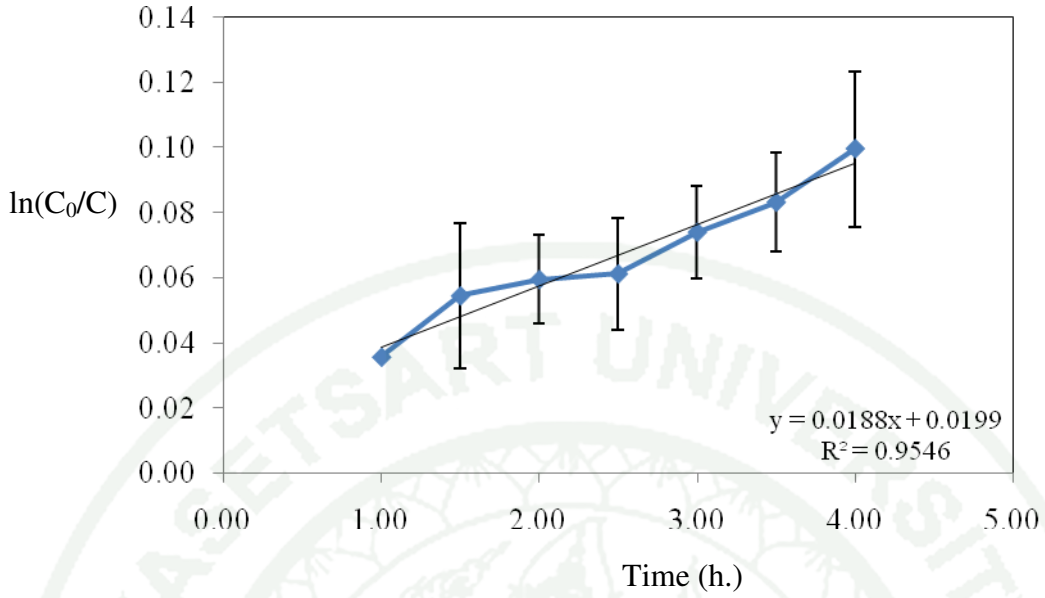

Figure 45 The relation between $\ln C_0/C$ and time (h) of photodegradation reaction of phenol from 200 ml of 100 ppm phenol solution by 0.4g of prepared-TiO_2 calcined at 400ºC.

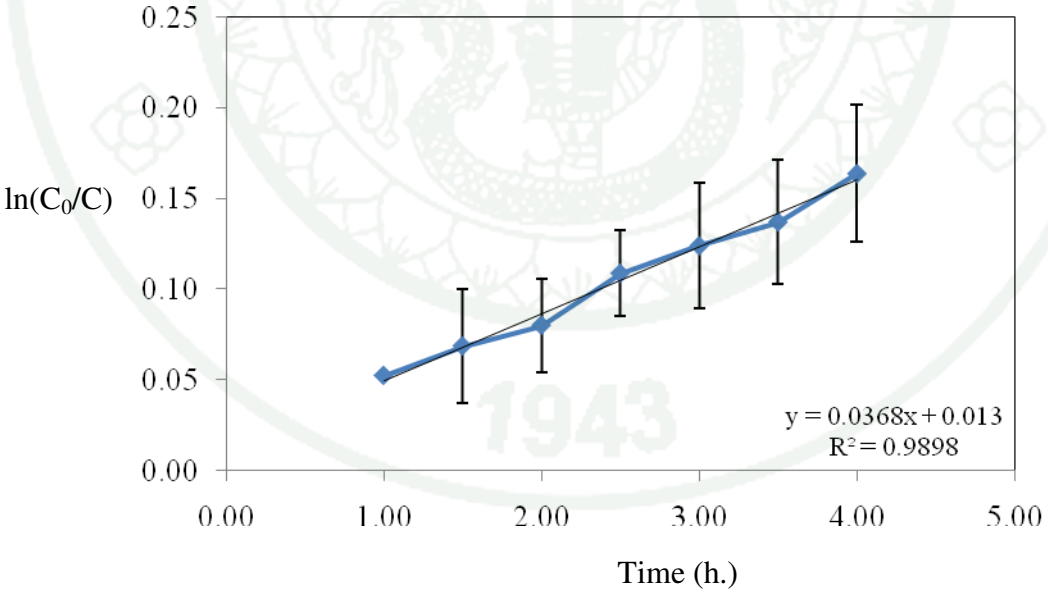

Figure 46 The relation between $\ln C_0/C$ and time (h) of photodegradation reaction of phenol from 200 ml of 100 ppm phenol solution by 0.4g of prepared-TiO_2 calcined at 500ºC.

Copyright by Kasetsart University All rights reserved

The rate of degradation (Figure 43 to 46) and %removal of phenol using prepared-TiO_2 catalysts are shown in Table 8. The results show that the prepared-TiO_2 calcined 500ºC has higher rate constant and %removal of phenol than the prepared-TiO_2 without calcination and calcined at 300ºC and 400ºC. This may be because the higher cystallinity in anatase phase of the prepared TiO_2 calcined at 500ºC.

Table 8 Percentage of phenol removal and rate constant for the photodegradation of phenol from 200 ml of 100 ppm phenol by 0.4g of prepared-TiO_2.

Catalysts	% Removal	R^2	Rate constant[a] (h^{-1})
Without calcination	3.29±0.011	0.9214	0.0064
Calcined at 300ºC	6.28±0.021	0.9030	0.0164
Calcined at 400ºC	9.45±0.041	0.9546	0.0188
Calcined at 500ºC	15.03±0.075	0.9898	0.0368

[a] Rate constants obtained form slope of graph in Figure 43 to 46.

The TiO_2/AC catalysts with various calcination temperatures and without calcination were used to degrade phenol under UV-irradiation and the results are shown in Figure 47 to 51. From the results, the TiO_2/AC calcined at 400ºC exhibited the highest %removal compared to TiO_2/AC calcined at 300ºC, 500ºC and without calcination under the same condition.

Copyright by Kasetsart University. All rights reserved

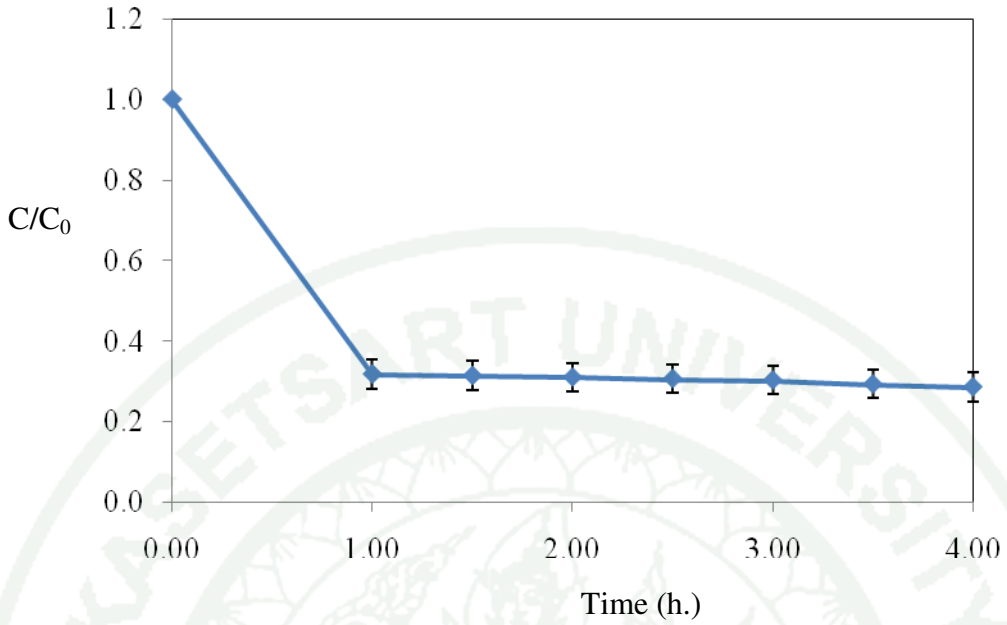

Figure 47 The removal of phenol from 200 ml of 100 ppm phenol by 0.4 g of TiO_2/AC using titanium(IV) isopropoxide without calcination.

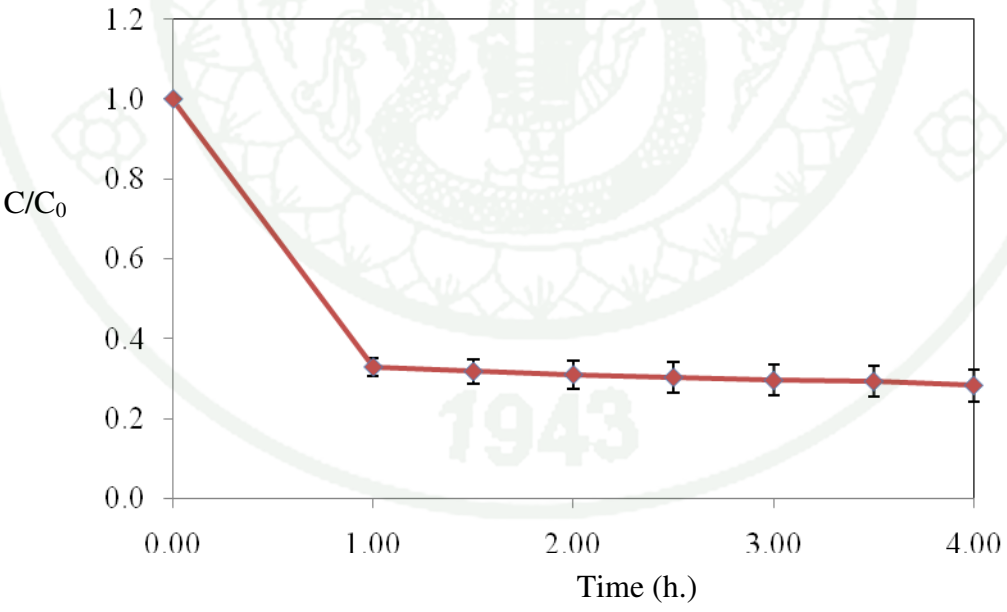

Figure 48 The removal of phenol from 200 ml of 100 ppm phenol by 0.4 g of TiO_2/AC using titanium(IV) isopropoxide calcined at 300ºC.

Copyright by Kasetsart University All rights reserved

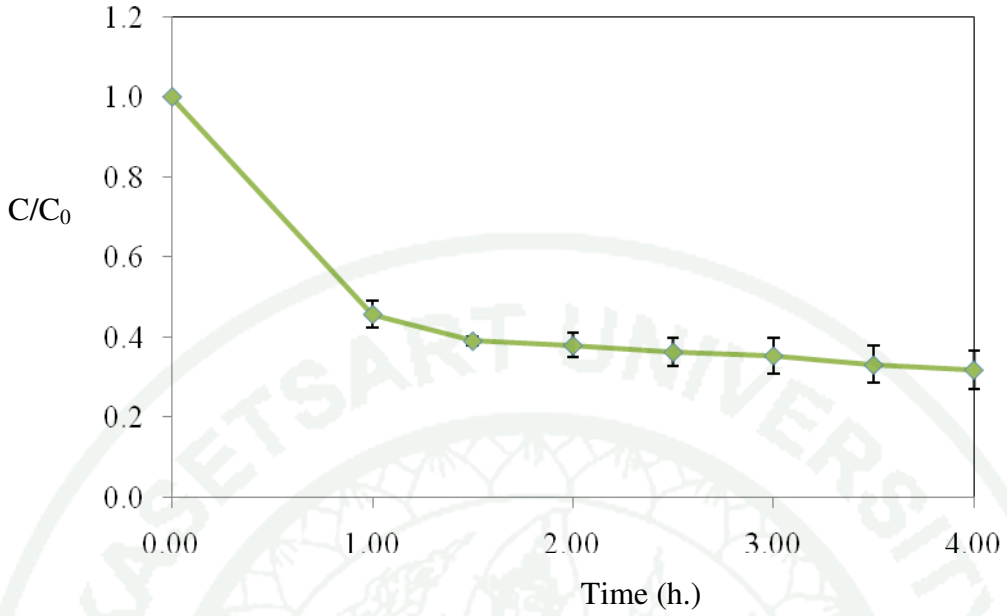

Figure 49 The removal of phenol from 200 ml of 100 ppm phenol by 0.4 g of TiO_2/AC using titanium(IV) isopropoxide calcined at 400ºC.

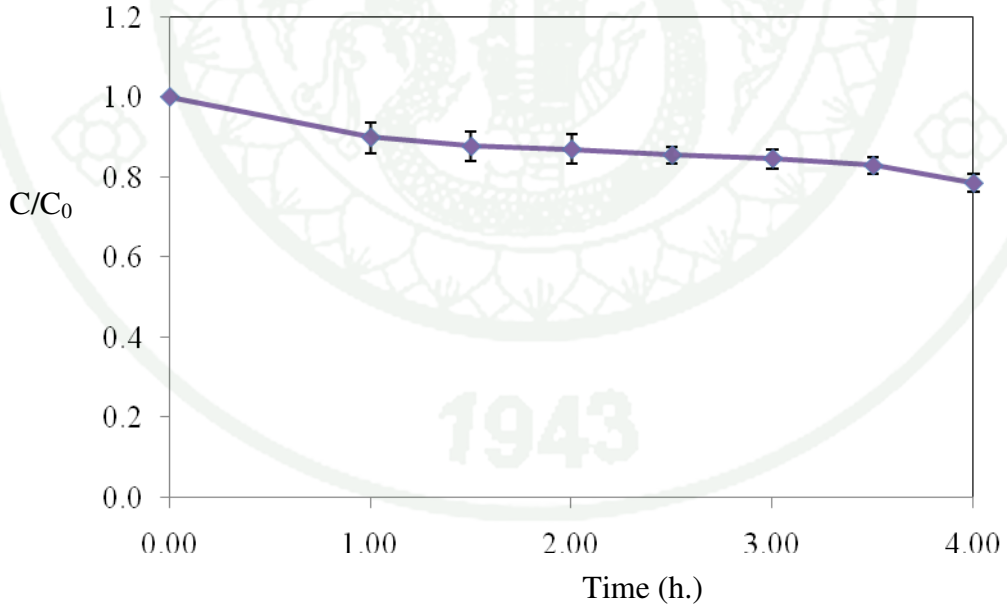

Figure 50 The removal of phenol from 200 ml of 100 ppm phenol by 0.4 g of TiO_2/AC using titanium(IV) isopropoxide calcined at 500ºC.

Copyright by Kasetsart University All rights reserved

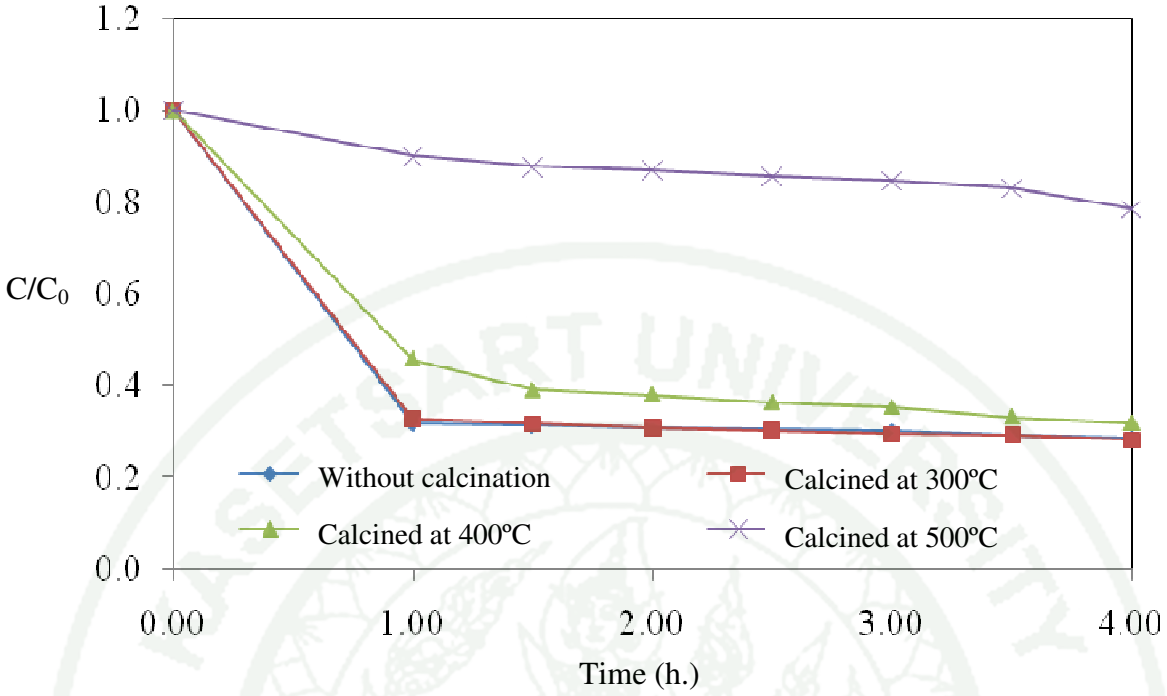

Figure 51 The removal of phenol from 200 ml of 100 ppm phenol by 0.4 g of TiO_2/AC using titanium(IV) isopropoxide without calcination and with calcined at various temperatures.

The removal of phenol from solution using TiO_2/AC without calcination and with calcined at 300ºC, 400ºC and 500ºC are shown in Figure 51. The process composed of adsorption activity (first 60 min) and photodegradation activity (after 60 min). The TiO_2/AC calcined at 500ºC provided the lowest %removal, and it showed only photodegradation activity because all of activated carbon was completely oxidized. For the TiO_2/AC without calcination and calcined at 300ºC that were still amorphous phase provided the highest %removal, but it showed only adsorption activity. Accordingly, the TiO_2/AC calcined at 400ºC has higher removal efficiency than other catalysts due to the combination from both adsorption and photodegradation.

Copyright by Kasetsart University All rights reserved

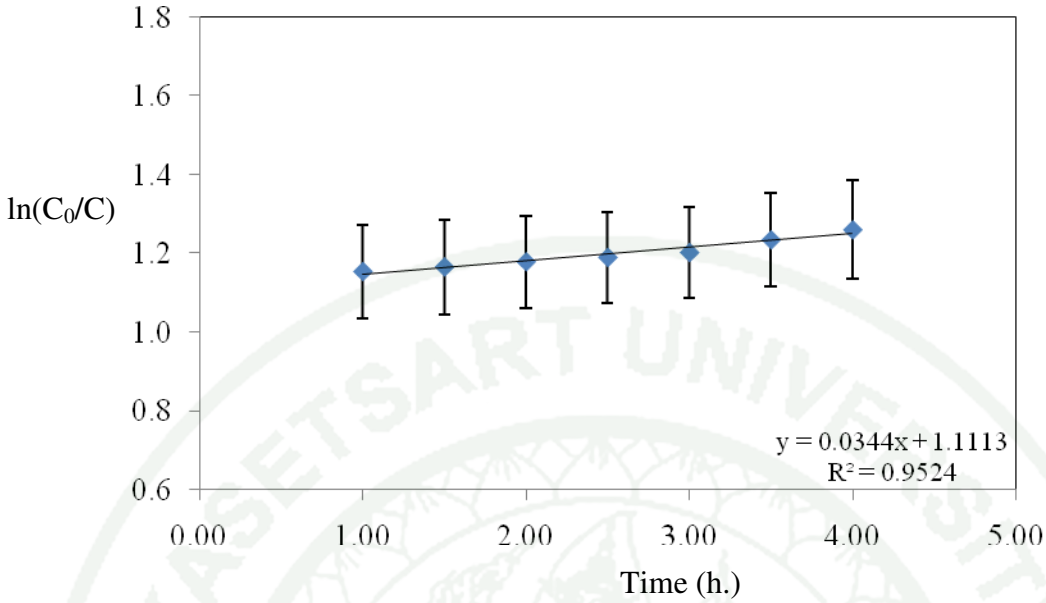

Figure 52 The relation between $\ln C_0/C$ and time (h) of photodegradation reaction of phenol from 200 ml of 100 ppm phenol solution by TiO_2/AC using titanium(IV) isopropoxide without calcination.

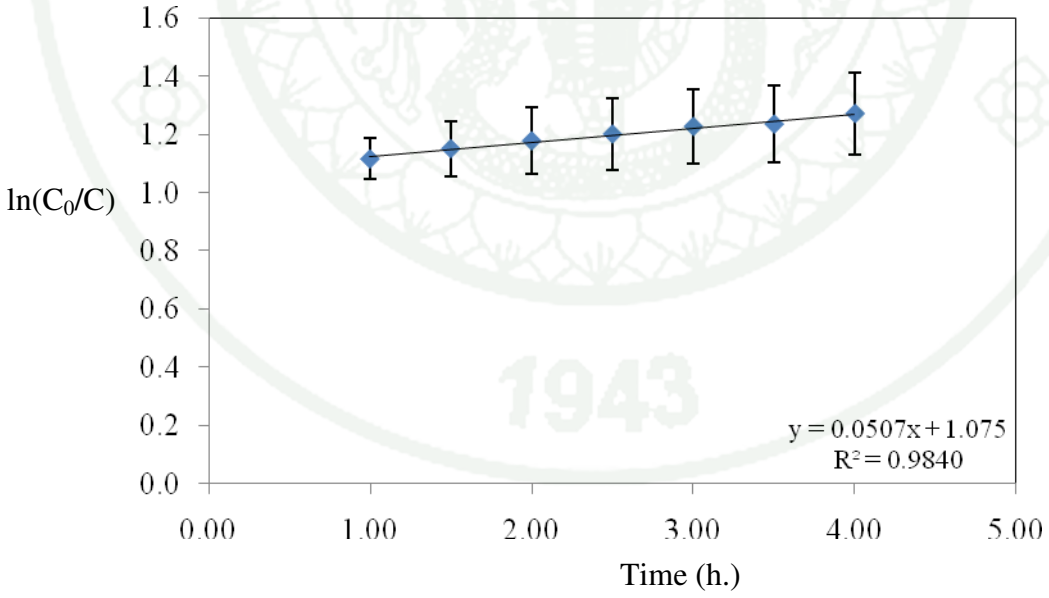

Figure 53 The relation between $\ln C_0/C$ and time (h) of photodegradation reaction of phenol from 200 ml of 100 ppm phenol solution by TiO_2/AC using titanium(IV) isopropoxide calcined at 300ºC.

Copyright by Kasetsart University All rights reserved

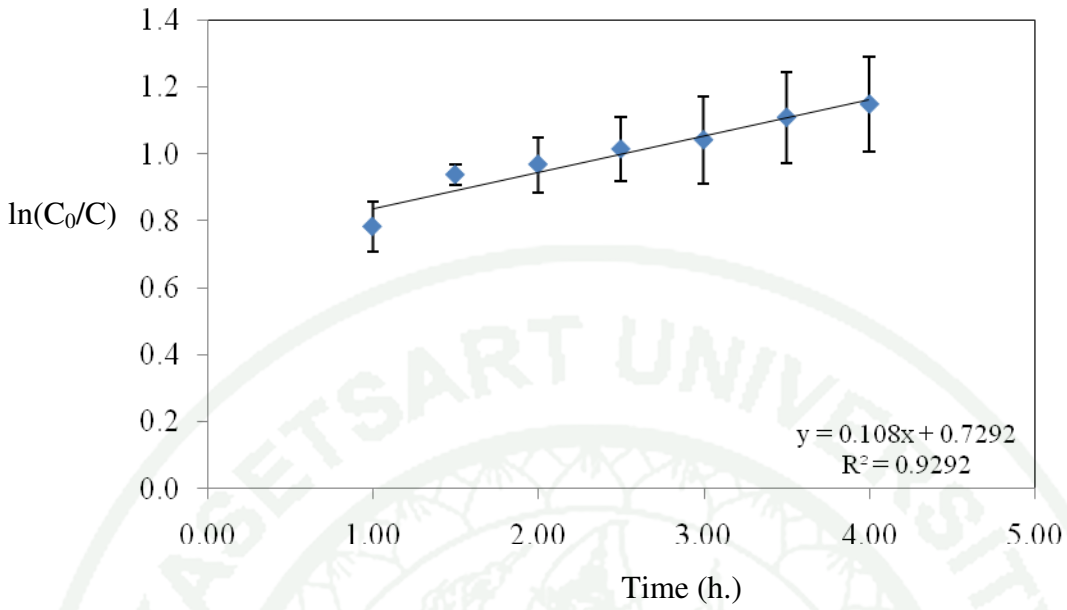

Figure 54 The relation between $\ln C_0/C$ and time (h) of photodegradation reaction of phenol from 200 ml of 100 ppm phenol solution by TiO_2/AC using titanium(IV) isopropoxide calcined at 400ºC.

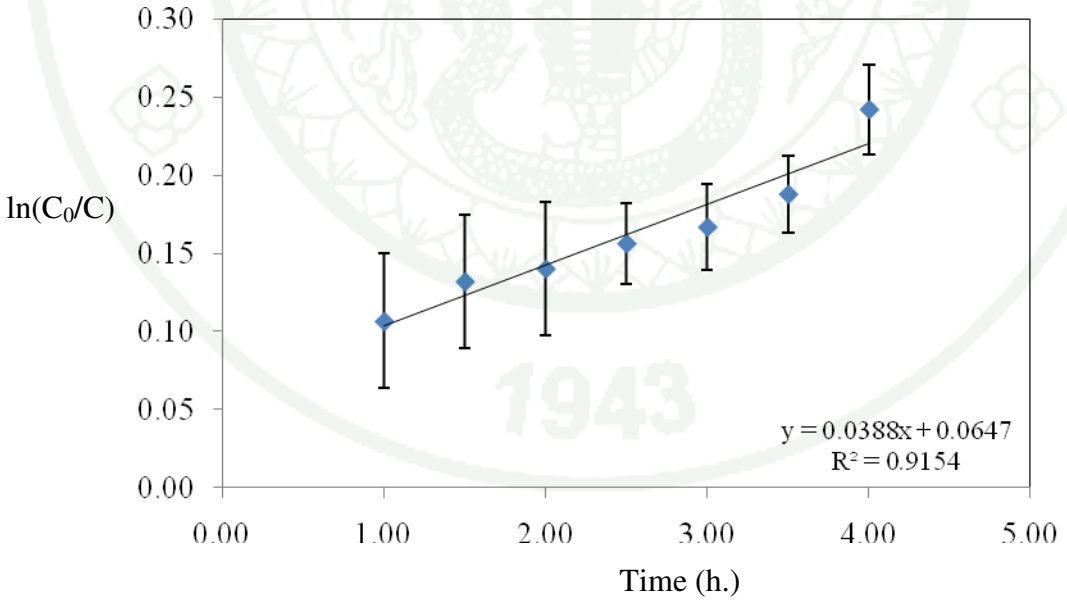

Figure 55 The relation between $\ln C_0/C$ and time (h) of photodegradation reaction of phenol from 200 ml of 100 ppm phenol solution by TiO_2/AC using titanium(IV) isopropoxide calcined at 500ºC.

Copyright by Kasetsart University All rights reserved

Furthermore, the rate constant (Figure 52 to 55) of photodegradation using TiO_2/AC calcined at 400ºC was faster than using others catalysts, which shown in Table 9. This can be concluded that the TiO_2/AC calcined at 400ºC was effective photocatalyst because the TiO_2 was anatase phase and activated carbon still remained in the catalyst.

Table 9 Percentage of phenol removal and rate constant for the photodegradation of phenol from 200 ml of 100 ppm phenol by 0.4g of TiO_2/AC (prepared by titanium(IV) isopropoxide as a precursor).

Catalysts	% Removal			R^2	Rate constant[a] (h^{-1})
	Adsorption	Degradation	Total		
Without calcination	67.55±0.037	4.48±0.036	72.03±0.073	0.9524	0.0345
Calcined at 300ºC	68.36±0.023	3.78±0.039	72.15±0.062	0.9840	0.0507
Calcined at 400ºC	54.14±0.034	13.88±0.047	68.03±0.081	0.9292	0.1080
Calcined at 500ºC	8.15±0.038	10.83±0.022	18.98±0.060	0.9154	0.0388

[a] Rate constants obtained form slope of graph in Figure 52 to 55.

The TiO_2/AC, using titanium(IV) n-butoxide as precursor, without calcination and with calcined at 300ºC, 400ºC and 500ºC (Figure 56 to 60) show similar results with TiO_2/AC using titanium(IV) n-butoxide as precursor. The catalyst which calcined at 400ºC was the most effective catalyst compared with catalyst calcined at 300ºC and 500ºC and without calcination under the same condition.

Copyright by Kasetsart University All rights reserved

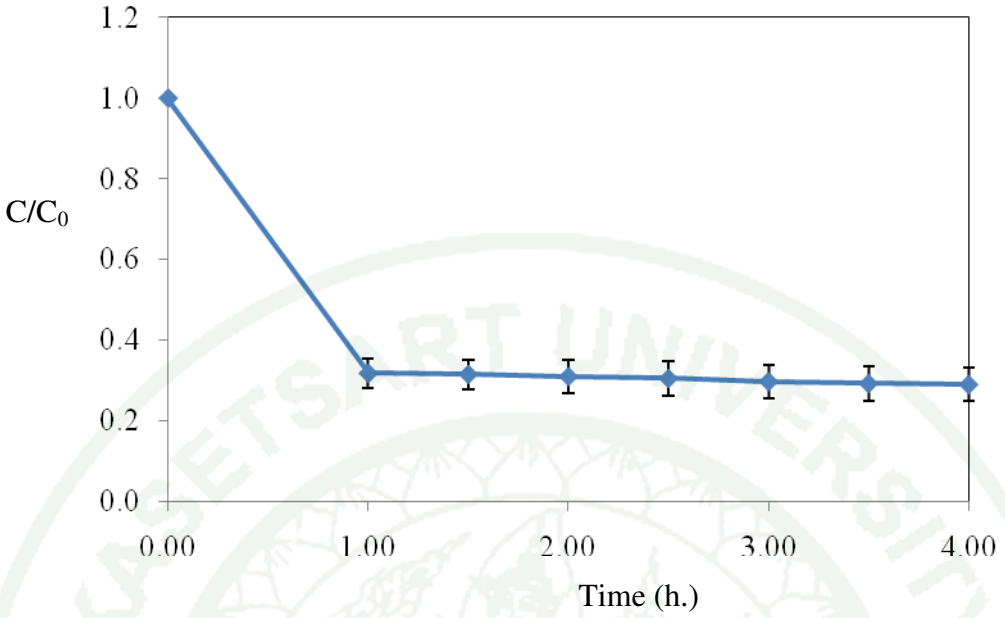

Figure 56 The removal of phenol from 200 ml of 100 ppm phenol by 0.4 g of TiO_2/AC using titanium(IV) n-butoxide without calcination.

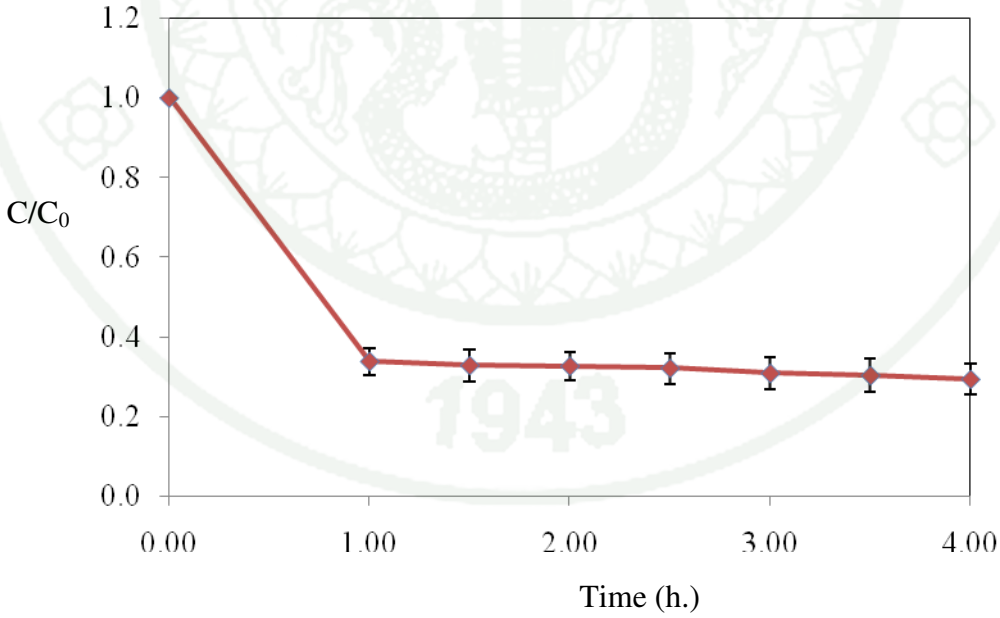

Figure 57 The removal of phenol from 200 ml of 100 ppm phenol by 0.4 g of TiO_2/AC using titanium(IV) n-butoxide calcined at 300ºC.

Copyright by Kasetsart University All rights reserved

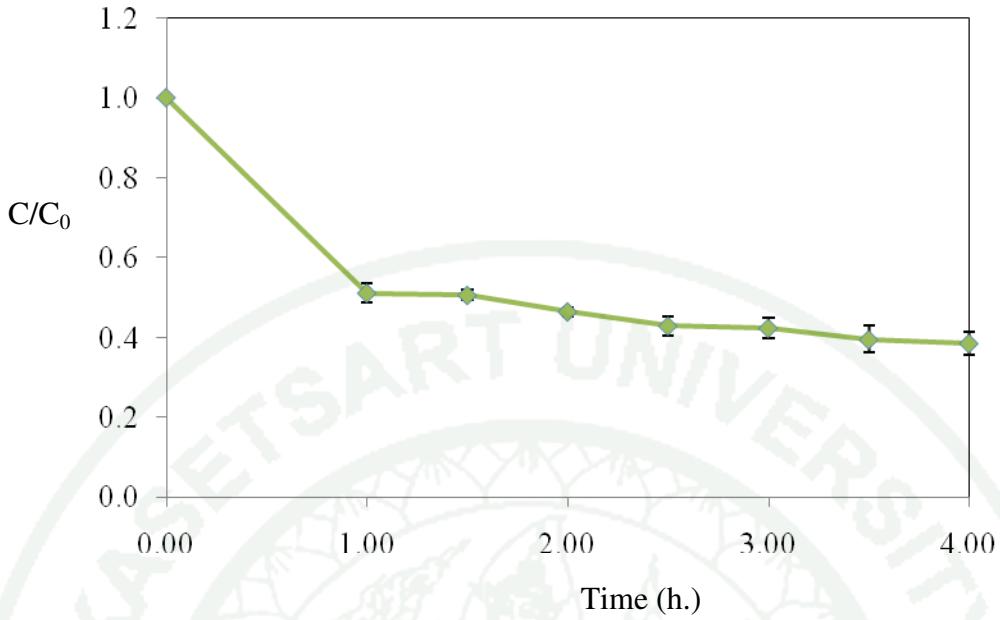

Figure 58 The removal of phenol from 200 ml of 100 ppm phenol by 0.4 g of TiO_2/AC using titanium(IV) n-butoxide calcined at 400ºC.

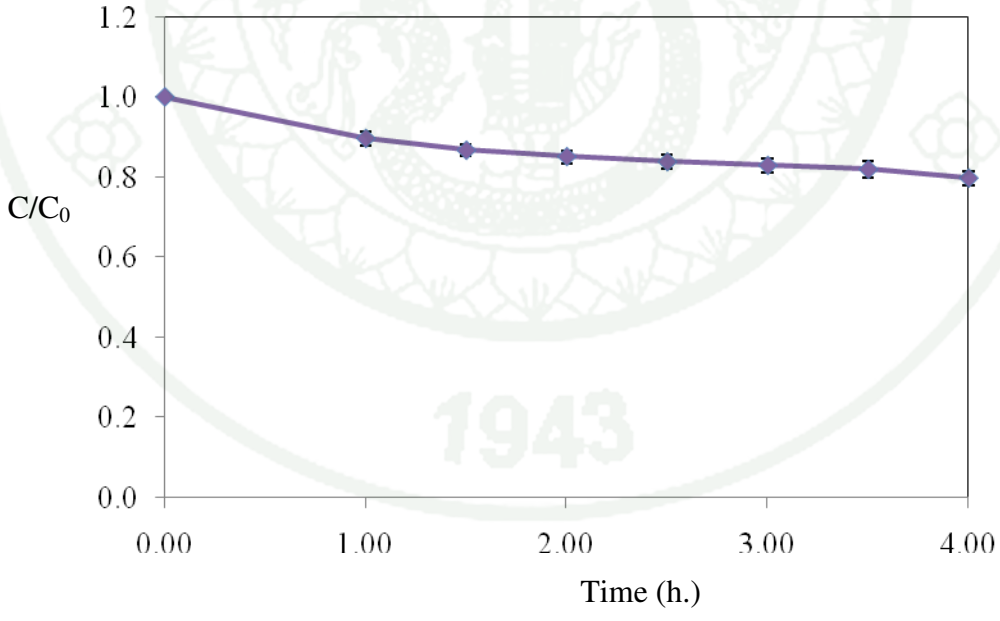

Figure 59 The removal of phenol from 200 ml of 100 ppm phenol by 0.4 g of TiO_2/AC using titanium(IV) n-butoxide calcined at 500ºC.

Copyright by Kasetsart University All rights reserved

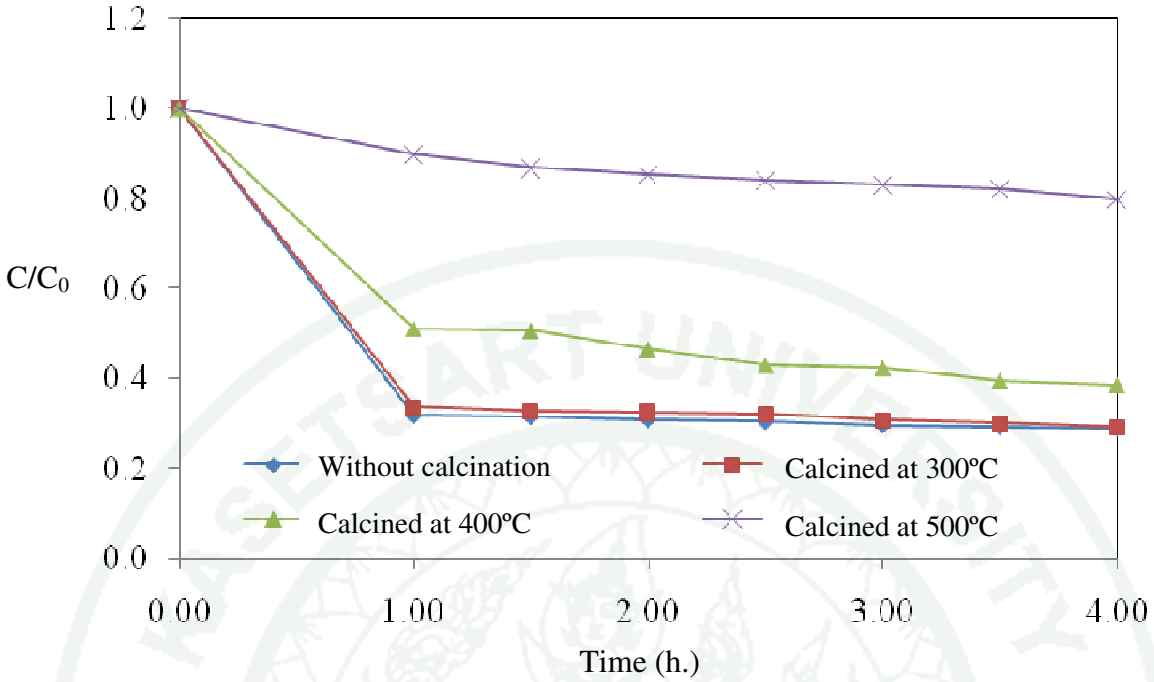

Figure 60 The removal of phenol from 200 ml of 100 ppm phenol by 0.4 g of TiO_2/AC using titanium(IV) n-butoxide without calcination and with calcined at various temperatures.

Figure 60 shows the removal of phenol solution using TiO_2/AC using titanium(IV) n-butoxide without calcination and with calcined at 300ºC, 400ºC and 500ºC, adsorption activity and photodegradation activity of catalyst are shown in the first 60 min and after 60 min, respectively. The TiO_2/AC calcined at 500ºC gave the lowest %removal, and it showed only photodegradation activity because of the activated carbon completely oxidation. For the TiO_2/AC without calcination and calcined at 300ºC that were still amorphous phase provided the highest %removal, but it exhibited only adsorption activity. Therefore, the TiO_2/AC calcined at 400ºC has higher removal efficiency than other catalysts because of adsorption and photodegradation.

Copyright by Kasetsart University All rights reserved

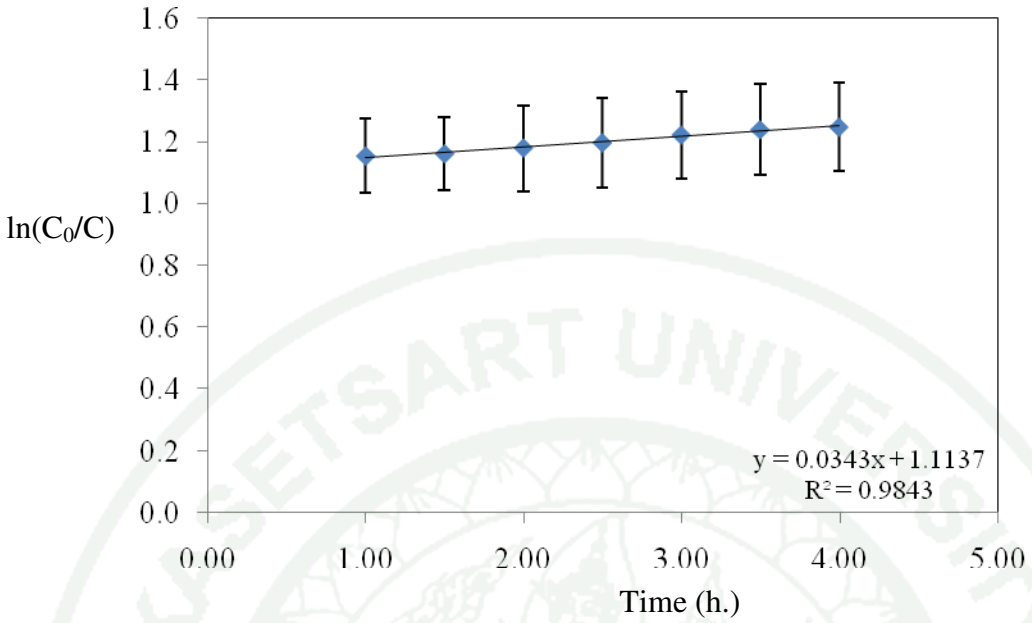

Figure 61 The relation between $\ln C_0/C$ and time (h) of photodegradation reaction of phenol from 200 ml of 100 ppm phenol solution by TiO_2/AC using titanium(IV) n-butoxide without calcination.

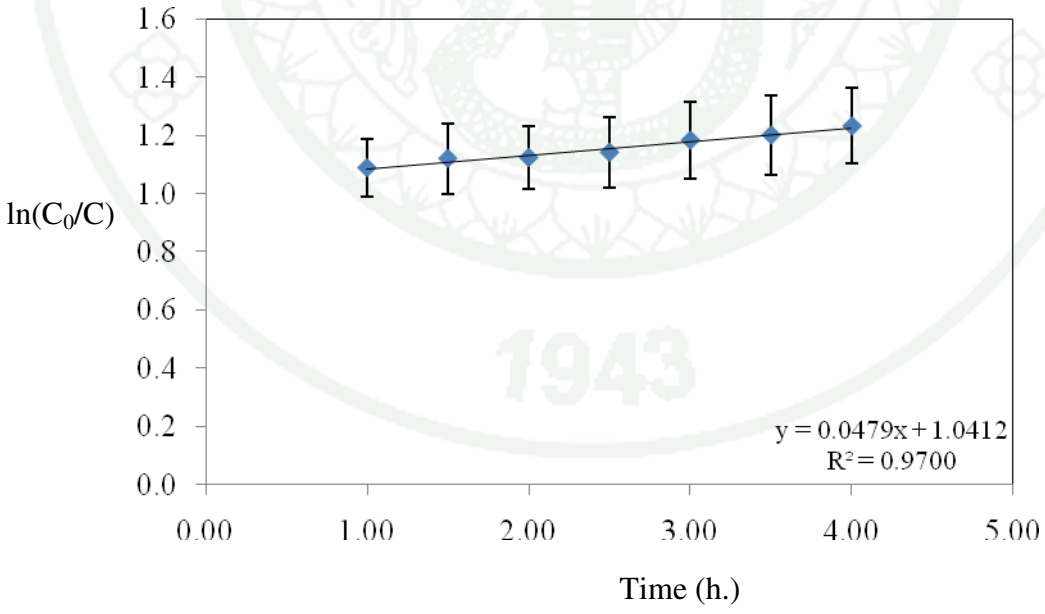

Figure 62 The relation between $\ln C_0/C$ and time (h) of photodegradation reaction of phenol from 200 ml of 100 ppm phenol solution by TiO_2/AC using titanium(IV) n-butoxide calcined at 300ºC.

Copyright by Kasetsart University All rights reserved

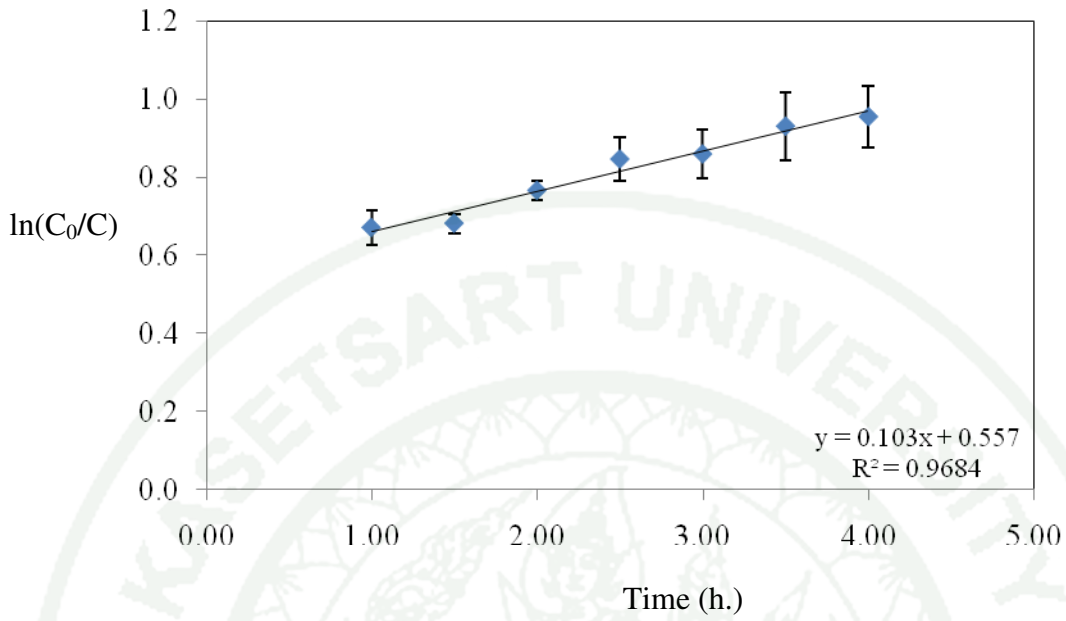

Figure 63 The relation between $\ln C_0/C$ and time (h) of photodegradation reaction of phenol from 200 ml of 100 ppm phenol solution by TiO_2/AC using titanium(IV) n-butoxide calcined at 400ºC.

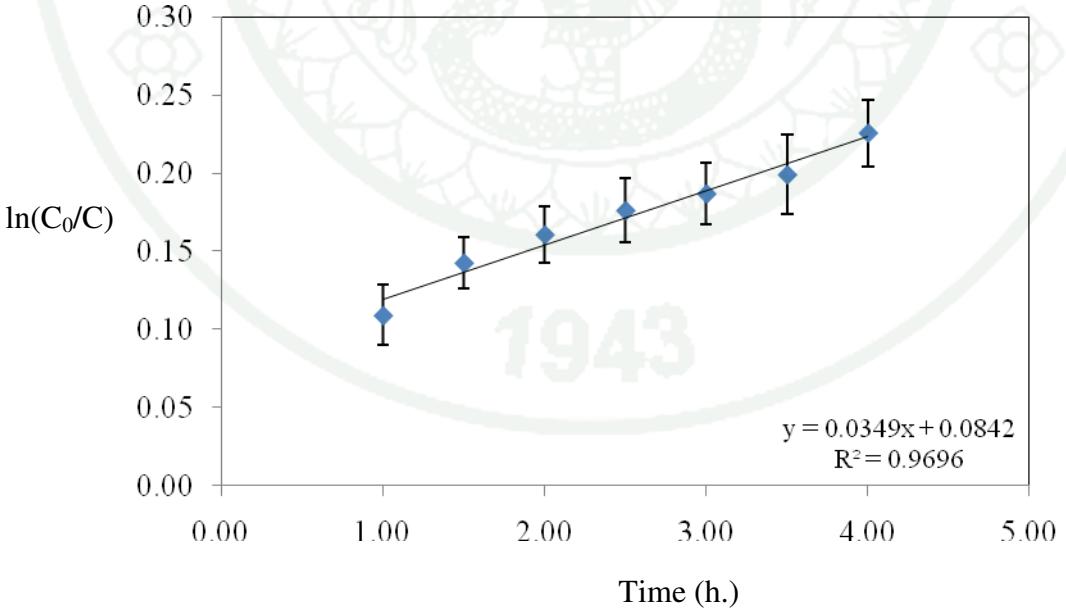

Figure 64 The relation between $\ln C_0/C$ and time (h) of photodegradation reaction of phenol from 200 ml of 100 ppm phenol solution by TiO_2/AC using titanium(IV) n-butoxide calcined at 500ºC.

Copyright by Kasetsart University All rights reserved

Moreover, the rate constant (Figure 51 to 64) of the photodegradation using TiO_2/AC calcined at 400ºC was faster than using others catalysts, as shown in Table 10. This can be concluded that the TiO_2/AC calcined at 400ºC was effective photocatalyst because the TiO_2/AC exhibited the synergistic effect of adsorption and photodegradation.

Table 10 Percentage of phenol removal and rate constant for the photodegradation of phenol from 200 ml of 100 ppm phenol by 0.4g of TiO_2/AC (prepared by using titanium(IV) n-butoxide as a precursor).

Catalysts	% Removal			R^2	Rate constant[a] (h^{-1})
	Adsorption	Degradation	Total		
Without calcination	68.28±0.037	5.79±0.041	74.08±0.078	0.9843	0.0343
Calcined at 300ºC	66.19±0.033	4.49±0.039	70.69±0.072	0.9700	0.0479
Calcined at 400ºC	48.78±0.023	12.60±0.029	61.39±0.052	0.9684	0.1030
Calcined at 500ºC	10.32±0.017	9.87±0.017	20.19±0.034	0.9696	0.0349

[a] Rate constants obtained form slope of graph in Figure 61 to 62.

Copyright by Kasetsart University All rights reserved

4.4. Effect of titania precursor

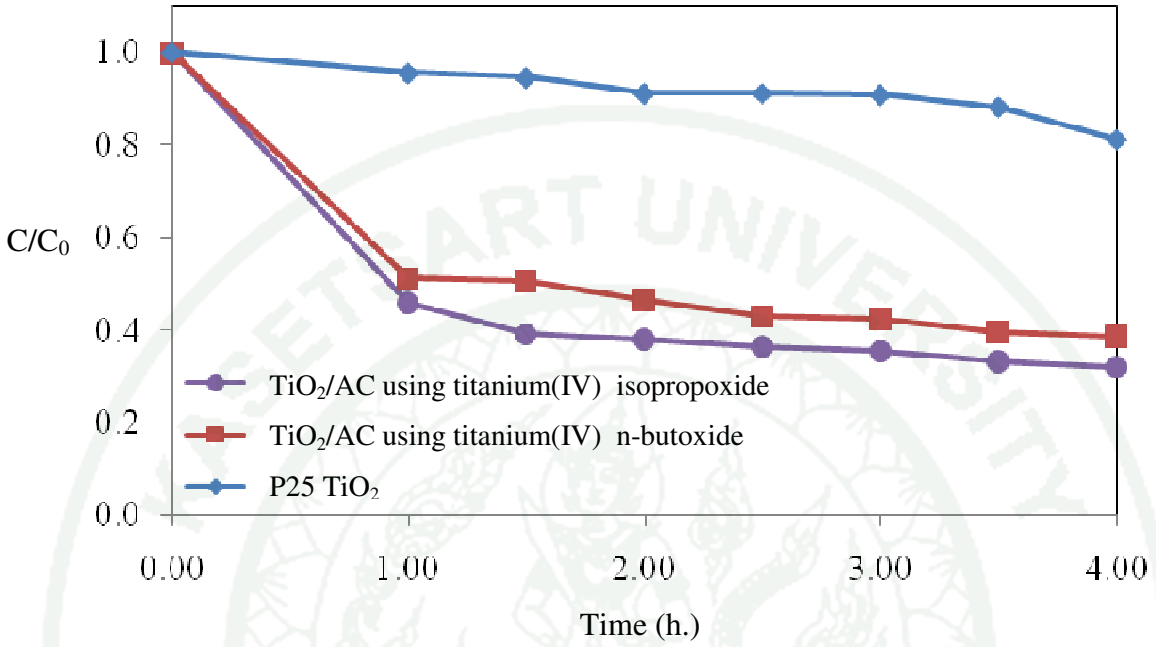

Figure 65 The removal of phenol from 200 ml of 100 ppm phenol by 0.4 g of TiO_2/AC calcined 400ºC using titanium(IV) isopropoxide and titanium(IV) n-butoxide compared to P25 TiO_2.

The results of removal activities (Figure 65) and rate constants (Table 11) of TiO_2/AC using titanium(IV) isopropoxide and titanium(IV) n-butoxide calcined at 400ºC, including P25 TiO_2 indicate that the removal efficiency of both TiO_2/AC catalysts are similar. However, TiO_2/AC using titanium(IV) isopropoxide was able to degrade phenol with the higher %removal of 68% and rate constant of 0.1101 h^{-1}, than TiO_2/AC using titanium(IV) n-butoxide, giving 61.38% removal of phenol with the rate constant of 0.1037 h^{-1}. This may be because of its crystallinity and crystallite size. As calculated from the Sherrer's equation, the crystallite size of TiO_2/AC using titanium(IV) isopropoxide and using titanium(IV) n-butoxide were 9.21 nm and 8.78 nm, respectively. This can be indicated that TiO_2/AC using titanium(IV) isopropoxide has higher crystallinity than TiO_2/AC using titanium(IV) n-butoxide.

Copyright by Kasetsart University All rights reserved

Table 11 Rate constant and %removal of phenol from 100 ppm phenol by 0.4g of TiO_2/AC calcined 400ºC using titanium(IV) isopropoxide and titanium(IV) n-butoxide compared to P25 TiO_2.

Catalysts	Precursor	% Removal			r^2	Rate constant (h^{-1})
		Adsorption	Degradation	Total		
TiO_2/AC	Titanium(IV) isopropoxide	54.14±0.034	13.88±0.047	68.03±0.081	0.9348	0.1101
	Titanium(IV) n-butoxide	48.78±0.023	12.60±0.029	61.39±0.052	0.9683	0.1037
P25 TiO_2	-	-	18.95±0.044	18.95±0.044	0.8909	0.0459

Copyright by Kasetsart University All rights reserved

5. Removal of acid orange 7 (AO7)

5.1. Calibration curve of AO7

A series of solution of AO7 was quantified by UV-Vis spectrophotometry. The absorbance of maximum wavelenght at 485 nm was plotted against concentration of AO7 from 5 to 25 ppm. The calibration curve of standard solution of AO7 was adjusted to pH 4.0, 7.0 and 10.0 that are shown in Figure 66, 67 and 68.

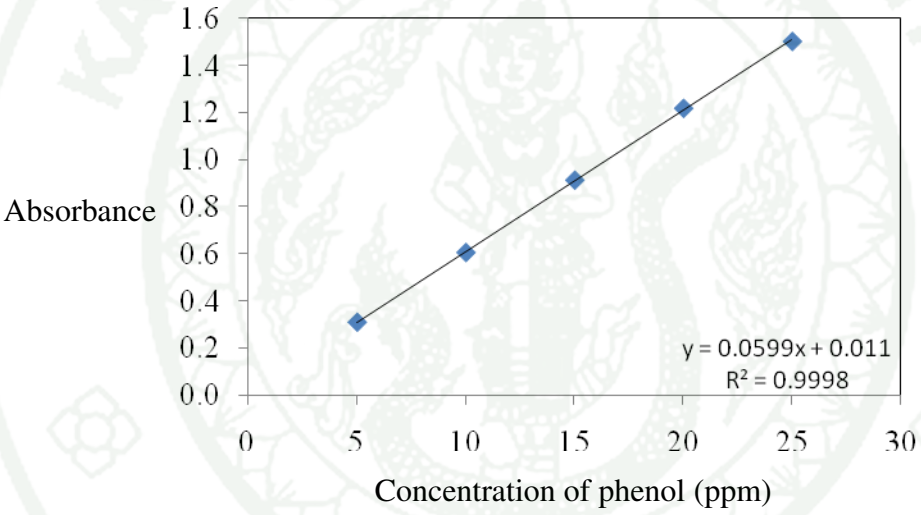

Figure 66 Calibration curve of standard AO7 at concentration from 5 to 25 ppm adjusted to pH 4.0 .

Copyright by Kasetsart University All rights reserved

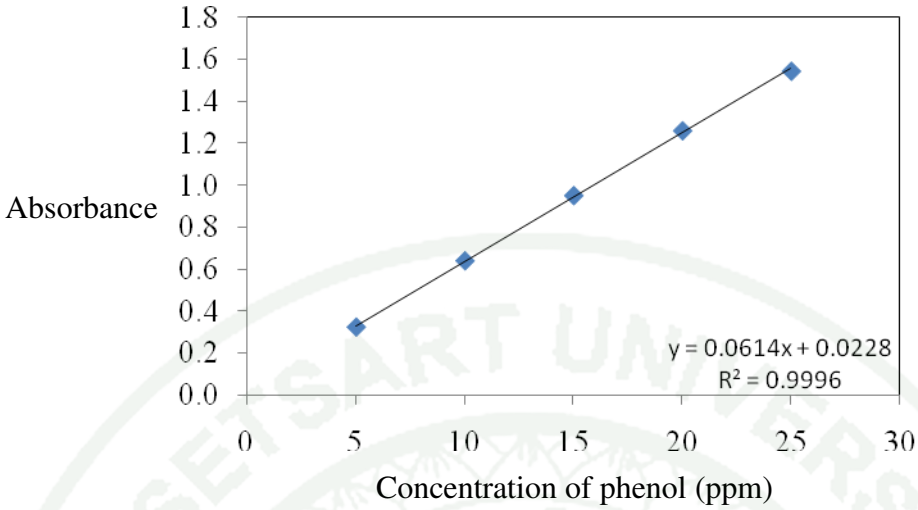

Figure 67 Calibration curve of standard AO7 at concentration from 5 to 25 ppm adjusted to pH 7.0 .

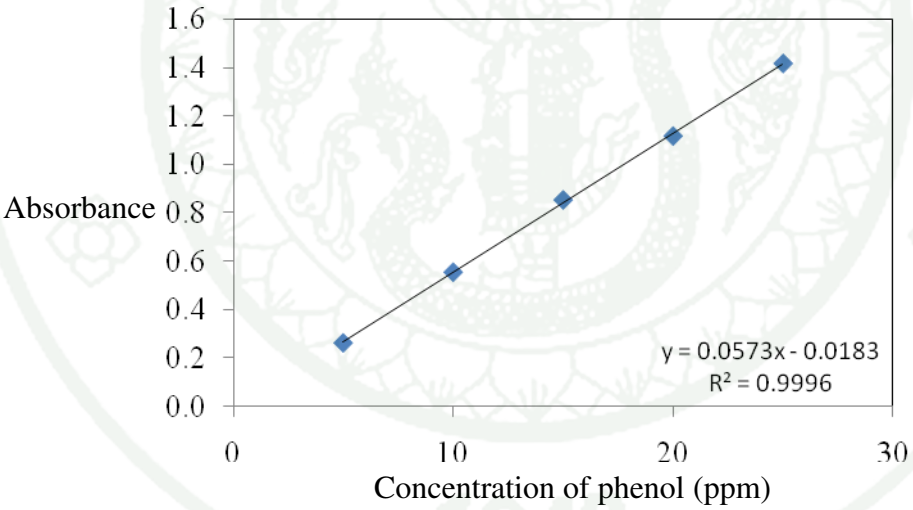

Figure 68 Calibration curve of standard AO7 at concentration from 5 to 25 ppm adjusted to pH 10.0 .

Copyright by Kasetsart University All rights reserved

5.2. Removal of acid orange 7 (AO7)

5.2.1. TiO_2/AC photocatalyst prepared by titanium(IV) isopropoxide

The concentration of AO7 at different pH after reached adsorption equilibrium (first hour) and photodegraded in each 30 minutes interval under artificial UV light were quantified by UV-Vis spectrophotometry at the maximum wavelenght of 485 nm. The removal results are shown in Figure 69 to 72, which composed of adsorption activity (first 60 min) and photodegradation activity (after 60 min). Figure 69 to 71 show the removal of AO7 at pH 4.0, 7.0 and 10.0, respectively. The 0.2 g of TiO_2/AC was used as a photocatalyst to remove AO7 from 200 ml of 100 ppm AO7 solutions.

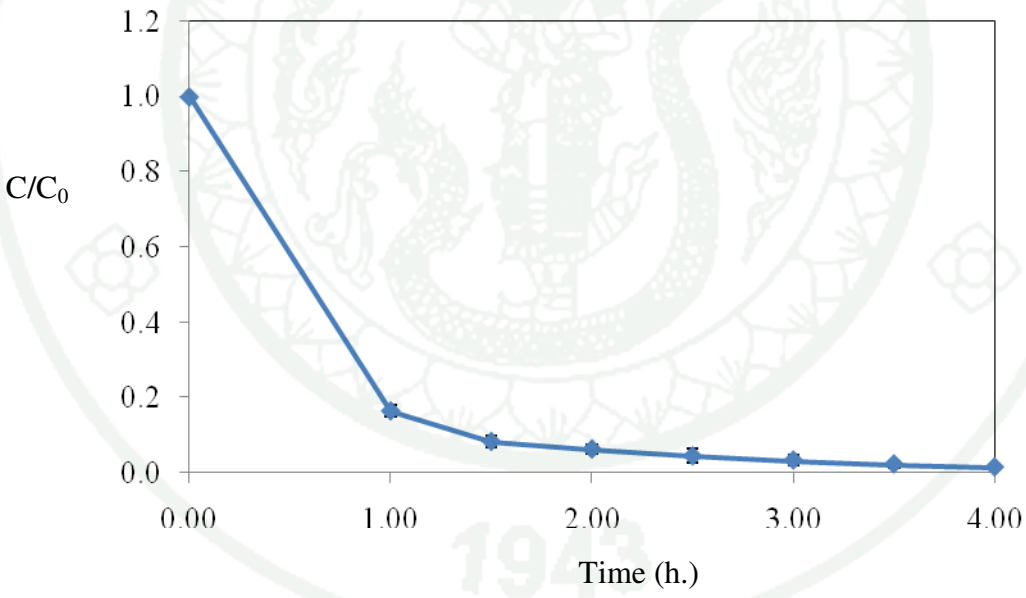

Figure 69 The removal of AO7 from 200 ml of 100 ppm AO7 solution by 0.2 g of TiO_2/AC at pH 4.0.

Copyright by Kasetsart University All rights reserved

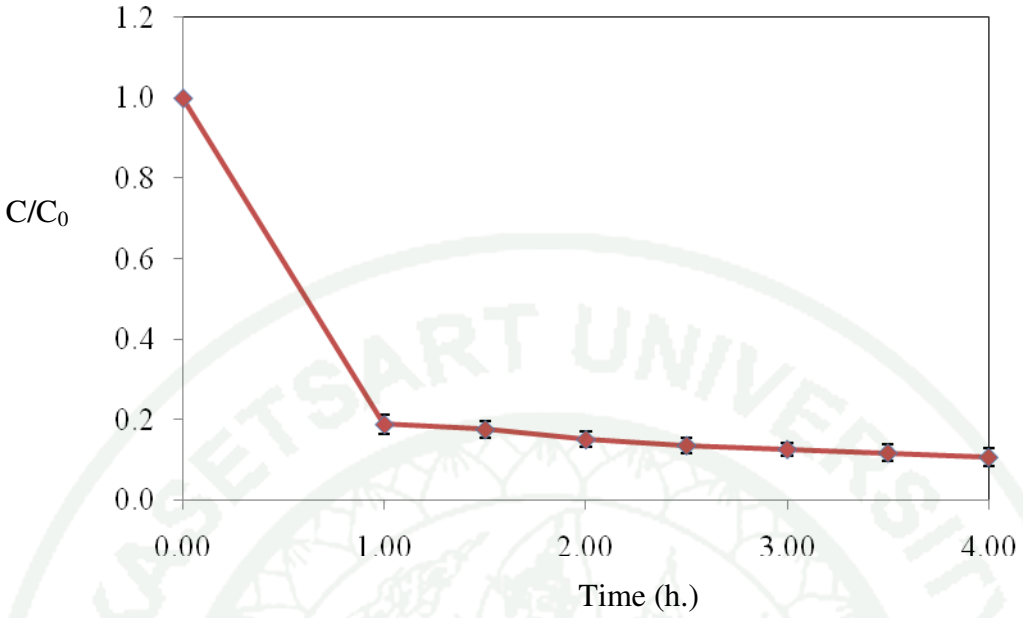

Figure 70 The removal of AO7 from 200 ml of 100 ppm AO7 solution by 0.2 g of TiO_2/AC at pH 7.0.

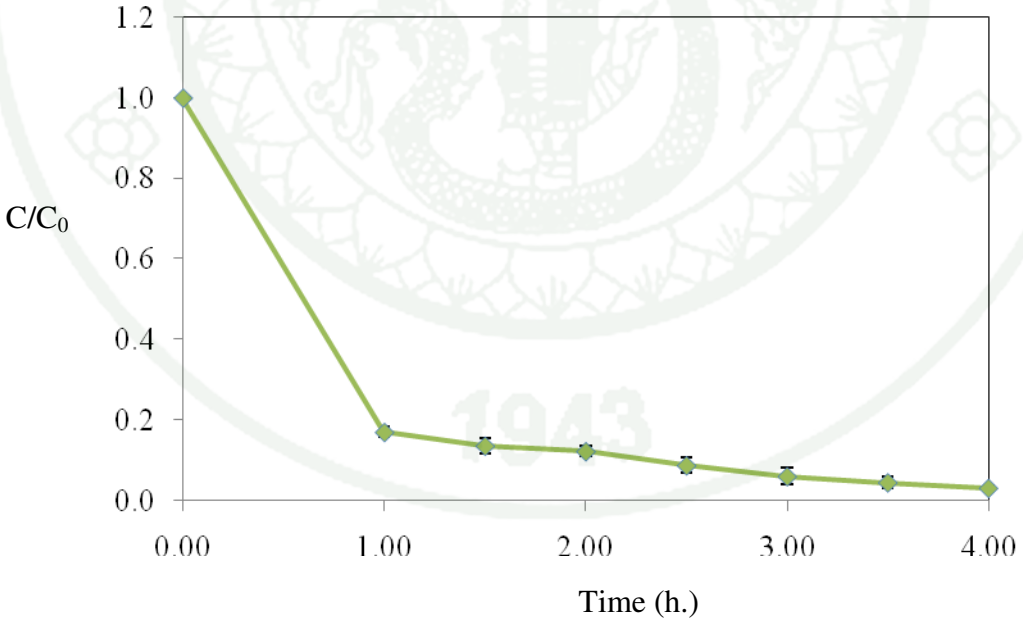

Figure 71 The removal of AO7 from 200 ml of 100 ppm AO7 solution by 0.2 g of TiO_2/AC at pH 10.0.

Copyright by Kasetsart University All rights reserved

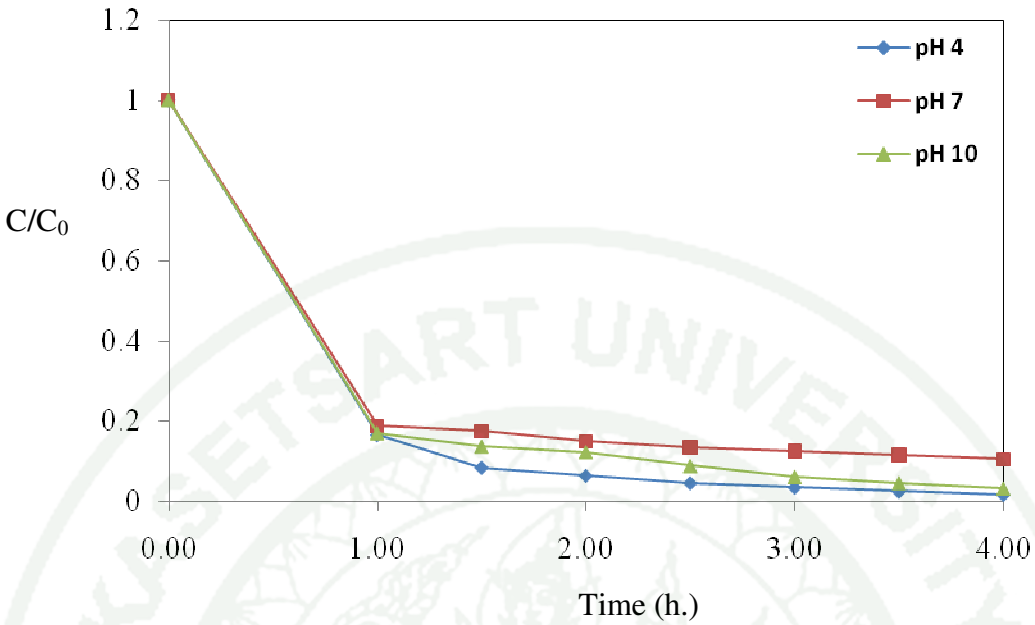

Figure 72 The removal of AO7 from 200 ml of 100 ppm AO7 solution by 0.2 g of TiO_2/AC calcined at 400ºC at different pH.

The removal of AO7 from solution at pH of 4, 7 and 10 using TiO_2/AC are shown in Figure 72. The %removal of AO7 at pH of 4, 7 and 10 were 97.94%, 91.05 and 96.77% as shown in Table 12, which showed the similar adsorption activity. Moreover, for the photodegradation activity, solution at pH 4 and 10 exhibited highest %photodegradation. Accordingly, the pH of solution at 4 and 10 had more effective than pH 7 for the removal of AO7 by TiO_2/AC photocatalyst.

Copyright by Kasetsart University All rights reserved

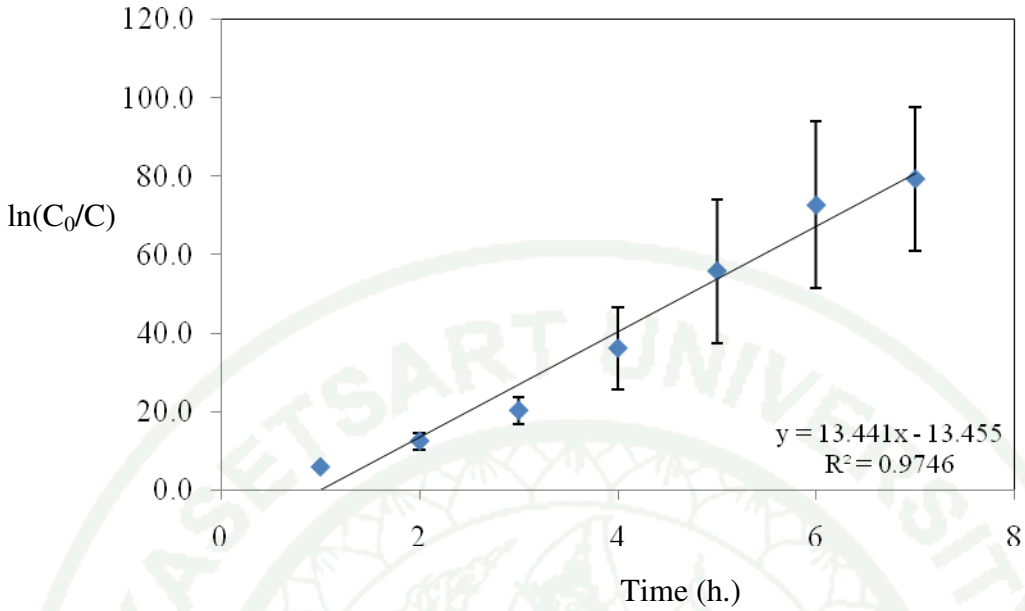

Figure 73 The relation between $\ln C_0/C$ and time (h) of photodegradation reaction of AO7 from 200 ml of 100 ppm AO7 solution at pH 4.0 by 0.2g TiO_2/AC.

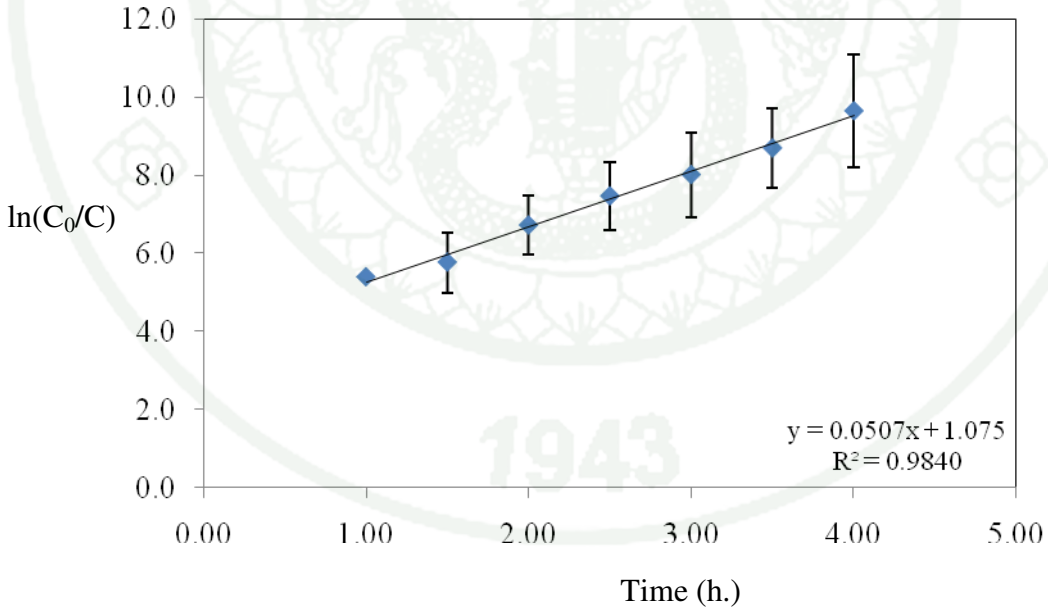

Figure 74 The relation between $\ln C_0/C$ and time (h) of photodegradation reaction of AO7 from 200 ml of 100 ppm AO7 solution at pH 7.0 by 0.2g TiO_2/AC.

Copyright by Kasetsart University All rights reserved

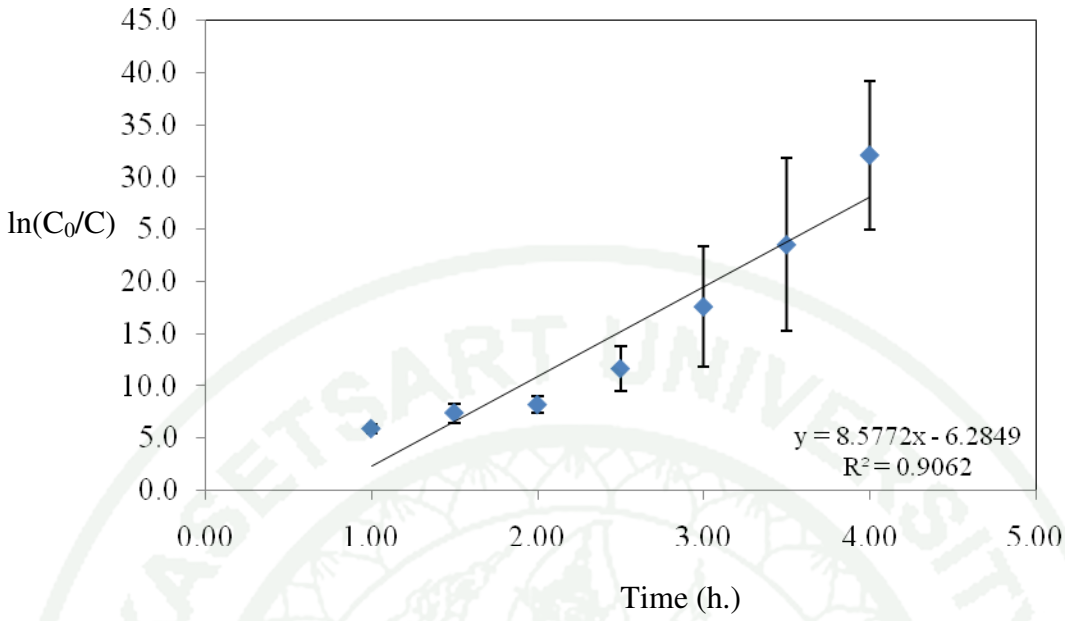

Figure 75 The relation between $\ln C_0/C$ and time (h) of photodegradation reaction of AO7 from 200 ml of 100 ppm AO7 solution at pH 10.0 by 0.2g TiO_2/AC.

The rate of degradation (Figure 73 to 75) and %removal of AO7 using TiO_2/AC photocatalyst are shown in Table 12. The results showed that the solution at pH 4.0 exhibited the highest degradation rate of AO7. This can be concluded that the pH of solution had effect to rate of photodegradation.

Copyright by Kasetsart University All rights reserved

Table 12 Percentage of AO7 removal for the photodegradation of AO7 from 200 ml of 100 ppm AO7 by 0.2 g of TiO_2/AC (prepared by using titanium(IV) isopropoxide as a precursor) at various pH of solution.

Catalysts	pH	% Removal			R^2	Rate constant[a] (h^{-1})
		Adsorption	Degradation	Total		
TiO_2/AC using titanium(IV) isopropoxide	4.0	82.55±1.59	15.39±0.47	97.94±2.06	0.9746	13.4410
	7.0	84.07±2.52	6.98±2.14	91.05±4.66	0.9840	0.0507
	10.0	82.91±1.24	13.86±0.72	96.77±1.96	0.9062	8.5772

[a] Rate constants obtained form slope of graph in Figure 73 to 75.

Copyright by Kasetsart University All rights reserved

5.2.2. TiO_2/AC photocatalyst prepared by titanium(IV) n-butoxide

The concentration of AO7 at different pH after reached adsorption equilibrium (first hour) and photodegraded in each 30 minutes interval under artificial UV light were quantified by UV-Vis spectrophotometry at the maximum wavelenght of 485 nm. The removal results are shown in Figure 76 to 79, which composed of adsorption activity (first 60 min) and photodegradation activity (after 60 min). Figure 76 to 78 show the removal of AO7 at pH 4.0, 7.0 and 10.0, respectively. The 0.2 g of TiO_2/AC was used as a photocatalyst to remove AO7 from 200 ml of 100 ppm AO7 solution.

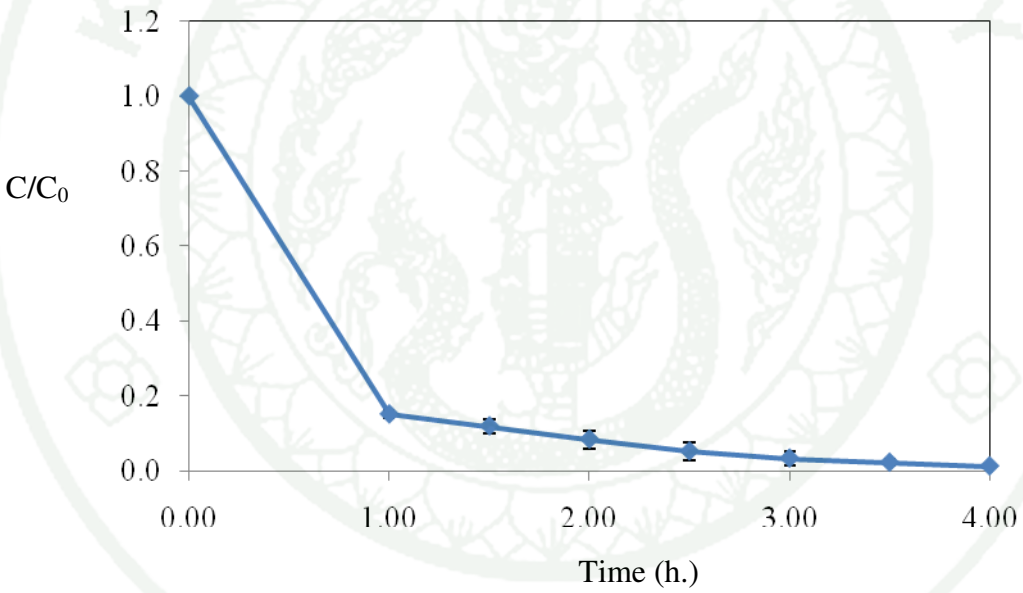

Figure 76 The removal of AO7 from 200 ml of 100 ppm AO7 solution by 0.2 g of TiO_2/AC at pH 4.0.

Copyright by Kasetsart University All rights reserved

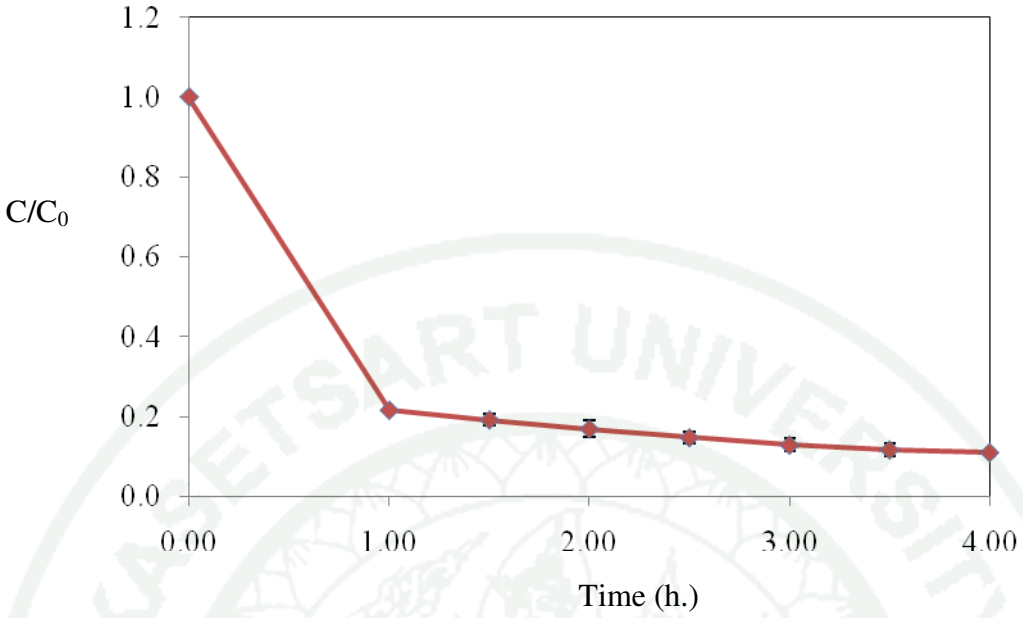

Figure 77 The removal of AO7 from 200 ml of 100 ppm AO7 solution by 0.2 g of TiO_2/AC at pH 7.0.

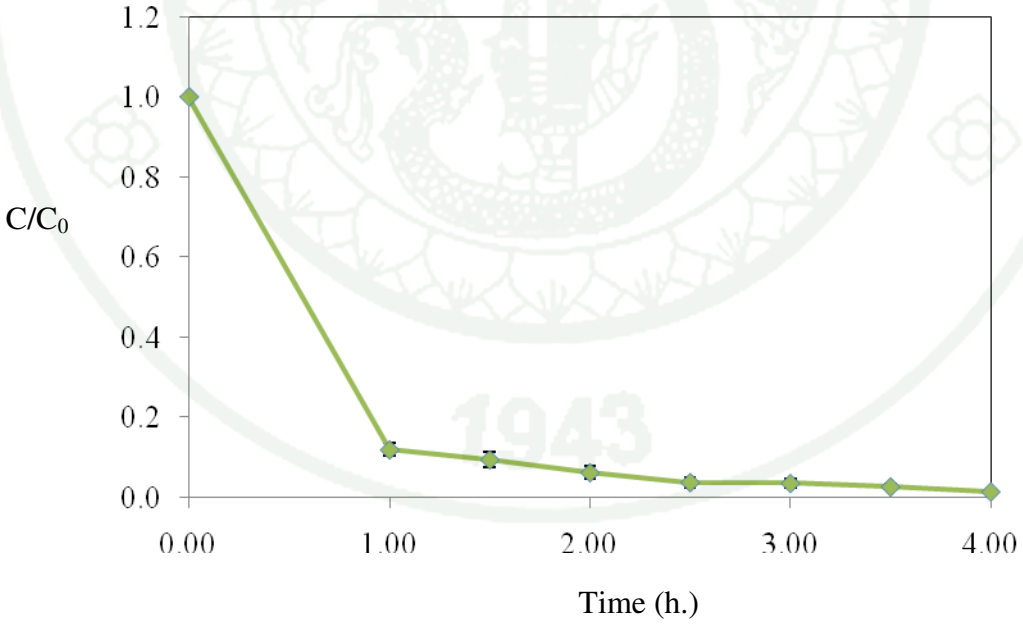

Figure 78 The removal of AO7 from 200 ml of 100 ppm AO7 solution by 0.2 g of TiO_2/AC at pH 10.0.

Copyright by Kasetsart University All rights reserved

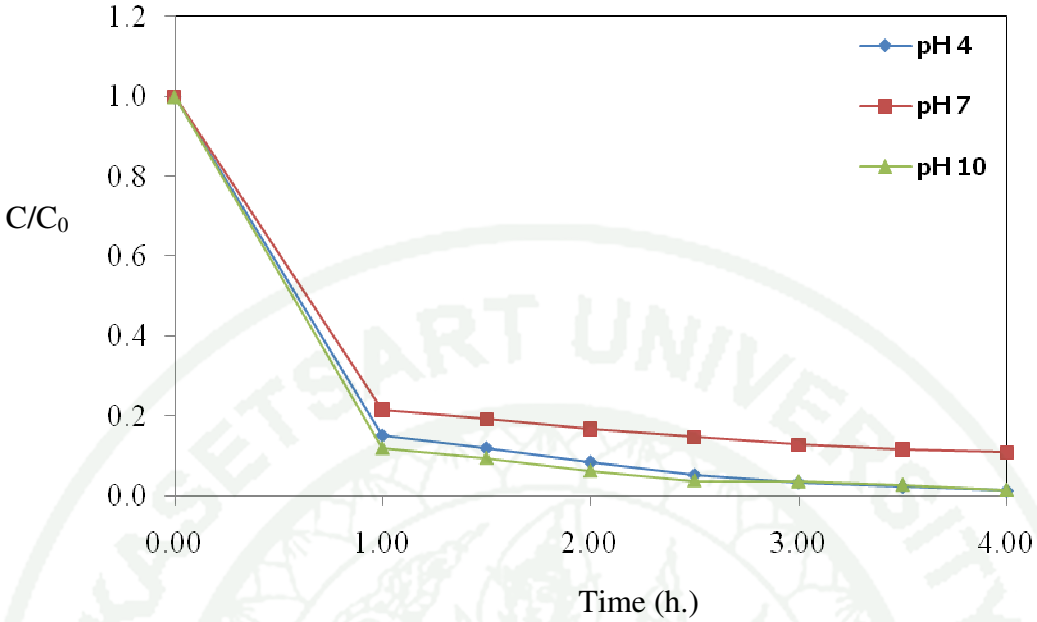

Figure 79 The removal of AO7 from 200 ml of 100 ppm AO7 solution by 0.2 g of TiO_2/AC calcined at 400ºC at different pH.

The removal of AO7 from solution at pH of 4, 7 and 10 using TiO_2/AC are shown in Figure 79. The %removal of AO7 at pH of 4, 7 and 10 were 98.76%, 88.80% and 98.52%, respectively as shown in Table 13, which showed the similar adsorption activity. Moreover, for the photodegradation activity, solution at pH 4 and 10 exhibited higher %photodegradation than at pH 7.0. Accordingly, the pH of solution at 4 and 10 are more effective than pH 7.0 for the removal of AO7 by TiO_2/AC photocatalyst.

Copyright by Kasetsart University All rights reserved

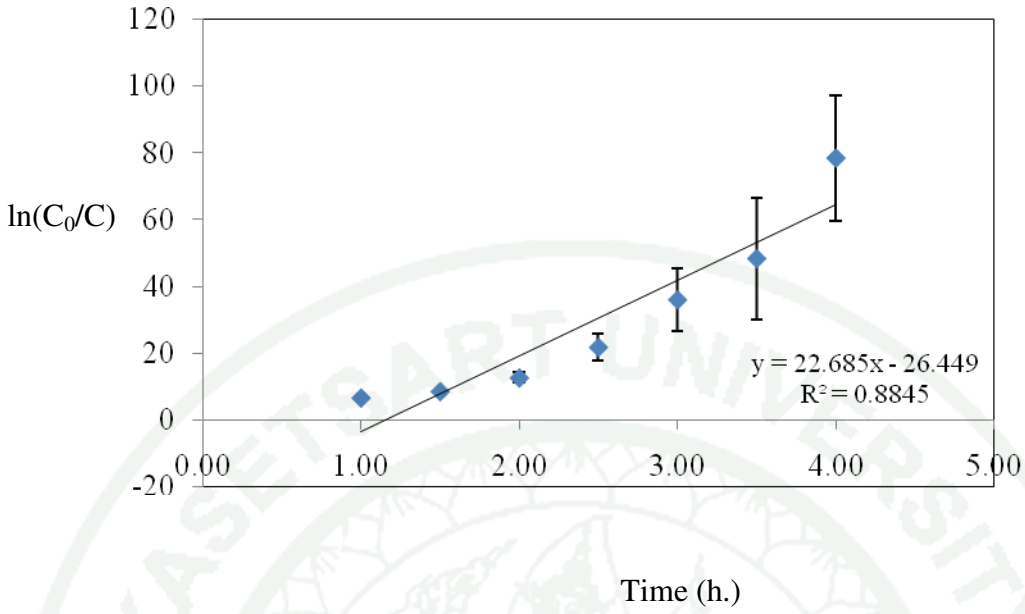

Figure 80 The relation between $\ln C_0/C$ and time (h) of photodegradation reaction of AO7 from 200 ml of 100 ppm AO7 solution at pH 4.0 by 0.2g TiO_2/AC.

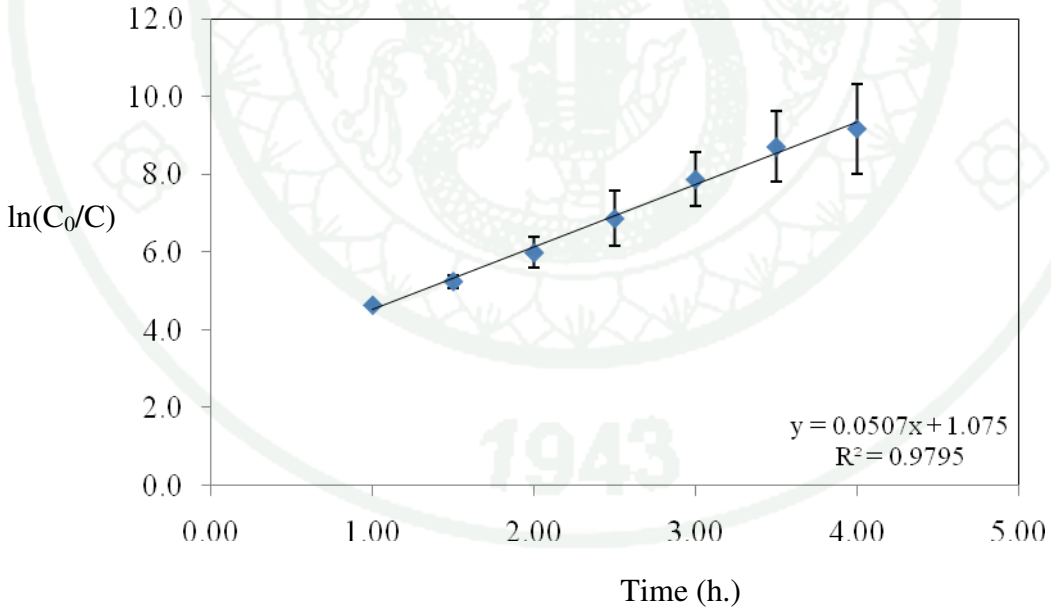

Figure 81 The relation between $\ln C_0/C$ and time (h) of photodegradation reaction of AO7 from 200 ml of 100 ppm AO7 solution at pH 7.0 by 0.2g TiO_2/AC.

Copyright by Kasetsart University All rights reserved

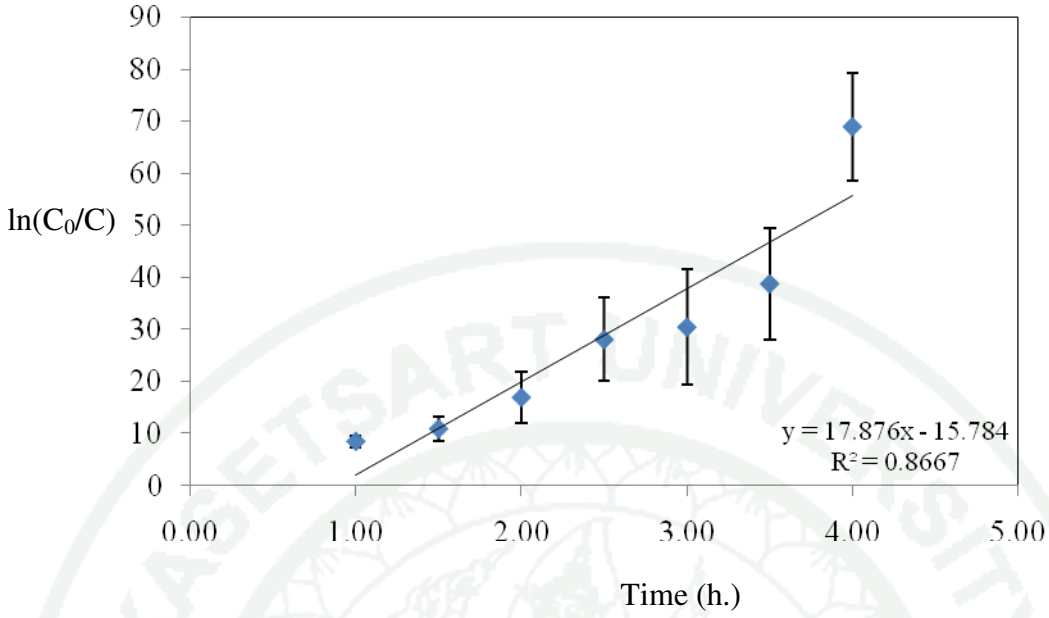

Figure 82 The relation between $\ln C_0/C$ and time (h) of photodegradation reaction of AO7 from 200 ml of 100 ppm AO7 solution at pH 10.0 by 0.2g TiO_2/AC.

The rate of degradation (Figure 80 to 82) and %removal of AO7 using TiO_2/AC photocatalyst are shown in Table 13. The results showed that the pH 4.0 exhibited the highest degradation rate of AO7. This can also be concluded that the pH of solution had effect to rate of photodegradation.

Copyright by Kasetsart University All rights reserved

Table 13 Percentage of AO7 removal for the photodegradation of AO7 from 200 ml of 100 ppm AO7 by 0.2 g of TiO_2/AC (prepared by using titanium(IV) n-butoxide as a precursor) at various pH of solution.

Catalysts	pH	% Removal			R^2	Rate constant[a] (h^{-1})
		Adsorption	Degradation	Total		
TiO_2/AC using titanium(IV) n-butoxide	4.0	83.84±1.04	14.92±0.04	98.76±1.08	0.8845	22.6850
	7.0	79.28±0.72	9.53±0.81	88.80±1.53	0.9795	0.0507
	10.0	88.07±1.57	10.45±0.20	98.52±1.77	0.8667	17.8760

[a] Rate constants obtained form slope of graph in Figure 80 to 82.

Copyright by Kasetsart University All rights reserved

In comparison with removal results of TiO_2/AC using two difference types of titania precursor, which showed the similar results in term of adsorption activity and photodegradation activity. Furthermore, for the photodegradation of AO7 at pH 4.0 and 10.0, which showed higher %degradation than pH 7.0. This could be discussed as follows;

As the previously studied by Fernandez *et al.*(2004), in neutral solution, titania at the surface would be the neutral molecule (uncharged specie). However, titania could form the positive charge ($Ti\text{-}OH_2^+$) in acidic solution and form the negative charge ($Ti\text{-}O^-$) in basis solution, which are shown in Figure 83.

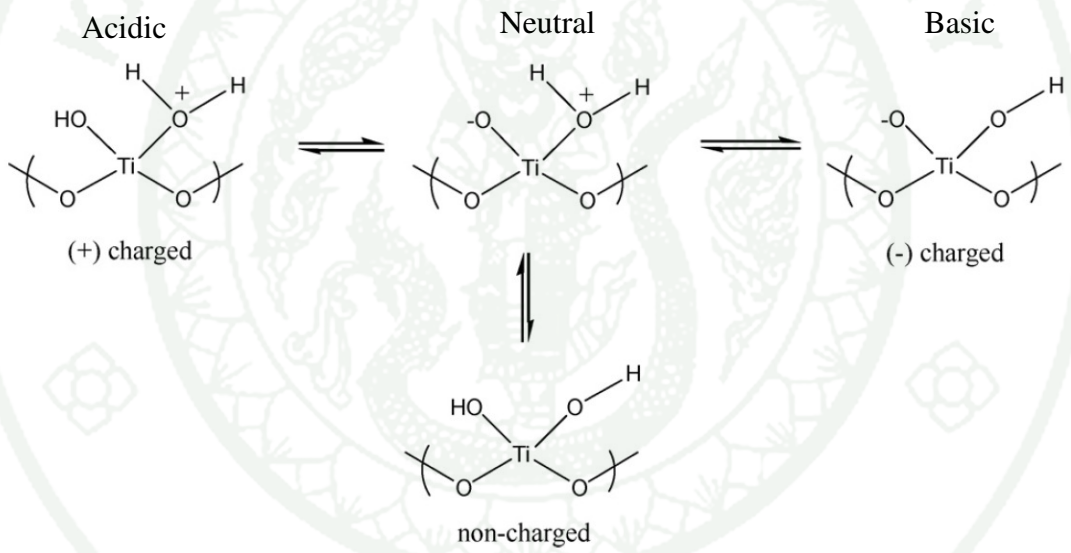

Figure 83 Effect of acidic and basic solution to surface of titania.

At the acidic solution (pH 4.0), the positive form at surface of titania ($TiOH_2^+$) could interact with the AO7 (anionic species) by electrostatic force. The interaction between positive form of titania ($Ti\text{-}OH_2^+$) and AO7 was stronger than at higher pH (pH 7.0 and pH 10.0) due to a higher density of acidic positive charges. As the reason mentioned above, it can be concluded that the pH 4.0 was the appropriate condition for degradation of AO7 using TiO_2/AC photocatalyst.

Copyright by Kasetsart University All rights reserved

In case of basic solution (pH 10.0), the high pH value of solution played an important role in the generation of hydroxide ions (OH^-) of solution, which would be able to generate hydroxyl radicals ($^{\bullet}OH$) extremely as shown in Figure 84. In other words, the increasing of hydroxide ion in solution could increase the number of hydroxyl radicals in solution, which helped in the degradation process accordance with the previous studied by Kaur and Singh (2007).

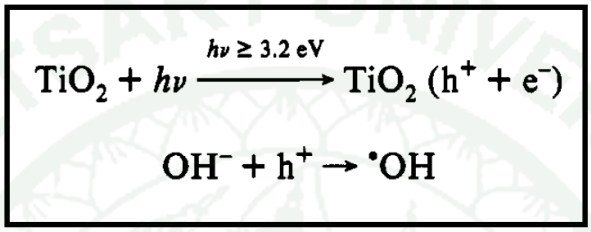

Figure 84 Mechanism of titania to generate hydroxyl radical ($^{\bullet}OH$) from hydroxide ion in basis solution

Source: Brezova *et al.*(1994)

Copyright by Kasetsart University All rights reserved

6. Proposed mechanism of photodegradation

6.1. Proposed photodegradation mechanism of phenol

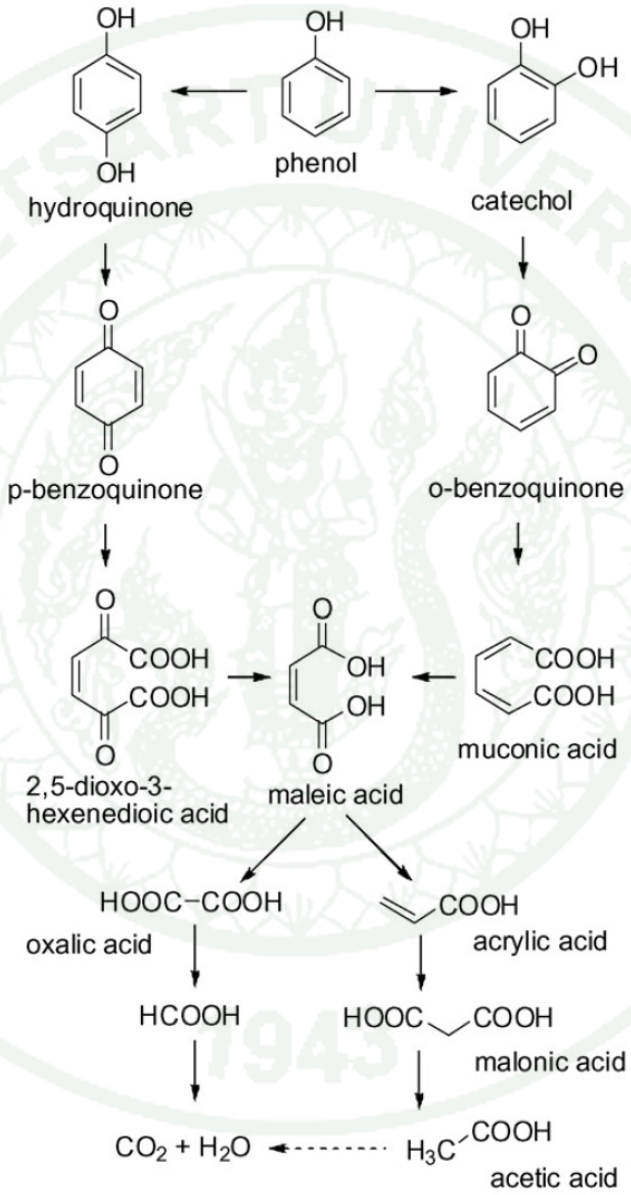

Figure 85 Possibly proposed mechanism of photodegradation of phenol by oxidation reaction of radical species.

Source : Liotta *et al.* (2008)

Copyright by Kasetsart University All rights reserved

Figure 85 shows the two possible degradation pathways of phenol by radical species ($^{\bullet}$OH). Firstly, the para- and meta-position of phenol molecule was reduced by $^{\bullet}$OH radical, which would be able to provide two possible intermediates that were hydroquinone and catechol, respectively. Then, both intermediates were reduced by $^{\bullet}$OH radical again, followed by ring opening of intermediates in accordance with the previous study by Liotta *et al.* (2008). Furthermore, the toxicity of each intermediate in pathways was presented by ChV and LC_{50} value which could be calculated by using EPI Suite software (version 4.00, January, 2009) with ECOSAR mode (Reuschenbach *et al.*, 2008) as shown in Appendix F. It was found that the ChV and LC_{50} of all the intermediates indicated that phenol has higher toxicity than the degradation products.

Copyright by Kasetsart University All rights reserved

6.2. Proposed photodegradation mechanism of AO7

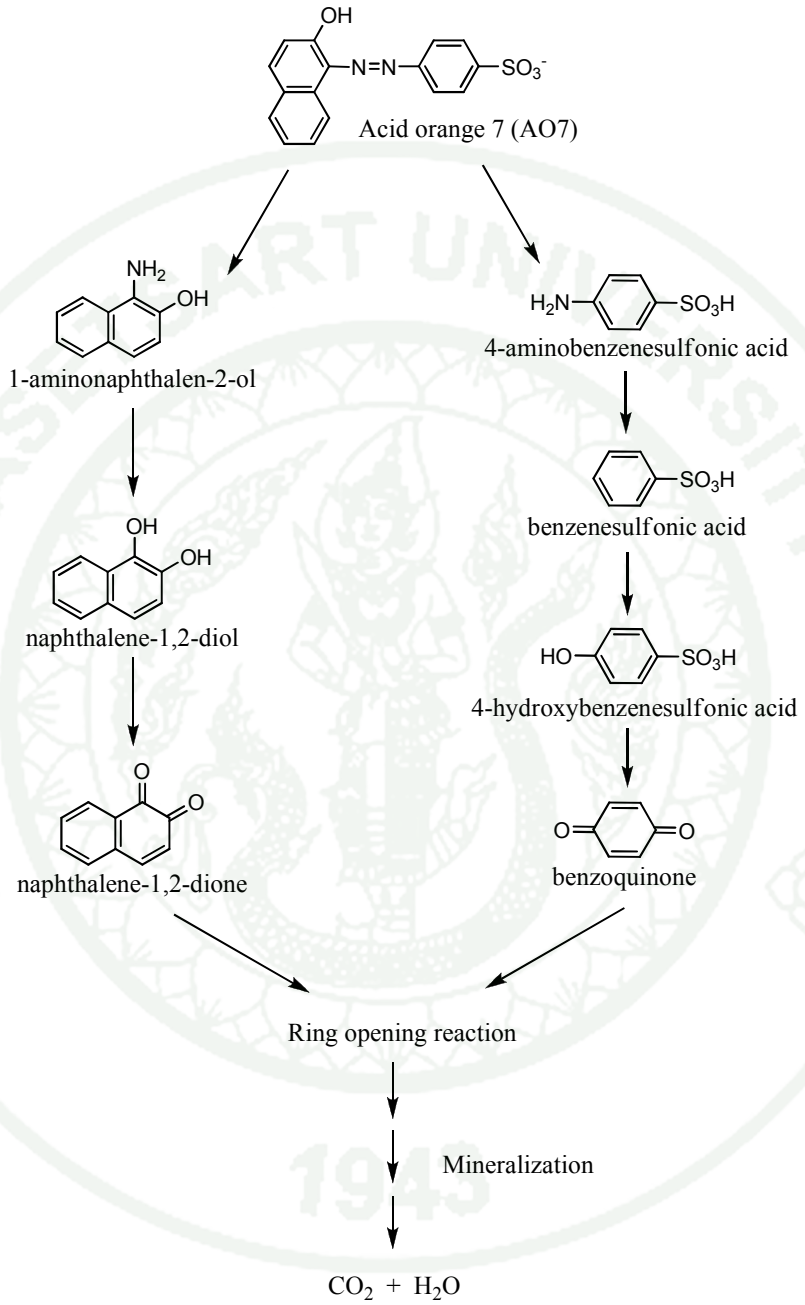

Figure 86 Possibly proposed mechanism of photodegradation of AO7 by oxidation reaction of radical species.

Source : Hammami *et al.* (2008)

Copyright by Kasetsart University All rights reserved

A plausible degradation pathway of AO7 by radical species ($^{\bullet}OH$) is shown in Figure 86. Initially, the AO7 molecule was attacked $^{\bullet}OH$ radical that lead to the cleavage of active azo bond, which provided 1-aminophthalen-2-ol and 4-aminobenzenesulfonic acid as an intermediate. Then, both intermediates were reduced again to generate quinine form (naphthalene-1,2-dione and benzoquinone), followed by ring opening of intermediates in accordance with the previous study by Hammami *et al.* (2008). Besides, the toxicity of each intermediate in pathways was presented by ChV and LC_{50} value which could be calculated by using EPI Suite software (version 4.00, January, 2009) with ECOSAR mode as (Reuschenbach *et al.*, 2008) shown in Appendix F. It was found that the ChV and LC_{50} of all the intermediates indicated that AO7 has higher toxicity than the degradation products.

7. Recycling experiment

The recyclability of the TiO_2/AC calcined at 400ºC (prepared by titanium(IV) isopropoxide) was determined for three photocatalytic runs. Table 14 and 15 show the %removal of phenol and AO7, respectively. It can be seen that the %removal of phenol and AO7 was decreased when the TiO_2/AC was repeatedly used in photocatalytic runs. This may be because the TiO_2/AC was deactivated by two reasons. First, the generation of reaction residues (by-products or intermediates) might be adsorbed onto the catalyst and block the active sites, which as a result reduced the photocatalytic reaction (Ollis, 2000). Second, the dirtiness (dust or impure particles) might change the catalyst surface by blocking pore (Zhao and Yang, 2003).

Copyright by Kasetsart University All rights reserved

Table 14 Removal of phenol by TiO_2/AC using titanium(IV) isopropoxide as precursor and calcined at 400ºC with three times recycle.

Cycle	Average %removal of phenol (%)		
	Adsorption	Degradation	Total
First run	54.20	13.90	61.10
Second run	48.96	9.45	58.41
Third run	41.03	6.15	46.19

Table 15 Removal of AO7 by TiO_2/AC using titanium(IV) isopropoxide as precursor and calcined at 400ºC with three times recycle.

Cycle	Average %removal of AO7 (%)		
	Adsorption	Degradation	Total
First run	81.20	8.20	89.40
Second run	43.15	7.50	50.65
Third run	18.59	7.37	25.96

Copyright by Kasetsart University All rights reserved

CONCLUSION AND RECOMMENDATIONS

Conclusion

TiO_2/AC photocatalyst prepared by titanium(IV) isopropoxide and titanium(IV) n-butoxide as titania precursors were able to be synthesized by the sol-gel method. From all characterization techniques, it can be indicated that the calcination temperature had a significant impact on the crystal structure of TiO_2 and the remaining of AC. With increasing temperature, TiO_2 of TiO_2/AC had the larger crystallite size, the higher crystallinity and the higher phase transformation of amorphous-to-anatase. TiO_2/AC using titanium(IV) isopropoxide as a titania precursor and calcined at 400ºC seemed to be closely within the scope of the ideal photocatalyst. It provided high crystallinity of TiO_2, small crystallite size and high abundant of AC. Its phase transformation was retarded by the effect of solvent and AC in preparation step. For the adsorption isotherm results, the TiO_2/AC using titanium(IV) isopropoxide as a titania precursor and calcined at 400ºC has the adsorption isotherm which fitted to the Langmuir isotherm, indicated the monolayer adsorption system, and gave the highest thermodynamic stability of adsorption compared with TiO_2/AC using titanium(IV) n-butoxide and P25 TiO_2.

Concerning the effect of titania precursor, the TiO_2/AC prepared by titanium(IV) isopropoxide showed the smaller crystallite size, higher crystallinity and adsorption stability than TiO_2/AC prepared by titanium(IV) n-butoxide.

Regarding to photocatalytic activity, TiO_2/AC using titanium(IV) isopropoxide calcined at 400ºC provided the highest %removal under UV light (composed of adsorption activity and degradation activity) of 68.03% for 100 ppm phenol with rate constant of 0.1101 h^{-1} and 97.94% for 100 ppm acid orange 7 (AO7) at pH 4.0 with the rate constant of 13.44 h^{-1}. In case of TiO_2/AC using titanium(IV) n-butoxide calcined at 400ºC, It also gave the highest %removal of 61.38% for 100 ppm phenol with rate constant of 0.1037 h^{-1} and 98.76% for 100 ppm acid orange 7 (AO7)

Copyright by Kasetsart University All rights reserved

at pH 4.0 with the rate constant of 22.68 h^{-1}. Interestingly, at the calcination at 500ºC, although the TiO_2/AC provided highest crystallinity of TiO_2, it showed only adsorption activity that due to the AC was completely oxidized at this temperature.

For the recycling of catalyst, the TiO_2/AC using titanium(IV) isopropoxide calcined at 400ºC also gave the highest %removal of phenol and AO7 from its solution in the first run. Which removal efficiency would be decreased by by-product and intermediate were adsorbed onto surface of catalyst and impure particle could be blocked the pore of catalyst.

Copyright by Kasetsart University All rights reserved

Recommendations

1. Regarding the synergistic effect between TiO_2 and AC, the removal by TiO_2/AC are composed of photodegradation activity (TiO_2) and adsorption activity (AC). Both activities are depended on amount and ratio of TiO_2 and AC. Therefore, the amount and ratio of TiO_2: AC should be optimized to obtain the maximum removal efficiency.

2. Concerning the recyclability of catalyst, the removal efficiency by using TiO_2/AC is dramatically decreased by blocking of substrates (phenol or AO7) on surface or pore of catalyst. Consequently, the used- catalyst can be characterized by Fourier-Transform Infrared spectroscopy (FTIR) in order to confirm changed-surface of catalyst.

3. In case of regeneration process before reusing of catalyst, the decreasing of removal efficiency cause by deactivation of surface or pore by substrate (phenol or AO7). Hence, the regeneration process should be improved by treating the used-catalyst by oxidizing agent in order to clean up surface of catalyst.

Copyright by Kasetsart University All rights reserved

LITERATURE CITED

Abdullah, M. 2008. Derivation of Sherrer realtion using an approach in basic physics course. **J. Nanosci. Nanotechnol.** 1:28-32.

Arana J., J.M. Dona-Rodriguez, E.T. Rendon, C. Garriga I Cabo, O. Gonzalez-Diaz, J.A. Herrera-Melian, J. Perez-Pena, G. Colon and J.A., Navio 2003. TiO_2 activation by using activated carbon as a support PartII. Photo activity and FTIR study. **Appl. Catal., B** 44: 153-160.

Ao, Y., J. Xu, D. Fu, X. Shen and C. Yuan. 2008. Low temperature preparation of anatase TiO_2-coated activated carbon. **Colloids Surf., A** 312: 125-130.

Brezova, V., A. Stasko, S. Biskupic, A. Blazkova and B. Havlinova. 1994. Kinetic of hydroxyl radical spin trapping in photoactivated homogeneous (H_2O_2) and heterogeneous (TiO_2, O_2) aqueous systems. **J. Phys. Chem.** 98; 8977-8984.

Carp, O., C.L. Huisman and A. Reller. 2004. Photoinduced reactivity of titanium dioxide. **Prog. Solid State Chem.** 32: 33-177.

Carpio E., P. Zuniga, S. Ponce, J. Solis, J. Rodriguez and W. Estrada 2005. Photocatalytic degradation of phenol using TiO_2 nanocrystals supported on activated carbon. **J. Mol. Catal. A: Chem.** 228: 293-298.

Colon G., M.C. Hidalgo, M. Macıas and J.A. Navıo 2004. Enhancement of TiO2/C photocatalytic activity by sulfate promotion. **Appl. Catal., A** 259: 235-243.

Cordero T., C. Duchamp, J. M. Chovelon, C. Ferronato and J. Matos 2007. Influence of L-type activated carbon on photocatalytic activity of TiO_2 in 4-chlorophenol photodegradation. **J. Photochem. Photobiol., A** 191: 122-131.

Copyright by Kasetsart University All rights reserved

Dabrowski, A., P. Podkoscielny, Z. Hubicki and M. Barczak. 2005. Adsorption of phenolic compounds by activated carbon - a critical review. **Chemosphere** 58: 1049-1070.

Fang, X., Z. Zhang, Q. Chen., H. Ji and X. Gao. 2007. Dependence of nitrogen doping TiO_2 precursor annealed under NH_3 flow. **J. Solid State Chem**. 180: 1325-1332.

Forgacs, E., T. Cserháti and G. Oros. 2004. Removal of synthetic dyes from wastewaters: a review. **Envir. Inter.** 30: 953-971.

Fu P., Y. Luan and X. Dai 2004. Preparation of activated carbon fibers supported TiO_2 photo catalyst act evaluation of its photocatalytic reactivity. **J. Mol. Catal., A: Chem.** 221: 81-88.

Gnaser, H., A. Orendorz, A. Brodyanski, J. Losch, L.H. Bai, Z.H. Chen, Y.K. Le and C. Ziegler. 2007. Phase transformation and particle growth in nanocrystalline anatase TiO_2 films analyzed by X-ray diffraction and Raman spectroscopy. **Surf. Sci.** 601: 4390-4394.

Guo, L., F. Chen, X. Fan, W. Cai and J. Zhang. 2010. S-doped α-Fe_2O_3 as a highly active heterogeneous fenton-like catalyst towards the degradation of acid orange 7 and phenol. **Appl. Catal., B** doi:10.1016/j.apcatb.2010.02.015

Hameed, B.H., A.L. Almad and K.N.A. Latiff. 2007. Adsorption of basic dye (methylene blue) onto activated carbon prepared from rattan saw dust. **Dyes and Pigments.** 75: 143-149.

Hammami, S., N. Bellakhal, N. Oturan, M.A. Oturan and M. Dachraoui. 2008. Degradation of acid orange 7 by electrochemically generated $OH^{\bullet}$ radicals in acidic aqueous medium using a boron-doped diamond or platinum anode: a mechanistic study. **Chemosphere.** 73: 678-684.

Copyright by Kasetsart University All rights reserved

Hoffmann, M.R., S.T. Martin, W. Choi, and D.W. Bahnemannt. 1995. Environmental applications of semiconductor photocatalysis. **Chem. Rev.** 95: 69-96.

Kaur, S. and V. Singh, 2007. TiO_2 mediated photocatalytic degradation studies of Reactive Red 198 by UV irradiation. **J. Hazard. Mater.** 141: 230-236.

Li, Y., M. Ma, S. Sun, W. Yan and Y. Ouyang. 2008. Preparation of TiO_2-carbon surface composites with high photoactivity by supercritical pretreatment and sol-gel processing. **Appl. Surf. Sci.** 254: 4154-4158

_____, X. Li, J. Li and J. Yin 2005. Photocatalytic degradation of methyl orange in a sparged tube reactor with TiO_2-coated activated carbon composites. **Cat. Comm.** 6: 650-655.

_____, Zhang S., Q. Yu and W. Yin 2007. The effects of activated carbon supports on the structure and properties of TiO_2 nanoparticles prepared by a sol–gel method. **App. Surf. Sci.** 253: 9254–9258.

Matos, J., J. Laine and J.M. Herrman. 1998. Synergistic effect in the photocatalytic degradation of phenol on a suspended mixture of titania and activated carbon. **Appl. Catal., B** 18: 218-291.

_____, J. Laine, J. Heremann, D. Uzcategui and J.L. Brito 2007. Influence of activated carbon upon titania on aqueous photocatalytic consecutive runs of phenol photodegradation. **Appl. Catal., B** 70: 461-469.

Mills, A. and S.L. Hunte. 1997. An overview of semiconductor photocatalysis. **J. Photochem. Photobiol. A** 108: 1-35.

Copyright by Kasetsart University All rights reserved

Mao, C.C. and H.S. Weng. 2009. Promoting effect of adding carbon black to TiO_2 for aqueous photocatalytic degradation o f methyl orange. **Chem. Eng. J.** 155: 744-749.

Muggli, D.S. and L. Ding. 2001. Photocatalytic performance of sulfated TiO_2 and Degussa P25 TiO_2 during oxidation of organics. **Appl. Catal., B** 32: 181-194.

Ollis, D.F., 2002, Photocatalytic purification and remediation of contaminated air and water. **C. R. Chim.** 3: 405-411.

Patterson, A.L. 1939. The Scherrer formula for X-Ray particle size determination. **Phys. Rev.** 56: 978 – 982.

Ravichandran, L., K. Selvam, and M. Swamimathan. 2010. Highl efficient activated carbon loaded TiO2 for photodefluoroidation of pentafluorobenzoic acid. **J. Mol. Catal. A: Chem.** 317: 89-96.

Reuschenbach, P., M. Silvani, M. Dammann, D. Warnecke and T. Knacker. 2008. ECOSAR model performance with a large test set of industrial chemicals. **Chemosphere** 71: 1986-1995.

Subramani, A.K., K. Byrappa, G.N. Kumaraswam , H.B. Ravikumar, C. Ranganathaiah, K.M. Lokanatharai, S. Ananda and M. Yoshimura 2007. Hydrothermal preparation and characterization of TiO_2:AC composites. **Mater. Lett.** 61: 4828-4831.

_____, Y. Liu, Z. Hu, Y. Chen, W. Lui and G. Zhao. 2009. Degradation of methyl orange by composite photocatalysts nano-TiO2 immobilized on activated carbons of different porosities. **J. Hazard. Mater.** 169: 1061-1067.

Copyright by Kasetsart University All rights reserved

Tryba, B., A.W. Morawski and M. Inagaki 2003. Application of TiO_2-mounted activated carbon to the removal of phenol from water. **Appl. Catal., B** 41: 427-433.

Wang, W., C.G. Silva and J.L. Faria 2007. Photocatalytic degradation of Chromotrope 2R using nanocrystalline TiO_2/activated-carbon composite catalysts. **Appl. Catal., B** 70: 470-478.

Wang, X., Z. Hu, Y. Chen, G. Zhao, Y. Li and Z. Wen. 2009. A novel approach towards high-performance compocite photocatalyst of TiO2 deposited in activated carbon. **Appl. Surf. Sci.** 255: 3953-3958.

Yates, J.T., A.L. Linsebigler and G. Lu. 1995. Photocatalysis on TiO_2 Surfaces: Principles, Mechanisms, and Selected Results. **Chem. Rev.** 95: 735-758.

Yuan R., J. Zheng, R. Guan and Y. Zhao 2005. Surface and Photocatalytic activity of TiO_2 loaded on activated fibers. **Colloids. Surf., A** 254: 131-136.

Zhang, X., A. Li, Z. Jiang and Q. Zhang. Adsorption of dyes and phenol from water in resin adsorbents: Effect of adsorbate size and pore size distribution. **J. Hazard. Mater.** 137: 1115-1122.

Zhang, J., M. Li, Z. Feng, J. Chen and C. Li. 2006. UV Raman spectroscopic study on TiO_2. I. phase transformation at the surface and in the bulk. **J. Phys. Chem. B** 110: 927-935.

Zhang X. and L. Lei. 2008. Effect of preparation methods on the structure and catalytic performance of TiO_2/AC photocatalysts. **J. Harzard. Mater.** 153: 827-833.

Zhao, J. and X.D. Yang. 2003. Photocatalytic oxidation for indoor air purification: a literature review. **Build. Environ.** 38: 645-654.

Copyright by Kasetsart University All rights reserved

Zhu, B. and L. Zou. 2009. Trapping and decomposition of color compounds from recycled water by TiO2 coated activated carbon. **J. Envir. Man.** 90: 3217-3225.

Copyright by Kasetsart University All rights reserved

APPENDICES

Copyright by Kasetsart University All rights reserved

Appendix A

Calculation of crystallite sizes, phase identification using the Sherrer's equation

Copyright by Kasetsart University All rights reserved

The crystallite size was also calculated applying the Sherrer's equation showed as follows;

$$d = \frac{k\lambda}{\beta \cos\theta_B}$$

where d is the crystallite size (nm)cc

k is the constant whose value is approximately 0.9

λ is the wavelength of the X-ray radiation source (0.154 nm for Cu Kα)

β is the full width at half maximum intensity (FWHM) (radians)

θ_B is the Bragg angle at the position of the peak maximum

Appendix Figure A1 shows an example of finding all constants involved in the Sherrer's equation by fityk 0.8.9 software (a curve fitting and data analysis program). The XRD pattern can be well fitted with Lorentzian function (Abdullah, 2008). The parameters for the peak were following; center of peak = 25.4228º, peak area = 133.948, peak height = 312.606 and FWHM = 0.272784.

Copyright by Kasetsart University All rights reserved

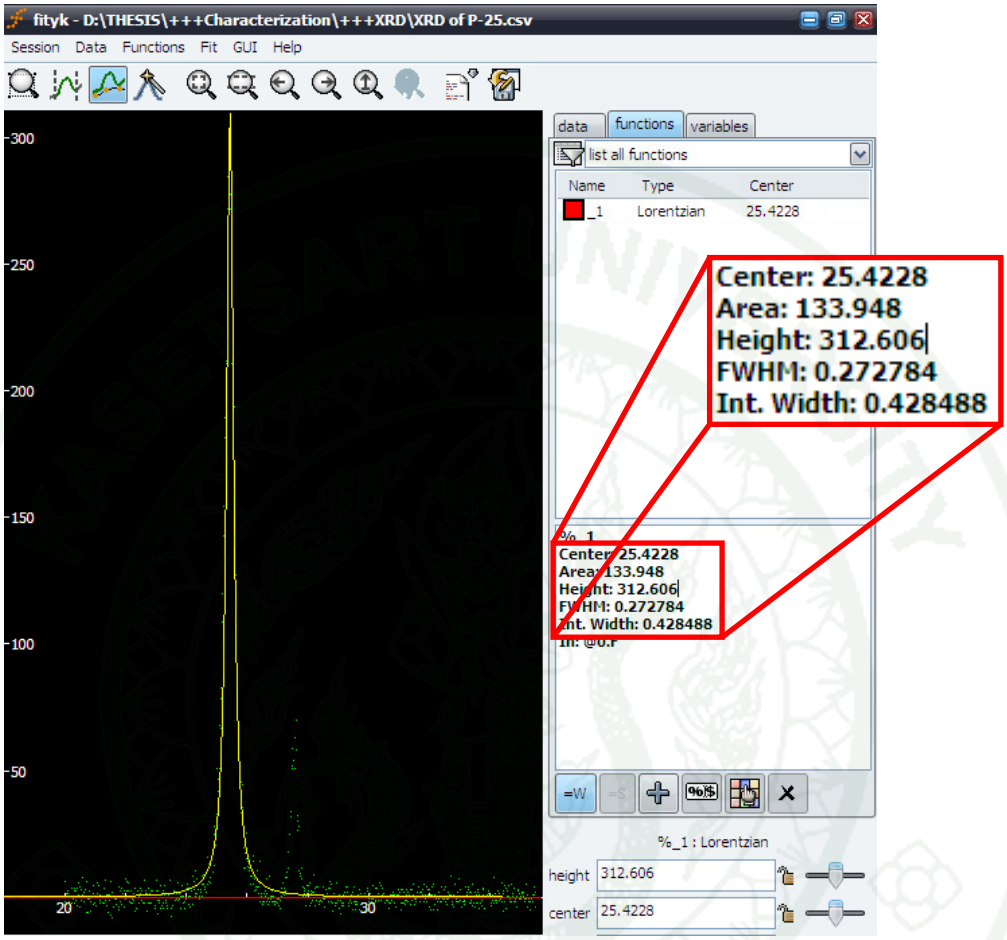

Appendix Figure A1 The fitting peak of P25 TiO_2 with Lorentzian function.

Copyright by Kasetsart University All rights reserved

Appendix B

Raw data of all adsorption isotherms

Copyright by Kasetsart University All rights reserved

. The analysis of the isotherm data by fitting them to different isotherm models is an important step to find the suitable model that can be used for design purpose (Hameed *et al.*, 2007). From the results in the present experiments, the adsorption data were fitted to the Langmuir isotherm model that indicated the monolayer adsorption system. Therefore, the Langmuir isotherm was used to describe the relationship between the amount of phenol adsorbed and its equilibrium concentration.

For the Langmuir isotherm, the procedure used to fit adsorption isotherm was adapted from Hameed *et al.*, which plotted a graph between C_e/ q_e and C_e. The relative coefficient (R^2) which obtained from plotted was close to 1. The Langmuir adsorption constant (b) and adsorption capacity (Q) from Langmuir equation as followed:

$$\frac{C_e}{q_e} = \frac{1}{bQ} + \frac{C_e}{Q}$$

C_e = liquid-phase concentration of phenol at equilibrium (mg/l)
q_e = equilibrium of solid-phase absorbed concentration (mg/g)
b = adsorption constant of Langmuir adsorption isotherm (l/mg)
Q = the maximum surface coverage (monolayer formation) (mg/g)

The q_e value can be calculated as followed;

$$q_e = \frac{(C_0 - C_e)V}{m}$$

C_0 = initial concentration of phenol (mg/l)
C_e = liquid-phase concentration of phenol at equilibrium (mg/l)
V = volume of solution (ml)(25 ml)
m = content of sample (mg) (0.05 g)

Copyright by Kasetsart University All rights reserved

Appendix Table B1 Raw data of the adsorption isotherm of phenol by AC.

C_0 (ppm)	Absorbance at λ_{max} 270 nm			Remaining concentration (C_e) (ppm)					q_e[a] (mg/g)
	Abs_1	Abs_2	Abs_3	$(C_e)_1$	$(C_e)_2$	$(C_e)_3$	$(C_e)_{ave}$	$Std._{(Ce)}$	
300	0.192	0.204	0.199	41.69	45.91	44.15	43.92	2.122	124.41×10^3
350	0.280	0.274	0.271	72.67	70.56	69.50	70.91	1.613	134.68×10^3
400	0.365	0.366	0.36	102.60	102.95	100.84	102.13	1.131	140.19×10^3
450	0.495	0.487	0.503	148.38	145.56	151.19	148.38	2.816	139.78×10^3
500	0.567	0.609	0.595	173.73	188.52	183.59	181.94	7.530	134.62×10^3

[a] q_e value was calculated as shown above.

Copyright by Kasetsart University All rights reserved

Appendix Table B2 Raw data of the adsorption isotherm of phenol by AC-400.

C_0 (ppm)	Absorbance at λ_{max} 270 nm			Remaining concentration (C_e) (ppm)					q_e[a] (mg/g)
	Abs_1	Abs_2	Abs_3	$(C_e)_1$	$(C_e)_2$	$(C_e)_3$	$(C_e)_{ave}$	$Std._{(Ce)}$	
300	0.210	0.215	0.218	48.23	49.78	50.84	49.55	1.423	122.47×10^3
350	0.322	0.295	0.309	87.46	77.95	82.88	82.76	4.754	132.62×10^3
400	0.411	0.416	0.419	118.80	120.56	121.61	120.32	1.423	142.02×10^3
450	0.515	0.540	0.540	155.42	164.22	202.95	161.17	4.983	139.84×10^3
500	0.642	0.655	0.655	200.14	204.71	183.59	202.60	2.308	134.62×10^3

[a] q_e value was calculated as shown above.

Copyright by Kasetsart University All rights reserved

Appendix Table B3 Raw data of the adsorption isotherm of phenol by TiO_2/AC using titanium(IV) isopropoxide as a precursor.

C_0 (ppm)	Absorbance at λ_{max} 270 nm			Remaining concentration (C_e) (ppm)					q_e[a] (mg/g)
	Abs_1	Abs_2	Abs_3	$(C_e)_1$	$(C_e)_2$	$(C_e)_3$	$(C_e)_{ave}$	$Std._{(Ce)}$	
100	0.129	0.137	0.130	19.50	22.32	19.85	20.56	1.534	33.09×10^3
150	0.262	0.267	0.270	66.33	68.09	69.15	67.86	1.423	36.56×10^3
200	0.379	0.384	0.380	107.53	109.29	107.88	108.23	0.931	43.48×10^3
250	0.526	0.523	0.520	159.29	158.23	157.18	158.24	1.056	46.65×10^3
300	0.672	0.648	0.625	210.70	202.25	203.66	205.53	4.527	47.30×10^3

[a] q_e value was calculated as shown above.

Copyright by Kasetsart University All rights reserved

Appendix Table B4 Raw data of the adsorption isotherm of phenol by TiO_2/AC using titanium(IV) n-butoxide as a precursor.

C_0 (ppm)	Absorbance at λ_{max} 270 nm			Remaining concentration (C_e) (ppm)					q_e[a] (mg/g)
	Abs_1	Abs_2	Abs_3	$(C_e)_1$	$(C_e)_2$	$(C_e)_3$	$(C_e)_{ave}$	$Std._{(Ce)}$	
100	0.125	0.139	0.135	18.09	23.02	21.62	20.91	1.539	38.24×10^3
150	0.266	0.262	0.273	67.74	66.33	70.21	68.09	1.960	39.79×10^3
200	0.372	0.387	0.383	105.07	110.35	108.94	108.12	2.735	44.60×10^3
250	0.530	0.520	0.518	160.70	157.18	156.47	158.12	2.263	45.13×10^3
300	0.668	0.659	0.651	209.29	206.12	203.31	206.24	2.994	42.27×10^3

[a] q_e value was calculated as shown above.

Copyright by Kasetsart University All rights reserved

Appendix C

Raw data of all photodegradation reactions

Copyright by Kasetsart University All rights reserved

Appendix Table C1 Raw data of the photodegradation reaction of phenol by prepared-TiO_2 without calcination.

Degrading time (min.)	Absorbance at λ_{max} 270 nm			Concentration[a] (ppm)			Relative concentration (C/C_o)				
	Abs_1	Abs_2	Abs_3	C_1	C_2	C_3	C_1/C_o	C_2/C_o	C_3/C_o	$(C/C_o)_{ave}$	$Std_{(C/Co)}$
Before on lamp	1.507	1.62	1.617	100.94	108.90	108.69	1	1	1	1	1.71E-08
0	1.500	1.618	1.61	100.45	108.76	108.19	0.9951	0.9987	0.9954	0.9964	0.001979
30	1.498	1.607	1.612	100.30	107.98	108.33	0.9937	0.9915	0.9967	0.9940	0.002596
60	1.490	1.598	1.599	99.74	107.35	107.42	0.9881	0.9857	0.9883	0.9874	0.001426
90	1.489	1.592	1.595	99.67	106.92	107.14	0.9874	0.9818	0.9857	0.9850	0.002843
120	1.475	1.581	1.596	98.69	106.15	107.21	0.9776	0.9747	0.9864	0.9796	0.006045
150	1.488	1.573	1.598	99.60	105.59	107.35	0.9867	0.9696	0.9876	0.9813	0.010178
180	1.482	1.569	1.594	99.18	105.30	107.07	0.9825	0.9670	0.9850	0.9782	0.009786

Copyright by Kasetsart University All rights reserved

Appendix Table C2 Raw data of the photodegradation reaction of phenol by prepared-TiO_2 calcined at 300ºC.

Degrading time (min.)	Absorbance at λ_{max} 270 nm			Concentration[a] (ppm)			Relative concentration (C/C_o)				
	Abs_1	Abs_2	Abs_3	C_1	C_2	C_3	C_1/C_o	C_2/C_o	C_3/C_o	$(C/C_o)_{ave}$	$Std_{(C/Co)}$
Before on lamp	1.502	1.698	1.553	100.59	114.39	104.18	1	1	1	1	1.36E-08
0	1.480	1.69	1.545	99.04	113.83	103.61	0.9845	0.9950	0.9945	0.9914	0.005914
30	1.471	1.63	1.545	98.40	109.60	103.61	0.9782	0.9581	0.9945	0.9770	0.018261
60	1.465	1.643	1.537	97.98	110.52	103.05	0.9740	0.9661	0.9891	0.9764	0.011704
90	1.469	1.639	1.537	98.26	110.23	103.05	0.9768	0.9636	0.9891	0.9765	0.012755
120	1.432	1.621	1.521	95.66	108.97	101.92	0.9509	0.9525	0.9783	0.9606	0.015363
150	1.419	1.611	1.521	94.74	108.26	101.92	0.9418	0.9464	0.9783	0.9555	0.019877
180	1.411	1.572	1.483	94.18	105.52	99.25	0.9362	0.9224	0.9526	0.9371	0.015142

Copyright by Kasetsart University All rights reserved

Appendix Table C3 Raw data of the photodegradation reaction of phenol by prepared-TiO_2 calcined at 400ºC.

Degrading time (min.)	Absorbance at λ_{max} 270 nm			Concentration[a] (ppm)			Relative concentration (C/C_o)				
	Abs_1	Abs_2	Abs_3	C_1	C_2	C_3	C_1/C_o	C_2/C_o	C_3/C_o	$(C/C_o)_{ave}$	$Std_{(C/Co)}$
Before on lamp	1.320	1.400	1.456	87.77	93.40	97.35	1	1	1	1	1.20E-08
0	1.280	1.380	1.376	84.95	92.00	91.71	0.9679	0.9849	0.9421	0.9649	0.021545
30	1.249	1.349	1.368	82.77	89.81	91.15	0.9430	0.9615	0.9363	0.9469	0.013057
60	1.246	1.346	1.355	82.56	89.60	90.23	0.9406	0.9592	0.9269	0.9422	0.016238
90	1.241	1.341	1.359	82.21	89.25	90.52	0.9366	0.9555	0.9298	0.9406	0.013310
120	1.236	1.321	1.336	81.85	87.84	88.90	0.9326	0.9404	0.9131	0.9287	0.014026
150	1.250	1.290	1.318	82.84	85.66	87.63	0.9438	0.9170	0.9001	0.9203	0.022017
180	1.230	1.270	1.299	81.43	84.25	86.29	0.9277	0.9019	0.8864	0.9054	0.020891

Copyright by Kasetsart University All rights reserved

Appendix Table C4 Raw data of the photodegradation reaction of phenol by prepared-TiO_2 calcined at 500ºC.

Degrading time (min.)	Absorbance at λ_{max} 270 nm			Concentration[a] (ppm)			Relative concentration (C/C_o)				
	Abs_1	Abs_2	Abs_3	C_1	C_2	C_3	C_1/C_o	C_2/C_o	C_3/C_o	$(C/C_o)_{ave}$	$Std_{(C/Co)}$
Before on lamp	1.564	1.501	1.597	104.95	100.52	107.28	1	1	1	1	1.97E-08
0	1.458	1.478	1.498	97.49	98.90	100.30	0.9288	0.9838	0.9350	0.9492	0.030144
30	1.440	1.446	1.48	96.22	96.64	99.04	0.9168	0.9614	0.9231	0.9338	0.024154
60	1.420	1.425	1.474	94.81	95.1	98.61	0.9033	0.9467	0.9192	0.9231	0.021945
90	1.375	1.405	1.423	91.64	93.76	95.02	0.8731	0.9327	0.8857	0.8972	0.031387
120	1.353	1.383	1.407	90.09	92.21	93.90	0.8584	0.9173	0.8752	0.8836	0.030337
150	1.329	1.369	1.394	88.40	91.22	92.98	0.8423	0.9075	0.8667	0.8721	0.032940
180	1.301	1.361	1.328	86.43	90.66	88.33	0.8235	0.9019	0.8234	0.8496	0.045281

Copyright by Kasetsart University All rights reserved

Appendix Table C5 Raw data of the photodegradation reaction of phenol by TiO_2/AC prepared from titanium(IV) isopropoxide without calcination.

Degrading time (min.)	Absorbance at λ_{max} 270 nm			Concentration[a] (ppm)			Relative concentration (C/C_o)				
	Abs_1	Abs_2	Abs_3	C_1	C_2	C_3	C_1/C_o	C_2/C_o	C_3/C_o	$(C/C_o)_{ave}$	$Std_{(C/Co)}$
Before on lamp	1.459	1.548	1.502	97.56	103.83	100.59	1	1	1	1	7.72E-08
0	0.457	0.590	0.537	27.00	36.36	32.63	0.2767	0.3502	0.3244	0.3171	0.037287
30	0.454	0.587	0.527	26.78	36.15	31.92	0.2745	0.3482	0.3174	0.3134	0.036977
60	0.450	0.579	0.521	26.50	35.59	31.50	0.2716	0.3427	0.3132	0.3092	0.035713
90	0.448	0.575	0.512	26.36	35.30	30.87	0.2702	0.3400	0.3069	0.3057	0.034929
120	0.442	0.568	0.509	25.94	34.81	30.66	0.2659	0.3353	0.3048	0.3020	0.034787
150	0.433	0.559	0.486	25.30	34.18	29.04	0.2594	0.3292	0.2887	0.2924	0.035049
180	0.423	0.551	0.473	24.60	33.61	28.12	0.2522	0.3237	0.2796	0.2852	0.036121

Copyright by Kasetsart University All rights reserved

Appendix Table C6 Raw data of the photodegradation reaction of phenol by TiO_2/AC prepared from titanium(IV) isopropoxide calcined at 300ºC.

Degrading time (min.)	Absorbance at λ_{max} 270 nm			Concentration[a] (ppm)			Relative concentration (C/C_o)				
	Abs_1	Abs_2	Abs_3	C_1	C_2	C_3	C_1/C_o	C_2/C_o	C_3/C_o	$(C/C_o)_{ave}$	$Std_{(C/Co)}$
Before on lamp	1.655	1.549	1.605	111.36	103.90	107.84	1	1	1	1	5.51E-08
0	0.569	0.598	0.558	34.88	36.92	34.11	0.3132	0.355	0.3163	0.3283	0.023512
30	0.532	0.589	0.552	32.28	36.29	33.69	0.2898	0.3493	0.3123	0.3171	0.030019
60	0.512	0.587	0.537	30.87	36.15	32.63	0.2772	0.3479	0.3025	0.3092	0.035843
90	0.498	0.578	0.528	29.88	35.52	32.00	0.2683	0.3418	0.2967	0.3023	0.037070
120	0.483	0.568	0.518	28.83	34.81	31.29	0.2588	0.3350	0.2901	0.2947	0.038307
150	0.478	0.565	0.515	28.47	34.60	31.08	0.2557	0.3330	0.2882	0.2923	0.038832
180	0.460	0.551	0.500	27.21	33.61	30.02	0.2443	0.3235	0.2784	0.2821	0.039744

Copyright by Kasetsart University All rights reserved

Appendix Table C7 Raw data of the photodegradation reaction of phenol by TiO_2/AC prepared from titanium(IV) isopropoxide calcined at 400ºC.

Degrading time (min.)	Absorbance at λ_{max} 270 nm			Concentration[a] (ppm)			Relative concentration (C/C_o)				
	Abs_1	Abs_2	Abs_3	C_1	C_2	C_3	C_1/C_o	C_2/C_o	C_3/C_o	$(C/C_o)_{ave}$	$Std_{(C/Co)}$
Before on lamp	1.579	1.495	1.495	106.01	100.09	100.06	1	1	1	1	1.56092 E-08
0	0.717	0.778	0.717	45.30	49.60	45.30	0.4273	0.4955	0.4526	0.4585	0.034465
30	0.645	0.634	0.645	40.23	39.46	40.23	0.3795	0.3942	0.4019	0.3919	0.011393
60	0.595	0.629	0.650	36.71	39.11	40.59	0.3463	0.3907	0.4055	0.3808	0.030791
90	0.565	0.601	0.635	34.60	37.14	39.53	0.3264	0.3710	0.3949	0.3641	0.034785
120	0.536	0.589	0.636	32.56	36.29	39.60	0.3071	0.3626	0.3956	0.3551	0.044721
150	0.521	0.521	0.621	31.50	31.50	38.54	0.2971	0.314	0.3851	0.3323	0.046524
180	0.505	0.498	0.605	30.38	29.88	37.42	0.2865	0.2985	0.3738	0.3196	0.047311

Copyright by Kasetsart University All rights reserved

Appendix Table C8 Raw data of the photodegradation reaction of phenol by TiO_2/AC prepared from titanium(IV) isopropoxide calcined at 500ºC.

Degrading time (min.)	Absorbance at λ_{max} 270 nm			Concentration[a] (ppm)			Relative concentration (C/C_o)				
	Abs_1	Abs_2	Abs_3	C_1	C_2	C_3	C_1/C_o	C_2/C_o	C_3/C_o	$(C/C_o)_{ave}$	$Std_{(C/Co)}$
Before on lamp	1.574	1.574	1.754	105.66	105.66	118.33	1	1	1	1	1.27E-07
0	1.460	1.357	1.617	97.63	90.38	108.69	0.9240	0.8553	0.9184	0.8992	0.038133
30	1.446	1.334	1.545	96.64	88.76	103.61	0.9146	0.8400	0.8756	0.8767	0.037336
60	1.415	1.315	1.565	94.46	87.42	105.02	0.8940	0.8273	0.8875	0.8696	0.036747
90	1.374	1.319	1.535	91.57	87.70	102.91	0.8667	0.8300	0.8696	0.8554	0.022071
120	1.343	1.309	1.536	89.39	87.00	102.98	0.8460	0.8233	0.8702	0.8465	0.023448
150	1.318	1.286	1.501	87.63	85.38	100.52	0.8293	0.8080	0.8494	0.8289	0.020698
180	1.244	1.223	1.435	82.42	80.94	95.87	0.7800	0.7660	0.8101	0.7854	0.022536

Copyright by Kasetsart University All rights reserved

Appendix Table C9 Raw data of the photodegradation reaction of phenol by TiO_2/AC prepared from titanium(IV) n-butoxide without calcination.

Degrading time (min.)	Absorbance at λ_{max} 270 nm			Concentration[a] (ppm)			Relative concentration (C/C_o)				
	Abs_1	Abs_2	Abs_3	C_1	C_2	C_3	C_1/C_o	C_2/C_o	C_3/C_o	$(C/C_o)_{ave}$	$Std_{(C/Co)}$
Before on lamp	1.459	1.548	1.502	97.56	103.83	100.59	1	1	1	1	7.72E-08
0	0.457	0.590	0.537	27.00	36.36	32.63	0.2767	0.3502	0.3244	0.3171	0.037287
30	0.456	0.587	0.531	26.92	36.15	32.21	0.2760	0.3482	0.3202	0.3148	0.036395
60	0.439	0.583	0.529	25.73	35.87	32.07	0.2637	0.3454	0.3188	0.3093	0.041686
90	0.431	0.579	0.520	25.16	35.59	31.43	0.2579	0.3427	0.3125	0.3044	0.042978
120	0.426	0.572	0.499	24.81	35.09	29.95	0.2543	0.3380	0.2978	0.2967	0.041844
150	0.421	0.569	0.486	24.46	34.88	29.04	0.2507	0.3360	0.2887	0.2918	0.042706
180	0.419	0.563	0.483	24.32	34.46	28.83	0.2493	0.3319	0.2866	0.2892	0.041373

Copyright by Kasetsart University All rights reserved

Appendix Table C10 Raw data of the photodegradation reaction of phenol by TiO_2/AC prepared from titanium(IV) n-butoxide calcined at 300ºC.

Degrading time (min.)	Absorbance at λ_{max} 270 nm			Concentration[a] (ppm)			Relative concentration (C/C_o)				
	Abs_1	Abs_2	Abs_3	C_1	C_2	C_3	C_1/C_o	C_2/C_o	C_3/C_o	$(C/C_o)_{ave}$	$Std_{(C/Co)}$
Before on lamp	1.395	1.364	1.410	93.05	90.87	94.11	1	1	1	1	1.79E-08
0	0.479	0.504	0.573	28.54	30.30	35.16	0.3067	0.3335	0.3736	0.3380	0.033670
30	0.462	0.483	0.571	27.35	28.83	35.02	0.2939	0.3172	0.3721	0.3277	0.040180
60	0.465	0.484	0.561	27.56	28.90	34.32	0.2962	0.3180	0.3647	0.3263	0.034996
90	0.450	0.480	0.558	26.50	28.61	34.11	0.28489	0.3149	0.3624	0.3207	0.039133
120	0.429	0.467	0.541	25.02	27.70	32.91	0.26897	0.3048	0.3497	0.3078	0.040477
150	0.422	0.458	0.536	24.53	27.07	32.56	0.2636	0.2978	0.3460	0.3025	0.041366
180	0.424	0.430	0.525	24.67	25.09	31.78	0.2651	0.2761	0.3377	0.2930	0.039124

Copyright by Kasetsart University All rights reserved

Appendix Table C11 Raw data of the photodegradation reaction of phenol by TiO_2/AC prepared from titanium(IV) n-butoxide calcined at 400ºC

Degrading time (min.)	Absorbance at λ_{max} 270 nm			Concentration[a] (ppm)			Relative concentration (C/C_o)				
	Abs_1	Abs_2	Abs_3	C_1	C_2	C_3	C_1/C_o	C_2/C_o	C_3/C_o	$(C/C_o)_{ave}$	$Std_{(C/Co)}$
Before on lamp	1.424	1.424	1.410	95.09	95.09	94.11	1	1	1	1	3.35E-08
0	0.763	0.735	0.790	48.54	46.57	50.45	0.5105	0.4897	0.5360	0.5121	0.023184
30	0.757	0.741	0.767	48.12	47.00	48.83	0.5060	0.4942	0.5188	0.5063	0.012319
60	0.718	0.701	0.681	45.38	44.18	42.77	0.4771	0.4646	0.4545	0.4654	0.011366
90	0.673	0.672	0.612	42.21	42.14	37.91	0.4438	0.4431	0.4028	0.4299	0.023457
120	0.656	0.677	0.602	41.01	42.49	37.21	0.4312	0.4468	0.3953	0.4245	0.026381
150	0.617	0.648	0.554	38.26	40.45	33.83	0.4023	0.4253	0.3594	0.3957	0.033441
180	0.601	0.632	0.547	37.14	39.32	33.33	0.3905	0.4135	0.3542	0.3860	0.029885

Copyright by Kasetsart University All rights reserved

Appendix Table C12 Raw data of the photodegradation reaction of phenol by TiO_2/AC prepared from titanium(IV) n-butoxide calcined at 500ºC

Degrading time (min.)	Absorbance at λ_{max} 270 nm			Concentration[a] (ppm)			Relative concentration (C/C_o)				
	Abs_1	Abs_2	Abs_3	C_1	C_2	C_3	C_1/C_o	C_2/C_o	C_3/C_o	$(C/C_o)_{ave}$	$Std_{(C/Co)}$
Before on lamp	1.340	1.340	1.383	89.18	89.18	92.21	1	1	1	1	5.87E-09
0	1.234	1.192	1.240	81.71	78.76	82.14	0.9162	0.8831	0.8907	0.8967	0.017364
30	1.193	1.161	1.198	78.83	76.57	79.18	0.8839	0.8586	0.8587	0.8670	0.014571
60	1.174	1.146	1.172	77.49	75.52	77.35	0.8689	0.8468	0.8388	0.8515	0.015576
90	1.161	1.124	1.157	76.57	73.97	76.29	0.8586	0.8294	0.8274	0.8384	0.017485
120	1.148	1.110	1.150	75.66	72.98	75.80	0.8483	0.8183	0.8220	0.8296	0.016367
150	1.138	1.085	1.147	74.95	71.22	75.59	0.8404	0.7986	0.8197	0.8196	0.020925
180	1.105	1.062	1.120	72.63	69.60	73.69	0.8144	0.7804	0.7991	0.7980	0.017005

Copyright by Kasetsart University All rights reserved

Appendix Table C13 Raw data of the photodegradation reaction of AO7 by TiO_2/AC prepared from titanium(IV) isopropoxide calcined at 400ºC at pH 4.0.

Degrading time (min.)	Absorbance at λ_{max} 485 nm			Concentration[a] (ppm)			Relative concentration (C/C_o)				
	Abs_1	Abs_2	Abs_3	C_1	C_2	C_3	C_1/C_o	C_2/C_o	C_3/C_o	$(C/C_o)_{ave}$	$Std_{(C/Co)}$
Before on lamp	1.216	1.216	1.469	100.58	100.58	121.70	1	1	1	1	1.96E-07
0	1.051	0.891	1.283	17.36	14.69	21.23	0.1726	0.1460	0.1744	0.1643	0.01589
30	0.496	0.431	0.736	8.09	7.01	12.1	0.0804	0.0697	0.0994	0.0832	0.01505
60	0.309	0.398	0.558	4.97	6.46	9.13	0.0494	0.0642	0.0750	0.0629	0.01283
90	0.178	0.257	0.488	2.78	4.10	7.96	0.0277	0.0408	0.06543	0.0446	0.01914
120	0.119	0.228	0.351	1.80	3.62	5.67	0.0179	0.0360	0.0466	0.0335	0.01451
150	0.094	0.191	0.201	1.38	3.00	3.17	0.0137	0.0298	0.0260	0.0232	0.00841
180	0.087	0.085	0.161	1.26	1.23	2.50	0.0126	0.0122	0.0205	0.015157	0.00469

Copyright by Kasetsart University All rights reserved

Appendix Table C14 Raw data of the photodegradation reaction of AO7 by TiO_2/AC prepared from titanium(IV) isopropoxide calcined at 400ºC at pH 7.0.

Degrading time (min.)	Absorbance at λ_{max} 485 nm			Concentration[a] (ppm)			Relative concentration (C/C_o)				
	Abs_1	Abs_2	Abs_3	C_1	C_2	C_3	C_1/C_o	C_2/C_o	C_3/C_o	$(C/C_o)_{ave}$	$Std_{(C/Co)}$
Before on lamp	1.218	1.218	1.569	100.75	100.75	130.05	1	1	1	1	2.01E-07
0	1.258	1.205	1.252	20.81	19.93	20.71	0.2066	0.1978	0.1593	0.1879	0.02517
30	1.091	1.191	1.191	18.03	19.69	19.69	0.1789	0.1955	0.1514	0.1753	0.02224
60	0.929	1.029	1.029	15.32	16.99	16.99	0.1521	0.1686	0.1306	0.1504	0.01905
90	0.840	0.940	0.914	13.83	15.50	15.07	0.1373	0.1539	0.1159	0.1357	0.01906
120	0.770	0.870	0.870	12.67	14.34	14.34	0.1257	0.1423	0.1102	0.1261	0.01603
150	0.688	0.855	0.788	11.30	14.09	12.97	0.1121	0.1398	0.0997	0.1172	0.02053
180	0.608	0.798	0.708	9.96	13.13	11.63	0.0989	0.1304	0.0894	0.1062	0.02143

Copyright by Kasetsart University All rights reserved

Appendix Table C15 Raw data of the photodegradation reaction of AO7 by TiO_2/AC prepared from titanium(IV) isopropoxide calcined at 400ºC at pH 10.0.

Degrading time (min.)	Absorbance at λ_{max} 485 nm			Concentration[a] (ppm)			Relative concentration (C/C_o)				
	Abs_1	Abs_2	Abs_3	C_1	C_2	C_3	C_1/C_o	C_2/C_o	C_3/C_o	$(C/C_o)_{ave}$	$Std_{(C/Co)}$
Before on lamp	1.143	1.143	1.541	101.33	101.33	136.06	1	1	1	1	5.29E-09
0	0.994	0.894	1.394	17.66	15.92	24.64	0.1743	0.1571	0.1811	0.1708	0.01238
30	0.715	0.715	1.215	12.79	12.79	21.52	0.1262	0.1262	0.1581	0.1369	0.01841
60	0.655	0.655	1.055	11.75	11.75	18.73	0.1159	0.1159	0.1376	0.1231	0.01253
90	0.435	0.432	0.835	7.910	7.85	14.89	0.0780	0.0775	0.1094	0.0883	0.01826
120	0.228	0.324	0.628	4.298	5.97	11.27	0.0424	0.0589	0.0828	0.0614	0.02035
150	0.160	0.251	0.460	3.111	4.69	8.34	0.0307	0.0463	0.0613	0.0461	0.01532
180	0.129	0.212	0.229	2.570	4.01	4.31	0.0253	0.0396	0.0317	0.0322	0.00716

Copyright by Kasetsart University All rights reserved

Appendix Table C16 Raw data of the photodegradation reaction of AO7 by TiO_2/AC prepared from titanium(IV) n-butoxide calcined at 400ºC at pH 4.0.

Degrading time (min.)	Absorbance at λ_{max} 485 nm			Concentration[a] (ppm)			Relative concentration (C/C_o)				
	Abs_1	Abs_2	Abs_3	C_1	C_2	C_3	C_1/C_o	C_2/C_o	C_3/C_o	$(C/C_o)_{ave}$	$Std_{(C/Co)}$
Before on lamp	1.225	1.225	1.469	101.33	101.33	121.70	1	1	1	1	5.00E-09
0	0.866	0.932	1.189	14.27	15.37	19.66	0.1408	0.1517	0.1615	0.1513	0.01037
30	0.605	0.781	0.991	9.91	12.86	16.36	0.0978	0.1268	0.1344	0.1197	0.01930
60	0.360	0.578	0.763	5.82	9.46	12.55	0.0574	0.0934	0.1031	0.0846	0.02404
90	0.201	0.311	0.572	3.17	5.00	9.36	0.0313	0.0494	0.0769	0.0525	0.02298
120	0.121	0.191	0.398	1.83	3.00	6.46	0.0181	0.0296	0.0530	0.0336	0.01781
150	0.098	0.186	0.192	1.45	2.92	3.02	0.0143	0.0288	0.0248	0.0226	0.00748
180	0.091	0.089	0.101	1.33	1.30	1.50	0.01318	0.01285	0.0123	0.0127	0.00041

Copyright by Kasetsart University All rights reserved

Appendix Table C17 Raw data of the photodegradation reaction of AO7 by TiO_2/AC prepared from titanium(IV) n-butoxide calcined at 400ºC at pH 7.0.

Degrading time (min.)	Absorbance at λ_{max} 485 nm			Concentration[a] (ppm)			Relative concentration (C/C_o)				
	Abs_1	Abs_2	Abs_3	C_1	C_2	C_3	C_1/C_o	C_2/C_o	C_3/C_o	$(C/C_o)_{ave}$	$Std_{(C/Co)}$
Before on lamp	1.385	1.213	1.213	110.92	96.92	96.92	1	1	1	1	7.06E-09
0	1.525	1.325	1.256	24.46	21.20	20.08	0.2205	0.2188	0.2072	0.2155	0.00724
30	1.421	1.16	1.076	22.77	18.52	17.15	0.2052	0.1910	0.1769	0.1911	0.01415
60	1.325	0.923	0.992	21.20	14.66	15.78	0.1911	0.1512	0.1628	0.1684	0.02053
90	1.121	0.81	0.891	17.88	12.82	14.14	0.1612	0.1322	0.1458	0.1464	0.01448
120	1.015	0.75	0.715	16.15	11.84	11.27	0.1456	0.1221	0.1163	0.1280	0.01553
150	0.932	0.631	0.693	14.80	9.90	10.91	0.1334	0.1022	0.1126	0.1161	0.01593
180	0.811	0.619	0.689	12.83	9.71	10.85	0.1157	0.1001	0.1119	0.1092	0.00810

Copyright by Kasetsart University All rights reserved

Appendix Table C18 Raw data of the photodegradation reaction of AO7 by TiO_2/AC prepared from titanium(IV) n-butoxide calcined at 400ºC at pH 10.0.

Degrading time (min.)	Absorbance at λ_{max} 485 nm			Concentration[a] (ppm)			Relative concentration (C/C_o)				
	Abs_1	Abs_2	Abs_3	C_1	C_2	C_3	C_1/C_o	C_2/C_o	C_3/C_o	$(C/C_o)_{ave}$	$Std_{(C/Co)}$
Before on lamp	1.181	1.181	1.431	104.65	104.65	126.46	1	1	1	1	5.68E-09
0	0.602	0.791	0.846	10.82	14.12	15.08	0.1034	0.1349	0.1192	0.1192	0.01575
30	0.427	0.672	0.667	7.77	12.04	11.95	0.0742	0.1151	0.0945	0.0946	0.02028
60	0.251	0.455	0.439	4.69	8.26	7.98	0.0449	0.0789	0.0631	0.0623	0.01702
90	0.154	0.294	0.223	3.00	5.45	4.21	0.0287	0.0520	0.0332	0.0380	0.01237
120	0.121	0.212	0.309	2.43	4.01	5.71	0.0232	0.0384	0.0451	0.0356	0.01123
150	0.099	0.169	0.201	2.04	3.26	3.82	0.0195	0.0312	0.0302	0.0270	0.00647
180	0.056	0.076	0.098	1.29	1.64	2.02	0.0123	0.0157	0.0160	0.0147	0.00202

Copyright by Kasetsart University All rights reserved

Appendix D

Calculation of rate constants

Copyright by Kasetsart University All rights reserved

The procedure used to find rate constants was adapted from previous research by Fang *et al.* (2007). They assumed that the degradation of methylene blue in the presence of photocatalysts was the first-order kinetic reaction because they plotted a graph between $\ln C_0/C$ and degrading time (h). Then, they obtained the relative coefficient (R^2) was close to 1 and the slope of the graph could be considered as the rate constant of the photodegradation reaction. Therefore, this work properly modified their method to find the rate constants. All raw data are shown in the Appendix C

For the first-order rate law (at t = 0, concentration of C is $[C]_0$);

$$Rate = \frac{d[A]_t}{[A]_0} = -kt$$

The integrated rate law is thus;

$$[A]_t = [A]_0 e^{-kt}$$

The rate law is applied in order to plot liner graph by taking natural logarithm

$$\ln[A]_t = \ln[A]_0 + \ln e^{-kt}$$

$$\ln[A]_0 - \ln[A]_t = kt$$

$$\ln \frac{[A]_0}{[A]_t} = kt$$

In experiment, the C_0 and C was used instead of $[A]_0$ and [A]t, respectively;

$$\ln \frac{C_0}{C} = kt$$

Therefore, the liner graph was plotted between $\ln C_0/C$ and t, the rate constant was obtained from slope of graph.

Copyright by Kasetsart University All rights reserved

Appendix E

Calculation of surface area for phenol adsorption

Copyright by Kasetsart University All rights reserved

The estimated surface area of catalyst could be calculated by maximum adsorption capacity (Q) and size of phenol. Regarding the Langmuir isotherm, adsorption was assumed as monolayer.

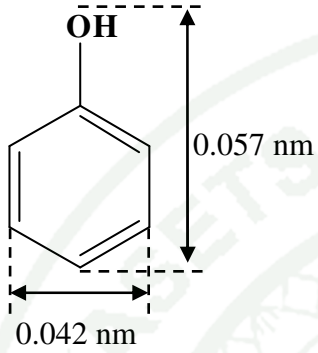

Size of phenol molecule = width x height

= 0.042 nm x 0.057 nm

$=2.394 \times 10^{-21}$ m^2

From Q-value of TiO_2/AC = 5.4×10^4 mg of phenol are adsorped

= 5.4×10^4 (mg) / 94 (g/mol)

= 0.5319 mol

Estimated surface area of phenol 1 mole

= $(6.02 \times 10^{23}$ molecule/mole$)(2.394 \times 10^{-21}$ $m^2)$(1 mole)

= 1441 m^2

Therefore, Estimated surface area of phenol 0.5319 mole

= $(6.02 \times 10^{23}$ molecule/mole$)(2.394 \times 10^{-21}$ $m^2)$(0.5319 mole)

= 766 m^2

Copyright by Kasetsart University All rights reserved

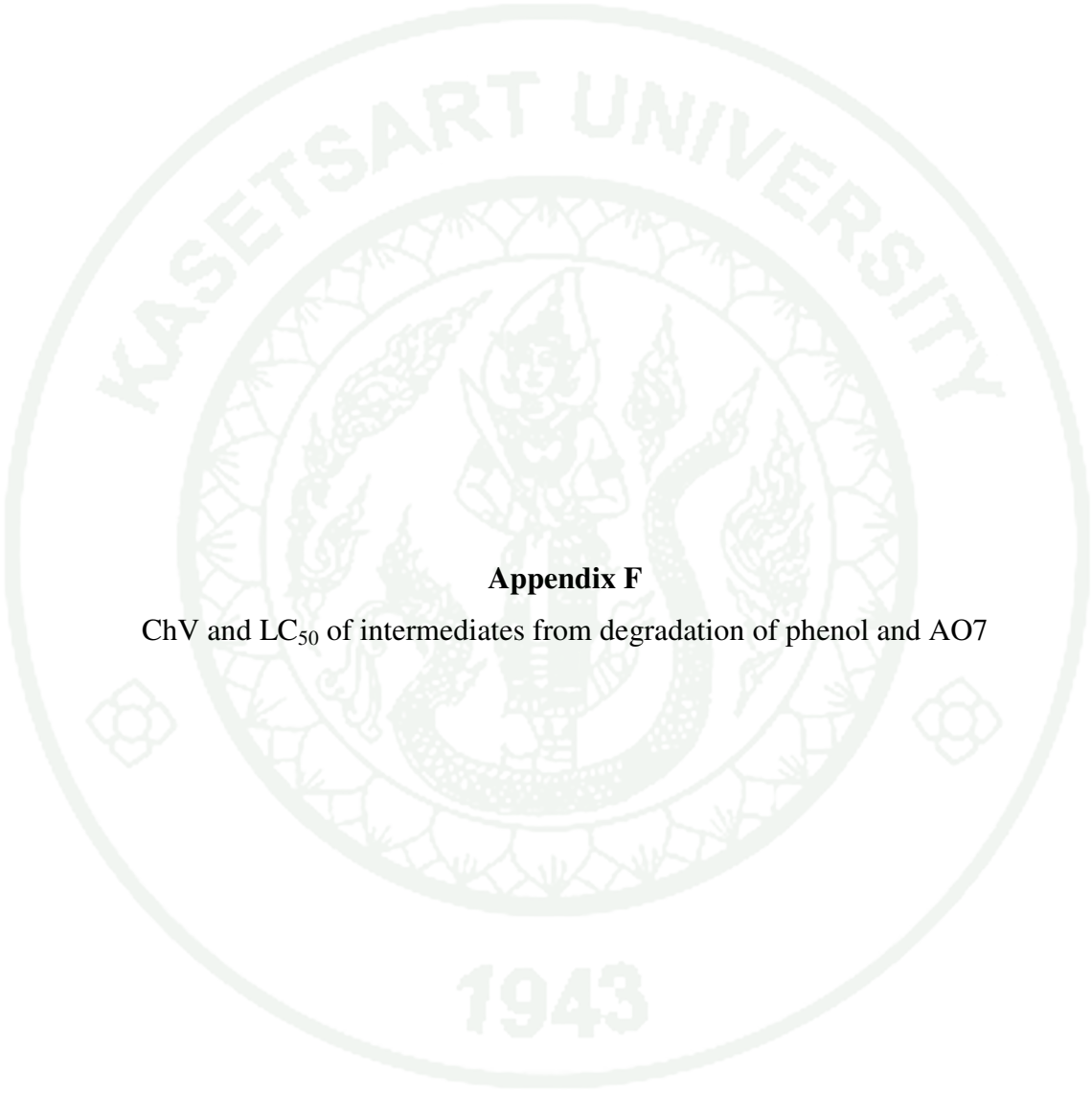

Appendix F

ChV and LC_{50} of intermediates from degradation of phenol and AO7

Copyright by Kasetsart University All rights reserved

The definition ChV and LC50 are chronic toxicity value and median lethal concentration. The toxicity of compounds and intermediates can be indicated by ChV and LC_{50} value, which are calculated by using EPI Suite software (version 4.00, January, 2009) with ECOSAR mode.(Reuschenbach *et al.*, 2008)

Copyright by Kasetsart University All rights reserved

Appendix Table F1 The ChV and LC_{50} value of each intermediate from degradation of phenol

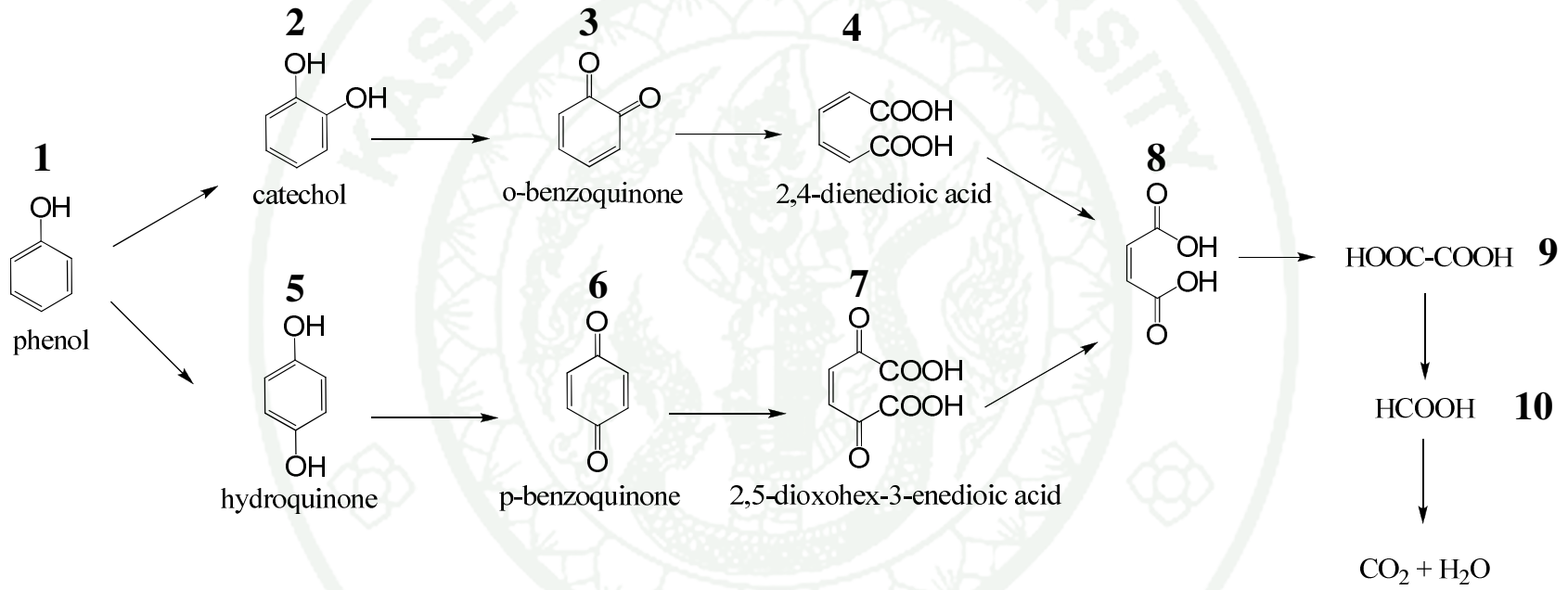

Compound	1	2	3	4	5	6	7	8	9	10
ChV(ppm)	2.02	14.17	1.2×10^{2}	8.5×10^{3}	14.17	2.5×10^{2}	5.4×10^{3}	5.6×10^{3}	1.1×10^{4}	4.5×10^{2}
LC_{50}(ppm)	31.89	38.15	1.2×10^{3}	9.4×10^{4}	38.14	2.5×10^{3}	6.3×10^{4}	6.2×10^{4}	1.4×10^{5}	5.2×10^{3}

[a]The ChV and LC50 value obtained from ECOSAR software (REF)

Copyright by Kasetsart University All rights reserved

Appendix Table F2 The ChV and LC_{50} value of each intermediate from degradation of AO7

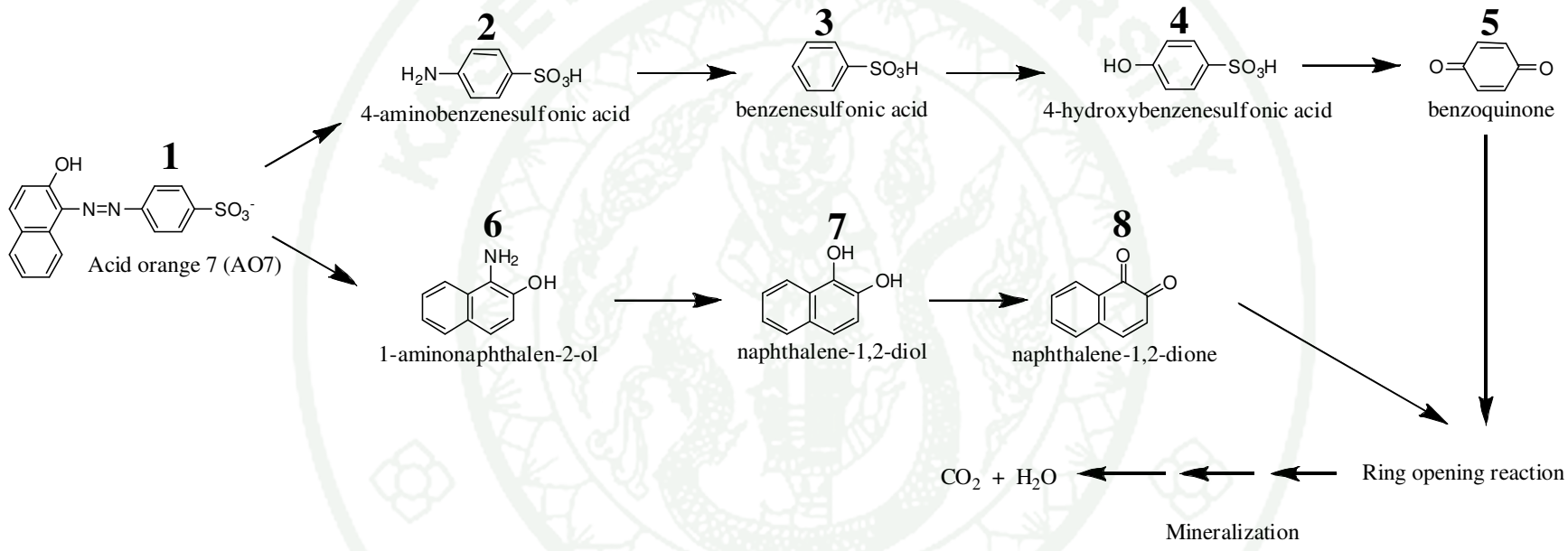

Compound	1	2	3	4	5	6	7	8
ChV(ppm)	2.02	14.17	1.2×10^{2}	8.5×10^{3}	14.17	2.5×10^{2}	5.4×10^{3}	5.6×10^{3}
LC_{50}(ppm)	31.89	38.15	1.2×10^{3}	9.4×10^{4}	38.14	2.5×10^{3}	6.3×10^{4}	6.2×10^{4}

[a]The ChV and LC50 value obtained from ECOSAR software (REF)

Copyright by Kasetsart University All rights reserved

CIRRICULUM VITAE

NAME : Mr. Chalermpan Ngamsopasirisun

BIRTH DATE : August 6, 1985

BIRTH PLACE : Bangkok, Thailand

EDUCATION	**: YEAR**	**INSTITUTE**	**DEGREE/DIPLOMA**
	2007	Kasetsart Univ.	B.Sc. (Chemistry)

POSITION/TITLE : Postgraduate student

WORKPLACE : Faculty of Science, Kasetsart University

SCHOLARSHIP/AWARDS : Center for Innovation in Chemistry: Postgraduate Education and Research Program in Chemistry (PERCH-CIC)

Copyright by Kasetsart University All rights reserved